

SCHOOL OF  
CIVIL ENGINEERING  
INDIANA  
DEPARTMENT OF HIGHWAYS

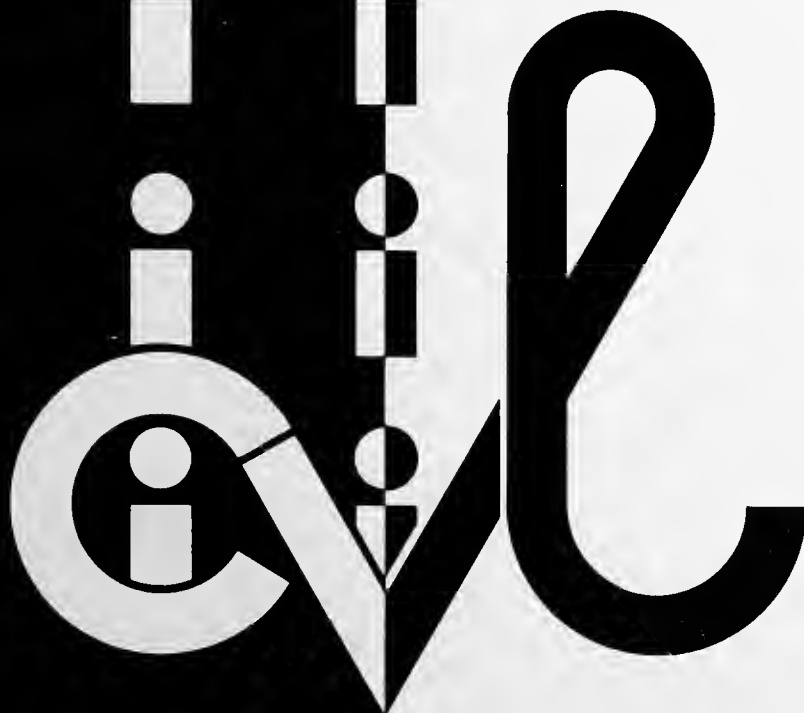
JOINT HIGHWAY RESEARCH PROJECT

JHRP-84-23

IDENTIFICATION OF FROST SUSCEPTIBLE  
AGGREGATE AND THEIR USE IN CONCRETE  
OR BITUMINOUS PAVEMENTS

FINAL REPORT

Marco Antonio Salcedo



PURDUE UNIVERSITY



JOINT HIGHWAY RESEARCH PROJECT

JHRP-84-23

IDENTIFICATION OF FROST SUSCEPTIBLE  
AGGREGATE AND THEIR USE IN CONCRETE  
OR BITUMINOUS PAVEMENTS

FINAL REPORT

Marco Antonio Salcedo



# FINAL REPORT

## IDENTIFICATION OF FROST SUSCEPTIBLE AGGREGATE AND THEIR USE IN CONCRETE OR BITUMINOUS PAVEMENTS

TO: H. L. Michael, Director  
Joint Highway Research Project

December 5, 1984

File: 5-9-13

FROM: C. F. Scholer, Research Engineer  
Joint Highway Research Project

Project: C-36-42N

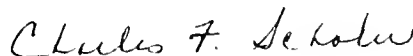
Attached is the Final Report on the approved JHRP research study titled, "Identification of Frost Susceptible Aggregate and Their Use in Concrete or Bituminous Pavements". The research was performed and the report authored by Mr. Marco A. Salcedo, Graduate Instructor in Research, under the direction of Professor Charles F. Scholer.

The report documents that the objectives of the research were achieved. Although it has been well known for many years that frost susceptible aggregates are a primary cause of damage to pavements where freezing and thawing occur, no totally successful method of detecting potentially deleterious aggregates has been available. Evidence exists that the pore structure of course aggregates is important in the resistance of aggregates to freeze-thaw action.

This report develops a discriminating function which differentiates between aggregates of varying frost resistance. The function is based on the details of the pore structure of course aggregates in concrete pavements.

The report is provided for the use of the IDOH and all others with interest in this pavement problem.

Sincerely,



Charles F. Scholer  
Research Engineer

CFS/tb

cc: A. G. Altschaeffl  
J. M. Bell  
W. F. Chen  
W. L. Dolch  
R. L. Eskew  
J. D. Fricker  
W. H. Goetz

G. K. Hallock  
J. F. McLaughlin  
R. D. Miles  
P. L. Owens  
B. K. Partridge  
G. T. Satterly  
C. F. Scholer

R. M. Shanteau  
K. C. Sinha  
J. R. Skinner  
C. A. Venable  
L. E. Wood  
S. R. Yoder

Digitized by the Internet Archive  
in 2011 with funding from  
LYRASIS members and Sloan Foundation; Indiana Department of Transportation

Final Report

IDENTIFICATION OF FROST SUSCEPTIBLE  
AGGREGATE AND THEIR USE IN  
CONCRETE OR BITUMINOUS PAVEMENTS

by

Marco Antonio Salcedo

Graduate Instructor in Research

Joint Highway Research Project

File No.: 5-9-13

Project No.: C-36-42N

Prepared as part of an Investigation

Conducted by the

Joint Highway Research Project  
Engineering Experiment Station  
Purdue University

in cooperation with the

Indiana Department of Highways

Purdue University

West Lafayette, Indiana

December 5, 1984





## ACKNOWLEDGMENTS

I would like to express my appreciation to my major professor, Dr. Charles F. Scholer, for his friendly support and encouragement during the course of this work. I am also very grateful to Dr. William L. Dolch for his active participation in all the stages of the present investigation; his careful review of the thesis and his constructive criticisms are deeply appreciated.

I am also grateful to Dr. V. L. Anderson for his suggestions with respect to the statistical analysis of the data, and to Dr. M. E. Harr for his comments and for reviewing the thesis.

Special thanks are extended to Dr. D. N. Winslow and to Dr. A. Shakoor for providing original data obtained in previous investigations.

I am also indebted to Mr. John Pirolo, Mr. Fred Glossic, Mr. Mark Yost, Mr. Joe Walters, and Mr. W. Cook for their participation in making several glass and plastic pieces, and for their valuable help with the instrumentation and testing of several specimens included in this study. My



gratitude also goes to Mrs. Agnes Meyers for typing the first draft, and to Mrs. Marian Sipes and Mrs. Dawn Leverknight for typing the final manuscript. Mr. Rodolfo Gonzembach and Miss Virginia May made all the drafting work; thanks are also extended to them.

This research was sponsored by the Indiana Department of Highways; this support and the help provided by the staff of the Division of Materials and Tests are gratefully acknowledged.

Finally, I would like to thank my wife, Maria; the successful completion of this work would not have been possible without her love and encouragement.



## TABLE OF CONTENTS

	Page
LIST OF TABLES . . . . .	vii
LIST OF FIGURES. . . . .	ix
ABSTRACT . . . . .	xii
CHAPTER I - INTRODUCTION . . . . .	1
CHAPTER II - CORRELATION BETWEEN FREEZING AND THAWING DURABILITY AND PORE STRUCTURE . . . . .	6
II.1 Introduction. . . . .	6
II.1.1 Statement of the Problem. . . . .	6
II.1.2 Statement of Objectives . . . . .	8
II.2 Literature Review . . . . .	8
II.3 Correlation Between Frost Durability and Pore Size Distribution. . . . .	18
II.3.1 Introduction. . . . .	18
II.3.2 Approach Used in this Study . . . . .	21
II.3.3 Comparative Analysis of Frost Resistant and Non-Resistant Argillaceous Aggregates . . . . .	23
II.3.4 Discriminant Analysis . . . . .	30
II.3.5 Permissible Amount of Deleterious Aggregates. . . . .	52
II.4 Summary of Chapter II . . . . .	69
CHAPTER III - SURFACE DETERIORATION. . . . .	71
III.1 Introduction. . . . .	71
III.1.1 Statement of the Problem. . . . .	71
III.1.2 Significance of the Problem . . . . .	72
III.1.3 Statement of Objectives . . . . .	73
III.2 Literature Review . . . . .	74
III.3 Experimental Work . . . . .	78
III.3.1 Determination of Osmotic Effect . . . . .	78
III.3.2 Significance of Osmotic Effect. . . . .	88
III.4 Summary of Chapter III. . . . .	98



## TABLE OF CONTENTS (Continued)

	Page
CHAPTER IV - FREEZING-POINT DEPRESSION OF WATER AND ITS EFFECT ON FROST ACTION IN ROCKS. . . . .	100
IV.1 Introduction . . . . .	100
IV.1.1 Statement of the Problem . . . . .	100
IV.1.2 Significance of the Problem. . . . .	101
IV.1.3 Statement of Objectives. . . . .	103
IV.2 Literature Review. . . . .	104
IV.3 Experimental Work. . . . .	108
IV.3.1 Conceptual Approach. . . . .	109
IV.3.2 Experimental Determinations. . . . .	111
IV.4 Considerations About Frost Action in Connection with Rate of Ice Formation and Pore Structure . . . . .	129
CHAPTER V - LABORATORY FROST SUSCEPTIBILITY OF BITUMINOUS SPECIMENS. . . . .	141
V.1 Introduction . . . . .	141
V.1.1 Statement of the Problem . . . . .	141
V.1.2 Statement of Objectives. . . . .	142
V.2 Experimental Work. . . . .	143
V.2.1 Statistical Design and Analysis of the Experiment. . . . .	144
V.2.2 Materials and Test Specimens . . . . .	147
V.2.3 Conditioning and Testing of Specimens. . . . .	148
V.2.4 Experimental Results . . . . .	148
V.3 Analysis and Interpretation of Results . . . . .	151
V.4 Recommendations for Further Studies Under Field Exposure . . . . .	156
CHAPTER VI - SUMMARY AND CONCLUSIONS. . . . .	157
VI.1 Summary. . . . .	157
VI.2 Conclusions. . . . .	163
REFERENCES. . . . .	166
APPENDICES . . . . .	172
Appendix A. . . . .	172
Appendix B. . . . .	174
VITA . . . . .	176





## LIST OF TABLES

Table		Page
II.1	Laboratory Results Reported in Reference (24) . . . . .	25
II.2	Unsound Aggregates on the Basis of Field Performance, Reference (24) . . . . .	25
II.3	Coarse Aggregate Fractions in a Concrete Mix . . . . .	37
II.4	Selected Group of Pavements from References (22) and (25). . . . .	42
II.5	Arbitrary Pore Size Ranges and Corresponding Limits. . . . .	43
II.6	Discriminant Scores of Aggregate Samples Studied by Shakoor (24) . . . . .	49
II.7	Discriminant Scores of Aggregate Samples Studied by Kaneuji (25) . . . . .	52
II.8	Data Reported in Reference (13) . . . . .	53
II.9	Permissible Percentages of Deleterious Aggregates. . . . .	55
II.10	Pavements in GROUP I. . . . .	62
II.11	Pavements in GROUP II . . . . .	62
III.1	Percentage of Pore Sizes Smaller than 0.06 $\mu\text{m}$ . . . . .	87
III.2	Percentage of Pore Sizes Smaller than 0.06 $\mu\text{m}$ . Shakoor's Data (24) . . . . .	88
III.3	Data Obtained from the Freezing of Rock Specimens Saturated with Water and 5% NaCl Salt Solution Respectively . . . . .	95



## LIST OF TABLES (Continued)

Table		Page
IV.1	Experimental Readings During Freezing of Rock Specimen. . . . .	119
IV.2	Empirical Models of the Freezing Process in a Porous Matrix. . . . .	120
IV.3	Potential Failure as it Depends on Pore Size Distribution (PSD). . . . .	137
IV.4	Volume of Pores in Ranges I, II, and III of Samples Taken from Reference (25). .	140
V.1	ANOVA Using Equation (22) . . . . .	146
V.2	Stability Values (Lbs.) . . . . .	149
V.3	Pulse Velocity Determinations (% Change). .	150
V.4	ANOVA for Data Shown in Table V.2 . . . . .	150
V.5	ANOVA for Data Shown in Table V.3 . . . . .	151



## LIST OF FIGURES

Figure		Page
II.1	Limiting Pore Sizes $d_u$ and $d_L$ . . . . .	12
II.2	Magnitude of $d_u$ and $d_L$ . . . . .	15
II.3	Pore Size Distribution of Samples L1, L3, L4, L5, K11 and K12. . . . .	26
II.4	Pore Size Distribution of Samples T1, T5, K19, and K20 . . . . .	27
II.5	Pore Size Distribution of Samples I265-C3 and I265-C5. . . . .	28
II.6	Pore Size Distribution of Samples US24-SR115-C2 and US24-STN4-C8 . . . . .	29
II.7	Determination of Pore Volume Increments from the Cumulative Pore Size Distribution . . . . .	35
II.8	Determination of Equivalent Pore Size Distribution . . . . .	38
II.9	Grouping of Pavements According to their Discriminant Scores. . . . .	45
II.10	Freeze-Thaw Resistance Versus (%) of Varying Quality Aggregates . . . . .	54
II.11	Deleterious Aggregate in the Center of Test Specimen . . . . .	57
II.12	Conventional Subdivision of the Discriminant Score Axis. . . . .	60
II.13	Acceptance and Rejection Regions in Q-P Plane. . . . .	65
II.14	Quarry Composed by n Ledges. . . . .	66



## LIST OF FIGURES (Continued)

Figure		Page
II.15	Location of Gropus I and II of Pavements in Q-P Plane . . . . .	68
III.1	Apparatus Used for the Determination of the Osmotic Phenomenon . . . . .	81
III.2	Test Specimens Bonded to Acrylic Tubes . . .	82
III.3	Test in Progress . . . . .	83
III.4	Volume of Solvent Permeating Toward Concentrated Solution, Against Time. . . . .	85
III.5	Volume Increase Observed in Rock Specimens Saturated with Water and Salt Solution Respectively . . . . .	91
III.6	Strain Readings During the Two Stages of the Experiment. . . . .	92
III.7	Strain Readings During Second Stage. . . . .	93
III.8	Temperature Readings During Second Stage . .	94
IV.1	Pore Size Distribution and Corresponding Volume Changes as Water Freezes . . . . .	110
IV.2	Dilatometer. . . . .	112
IV.3	Dummy Specimen for Temperature Measurements.	114
IV.4	Test Specimen in Dilatometer Filled with Mercury . . . . .	116
IV.5	Pipette Readings Against Mean Temperature. .	117
IV.6	Freezing Point of Water as a Function of Pore Diameter . . . . .	123
IV.7	Arbitrary Pore Size Distribution . . . . .	125
IV.8	Rock Test Specimen . . . . .	133
IV.9	Rock Samples with Equal Porosity and Different Pore Size Distribution . . . . .	138





## LIST OF FIGURES (Continued)

Figure		Page
V.1	Marshall Tests Results . . . . .	153
V.2	Pulse Velocity Results. First Experiment . . . . .	154
VI.1	Decision Making Process. . . . .	164
Appendix A		
Figure		
A-1	Pore Size Distribution of samples P, G, and CC-1 . . . . .	173



## ABSTRACT

Salcedo, Marco Antonio, Ph.D., Purdue University, December 1984. Identification of Frost Susceptible Aggregates and Their Use in Concrete or Bituminous Pavements. Major Professor: Charles F. Scholer.

Coarse aggregates have been recognized as potential sources of deterioration of concrete exposed to freezing and thawing action. Whenever coarse aggregates are involved, deterioration of pavement structures can take place as pitting, pop-outs, and varying extents of D-cracking.

Recently, serious damage of bituminous pavements was observed where the coarse aggregate fraction played an important role. In some concrete and bituminous pavements, a typical pattern of surface damage was also found associated to the application of deicers.

In order to prevent damage to concrete and bituminous pavements by frost susceptible aggregates, they must be identified by reliable testing procedures. Sometimes the identification of potentially deleterious aggregates is based on their physical properties alone, and some other times the identification is based on their performance under freezing and thawing surrounded by mortar. Neither method



has been entirely successful; however, from extensive experimental studies, the most significant factors involved in frost action have been identified. In this respect, strong evidence has been reported regarding the importance of the pore structure of coarse aggregates in their potential resistance to freeze-thaw action.

The present study was designed to investigate the significance of the details of the pore structure on the frost resistance of concrete aggregates. Likewise, the surface failure taking place in concrete and bituminous pavements exposed to deicers was closely analyzed. Two approaches were used to accomplish the objectives of this investigation: Statistical Analysis of observational data, and the Experimental Method. In addition, a simplified theoretical analysis of the freezing process was offered.

Based on field data, a discriminating function was obtained to differentiate between aggregates of varying frost resistance. This function was derived by taking into consideration the details of the pore structure of coarse aggregates in concrete pavements.



## CHAPTER I

### INTRODUCTION

The durability of concrete and bituminous pavements exposed to alternate freezing and thawing can be seriously affected by unsound coarse aggregates. In the case of portland cement concrete pavements the problem is known as D-cracking, and the negative effects of deleterious aggregates occur even if the cement paste is protected by an adequate air entrained system. Because most of the research related to this problem has been done in the area of Concrete Technology, it is imperative to study the problem in that context first; then, after the basic differences between portland cement concrete and bituminous concrete are identified, corresponding inferences can be drawn regarding the effects of unsound coarse aggregates in bituminous concrete.

The potential durability problem produced by frost susceptible aggregates in concrete has been recognized for a long time. From a survey of the research that has been conducted in connection with this problem, two major areas can be identified: first, investigations on the mechanisms of frost action, and second, identification of coarse

aggregates prone to D-cracking. These two areas are closely related to each other.

A chronological separation of reported research about frost action may be established as 1945, before and after the postulation of the hydraulic pressure hypothesis by T. C. Powers. It is important to mention that before and after the postulation of Powers' hypothesis, the same approach has been frequently used to understand the mechanism of frost action, i.e. the experimental method. In this respect, Powers (47) asserted:

"After the development of working hypothesis, there followed a long systematic research which made possible firm conclusions about the nature of frost action in concrete based on experimental observations rather than theory".

In order to minimize the negative effects of frost susceptible aggregates in concrete, a substantial amount of experimental research has been conducted to identify "good" and "poor" aggregates. Most of the physical properties of coarse aggregates have been studied for that purpose, but still no reliable procedures have been reported. Respect of this situation, Dolch (5) stated:

"The result of this less-than-satisfactory situation has been that freezing tests of concrete containing the aggregate in question have been considered superior to tests on the aggregate alone".



In addition, with regard to testing procedures to identify varying quality aggregates, the same author pointed out:

"...a test that could be performed on the aggregate alone is still desirable. It has long been considered that the details of the pore structure of the aggregate should be the most important factor in whether it will be durable or non-durable to frost in concrete".

As a result of experimental studies dealing with cement paste, rock samples, and concrete, the following main factors influencing the mechanism of frost action have been identified:

1. Pore Structure.
2. Rate of Cooling.
3. Geometry of test specimens.
4. Seasonal wetting and drying.

These variables combine to yield varying degrees of deterioration, ranging from no damage to complete disintegration after a few freezing and thawing cycles. The quantitative characterization of expected environmental conditions, and its proper inclusion in either experimental, theoretical, or semi-empirical analyses, has been a major practical problem. Therefore, if such variable is excluded, it should be recognized that the results of any effort to identify good and poor aggregates must be taken as estimates

of potential performance.

The negative effects of coarse aggregates on the durability of concrete and bituminous pavements, has been recently observed in several Indiana pavements, where argillaceous aggregates were used. Two distinctive features were observed in those cases: first, damage appeared as intense surface deterioration of concrete pavements and almost structural failure of bituminous pavements, second, damage occurred in one to two years after the completion of the pavements. In addition, there were indications that the problem was aggravated by the application of deicing salts.

The occurrence of the problem in such a short period; the fact that those aggregates were accepted from an approved aggregate source, and the fact that they may occur in different proportions in production samples, made necessary to perform further studies regarding their response to freezing action.

In this investigation, the response to frost action of the argillaceous aggregates under consideration was closely examined, as well as the frost resistance of concrete and bituminous mixes made of different percentages of unsound aggregates. For that purpose, the entire study was decomposed in various subproblems which were studied separately as follows. The problems of identifying coarse aggregates of varying frost resistance, and the estimation of permissi-

ble amounts of deleterious aggregates that can be safely used, were stated and analyzed in Chapter II. The particular problem of surface deterioration and its possible causes were discussed in Chapter III. The frost resistance of bituminous specimens made of different proportions of unsound aggregates was experimentally studied in Chapter V, and some recommendations were advanced for future studies regarding field exposure. In Chapter IV, the relationship between freezing point of water and capillary pore size was experimentally studied, and its implications with respect to freezing action in rocks were analyzed. The subject of the fourth chapter is a necessary step in any approach intended to develop a theoretical model of the freezing action in rocks. Finally, Chapter VI contains the summary and the major conclusions of this investigation.

CHAPTER II  
CORRELATION BETWEEN FREEZING AND THAWING  
DURABILITY AND PORE STRUCTURE

II.1 Introduction

II.1.1 Statement of the Problem

Coarse aggregates have long been recognized as a potential source of deterioration for concrete exposed to freezing and thawing. In order to minimize damage of concrete due to frost susceptible aggregates, extensive research has been conducted in the past to identify those aggregates potentially deleterious by studying their chemical and physical properties. Properties such as: Mineralogical Composition, Absorption, Specific Gravity, Degree of Saturation, etc., were determined to differentiate between frost resistant and non-resistant aggregates. Unconfined freezing and thawing tests were conducted using different building materials, as well as confined tests of concrete aggregates. As a result of such studies, identifying testing procedures and corresponding limiting values were recommended, but soon serious contradictions between predicted performance and field performance were found. Despite this problem,

important factors affecting the freezing and thawing resistance of concrete aggregates were determined through laboratory experimentation and by inspection of concrete under field exposure.

Pore structure has been identified as the most influential physical property in the durability of building materials. The significance of pore characteristics on frost durability was indicated by Rhodes and Mielenz in 1945 (1): "They significantly affect the strength of any material, and also determine absorption and permeability. As a result, they control durability under freezing and thawing conditions..." After an extensive review of related literature, Lewis, Dolch, and Woods, in 1953, concluded (2):

"It would be difficult to prove that any other physical property is of greater importance than the porosity characteristics (amount, size, and continuity of the pores) in either natural or artificial aggregates."

The influence of pore structure on freezing and thawing durability was studied and discussed by Dolch in 1956 and 1959 (3, 4), he stated that: "This influence is primarily due to the effect on the absorption and retention of water by the aggregate". He also emphasized the opposition of small capillary pores to the internal movement of water.

### II.1.2 Statement of Objectives

This study has been designed to investigate the influence of coarse aggregates on the durability of concrete exposed to freezing and thawing. The objectives of this study are:

1. To examine the pore structure of coarse aggregates in order to determine distinctive characteristics between frost resistant and non resistant aggregates.
2. To investigate the possible correlation between frost durability of concrete and the pore structure of its coarse aggregate fraction.
3. To analyze the effect on freeze-thaw durability of concrete of the proportion of the total coarse aggregate that is not frost resistant.

### II.2 Literature Review

In order to develop a systematic study of the pore structure of coarse aggregates and its possible relationship with freezing and thawing durability of concrete, it is necessary to define what pore structure is. The porous matrix of building materials is composed by various amounts of pores of different shape, size and continuity. Its complex internal relationship makes difficult its mathematical modeling and simplifying assumptions have to be made. By definition, the pore structure of a porous solid is

determined by the shape of the pores, which is commonly assumed to be round, and its pore size distribution (5).

The pore size distribution refers to the volume of pores of different sizes composing the porous matrix. The pore size distribution can be measured by several methods; two methods frequently used are the process of capillary condensation combined with the Kelvin equation, and the method of mercury porosimetry. This latter method has been extensively used for studying the pore structure of cement paste, mortar, concrete aggregates, ceramic materials, etc.

The possible relationship between pore structure and frost durability is suggested by the freezing mechanisms in a saturated porous matrix. The mechanism of frost action is complex, and it has been the subject of research for a long time. In 1945, Powers (6) postulated the Hydraulic Pressure Hypothesis to describe the frost damage mechanism in hardened cement paste. Later, Powers and Helmuth (7) extended the original hypothesis to take into account other phenomena produced by freezing of water in cement paste.

For the purpose of this investigation dealing with the frost resistance of coarse aggregates, it is assumed that the main source of damage is due to hydraulic pressure generated during the freezing process. In this respect, Powers (8) asserted:

"...it seems fairly certain that forces produced by freezing in rock are predominantly hydraulic."

According to the previous hypothesis, the magnitude of the hydraulic pressure generated within the porous matrix depends, among other factors, on its permeability. The larger the permeability, the smaller the internal hydraulic pressure for a given flow rate of fluid, and vice versa. Likewise, the smaller the internal hydraulic pressure, the smaller the structural damage to the porous matrix. This qualitative analysis implies that it might be possible to estimate the potential frost resistance of concrete aggregates by determining their permeability characteristics ( $K_o$ ). However, the difficulties involved in the determination of permeability demonstrate the need for less complicated testing procedures.

Given that there is a relationship between permeability and pore structure, other physical properties related to the pore structure may also be related to frost durability. Several physical properties such as absorption, porosity, saturation degree, surface area, permeability, absorptivity, etc. have been studied in order to establish correlations with frost durability. In reference (4) it was concluded that the rate of increase of the degree of saturation and the ratio of absorptivity to permeability are two significant indices of frost susceptibility for concrete aggregates. Other attempts to correlate frost durability with



one single property, i.e. absorption, total porosity, surface area, etc. have been only partially successful and are not reliable. It is important to recognize that those correlations have been established between frost durability and one or more parameters dependent on the pore structure; they are only indirect correlations between frost durability and pore structure.

In the present research, it is intended to correlate frost durability characteristics of coarse aggregates with a direct measurement of their pore structure as it is obtained by mercury porosimetry.

Before any correlation analysis is attempted, it is important to state the following basis. Several authors have advanced the hypothesis that it is the relative pore size distribution that primarily controls frost resistance, and that the total porosity is of secondary importance. This hypothesis can be stated from qualitative considerations as follows. In Figure 11.1, the pore structure of a solid is represented by its pore size distribution. Because of the dependence between freezing point of water and capillary pore size, it is expected that under normal field temperatures, water in fine capillaries will not freeze. Therefore, no contribution to frost damage is expected from water in capillary pores beyond a lower limiting diameter  $d_L$ . Water in large pores freezes at temperatures slightly below  $0^{\circ}$  C, and internal hydraulic pressures are

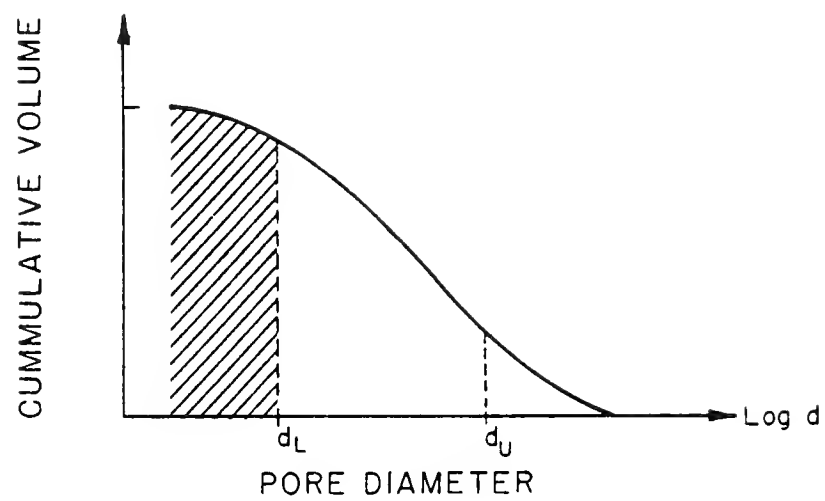


Figure II.1 Limiting Pore Sizes  $d_U$  and  $d_L$

simultaneously developed. Given that the magnitude of this pressure inversely depends on pore size, it is naturally deduced that an upper limiting diameter  $d_u$  should exist such that no disruptive pressures could be generated in the volume of pores beyond this diameter.

The existence of  $d_L$  is supported by experimental results obtained from the freezing of cement pastes (9). It was found that at temperatures as low as  $-70^{\circ}\text{C}$  not all the evaporable water could be frozen. The same phenomenon was reported by le Sage de Fontenay and Sellevold (10) for temperatures as low as  $-90^{\circ}\text{C}$ .

Although the existence of  $d_L$  has been recognized by many authors, its magnitude has only been discussed by few. Kaneuji et al obtained  $d_L = 45 \overset{\circ}{\text{A}}$  under the criterium of maximizing the correlation coefficient  $R$  of an empirical function (11). Litvan proposed  $d_L = 80 \overset{\circ}{\text{A}}$  but no discussion was given in support of this value (12).

The upper limit  $d_u$  has also been recognized by many authors, and specific values have been determined by different procedures using several building materials. Sweet (13) studied various concrete aggregates and he found that the fractional volume of pores smaller than  $5\mu$  correlated well with the freeze-thaw durability of concrete specimens made of those aggregates. Blanks (14) proposed  $4\mu$  as the

critical pore diameter. Walker and Hsieh (15) conducted an experiment similar to that reported by Sweet, and they concluded that: "The best separation between high and low-durability aggregates was with  $8\mu$  porosity values." Polach (16), from the study of heavy clay materials, stated: "The tests have revealed a negative impact of a large volume of pores in the size of  $r < 0.5\mu$  on frost resistance of the heavy clay materials". Lange and Modry (17) reported that concrete specimens made of limestone aggregates were severely damaged after a few freezing and thawing cycles. These aggregates had "...a distinct maximum of the existing pores in the range of the radii from  $100 \overset{\circ}{\text{A}}$  to  $500 \overset{\circ}{\text{A}}$ ". They also reported that concrete specimens made of aggregates with maximum volume of pores in the range  $1000 \overset{\circ}{\text{A}}$  to  $5000 \overset{\circ}{\text{A}}$  or  $10,000 \overset{\circ}{\text{A}}$ , resisted a substantially higher number of freeze-thaw cycles. Litvan (12) concluded that: "From the point of view of frost action, pores with radii in the range of  $40 \overset{\circ}{\text{A}}$  to  $300 \overset{\circ}{\text{A}}$  can cause frost damage most often". Koh and Kamada (18) investigated the frost resistance of several blended cement pastes, and they found that a large volume of pores in the range  $0.15\mu$  to  $1.5\mu$  was associated with low frost durability.

The set of some  $d_L$  and  $d_u$  values previously discussed is summarized in Figure II.2. It is observed in that figure

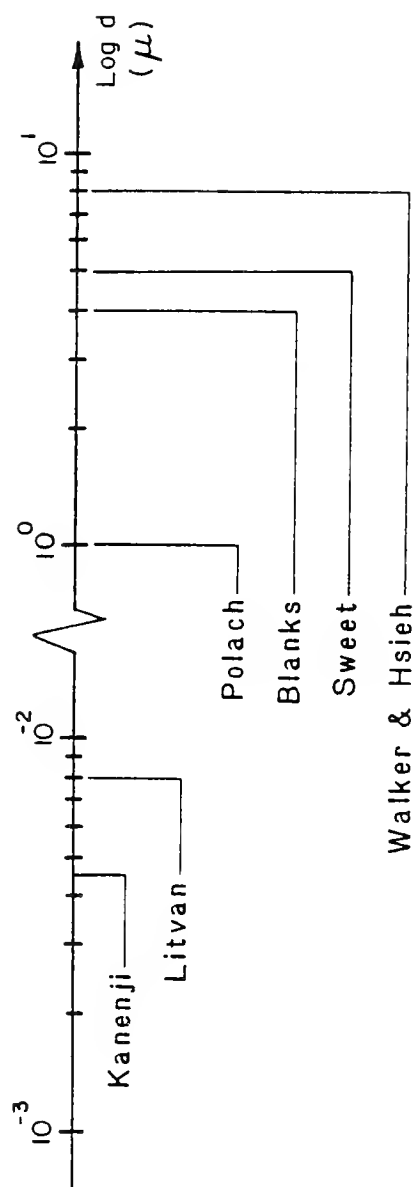


Figure II.2 Magnitude of  $d_u$  and  $d_L$

that most of the  $d_u$  values are within the range from  $1\mu$  to  $8\mu$ ; such difference should be expected because of the different severity of the applied freezing and thawing cycles. In addition to that, the different materials and the conditioning previous to testing should also be taken as influencing factors.

A retrospective analysis of the determination of  $d_L$  and  $d_u$  seems to be appropriated at this point. The existence of the Lower Limiting value  $d_L$  has been unquestioned; although its magnitude has been a matter of either speculation or quantified by assuming a correspondence with  $R^2$ , which does not provide causal evidence in support of the value thus obtained. Most of the efforts have been directed toward the determination of  $d_u$ , and it appears that its value is in the range  $1\mu$  to  $8\mu$ . Most of the times these values have been obtained by direct inspection of the PSD of concrete aggregates of varying frost resistance.

The existence of fixed limiting pore sizes,  $d_L$  and  $d_u$ , is unlikely. Their respective values depend on the expected minimum temperature in the case of  $d_L$ , and it depends on the rate of ice formation in the case of  $d_u$ . An estimate of the latter pore diameter is computed in Chapter IV.

Even the most reasonable estimate of those limiting pore sizes can not guarantee that, after the corresponding volumes of pores are deducted from the total volume, a

better correlation between frost susceptibility and the remaining pore volume will be found. This is understood if the basic failure mechanisms postulated by Verbeck and Langren (19) are taken into consideration. According to Verbeck and Langren, coarse aggregates can contribute to frost damage of concrete in two ways. First, by expulsion of water into the surrounding paste, where high disruptive pressures are generated. Second, by the internal failure of the aggregate which occurs whenever fine pores and a critical aggregate size are combined. Both types of failures have been reported by Scholer (20), Sweet (13), and Brown (21).

In the first type of failure, most of the capillary pores are large enough to preclude the generation of significant internal hydraulic pressure in the coarse aggregate. Presumably, in this case, most of the pores are larger than  $d_u$ , and the pore size distribution per se becomes irrelevant as an explanatory variable with respect to frost damage. Therefore, frost damage of concrete is more likely to be related to the total porosity. On the contrary, in the second type of failure, there is a significant volume of fine pores smaller than  $d_u$ , and internal failure of the aggregate occurs. It is in this situation where frost damage is expected to be correlated to the pore size distribution of the aggregate.

## II.3 Correlation Between Frost Durability and Pore Size Distribution

### II.3.1 Introduction

Finding an empirical correlation between freezing and thawing durability of concrete and the pore structure of its coarse aggregate fraction poses various problems. The first problem is to properly characterize measurable attributes of frost durability and pore structure. For the purpose of this discussion, frost durability and pore structure are taken as dependent and independent variables respectively.

Relative frost durability of concrete has been measured by attributes such as visual appearance, weight loss, critical expansion, ASTM Standard C 666, etc. How well each of these attributes represents freezing and thawing durability has been a matter of discussion. With respect to the independent variable, several characteristic parameters of the pore structure have been already mentioned. Whatever the measurable attributes of frost durability and pore structure might be, they must be closely related by the physical mechanism responsible of damage; otherwise, any correlation attempt may be unsuccessful.

After the dependent and independent variables are properly selected, the second major problem is to decide the conditioning of the materials prior to testing, and to



define the characteristics of the freezing and thawing cycle. These are necessary steps in any laboratory study. Powers discussed this problem, and corresponding recommendations were presented in reference (8). In addition, Polach reported that after applying severe freeze-thaw cycles it was not possible to identify any correlation between frost resistance and pore size distribution. After the severity of the cycles was reduced, such correlation was apparent (16).

Finally, the details of two basic failure mechanisms by which coarse aggregates contribute to frost damage of concrete were discussed by Verbeck and Langren; that discussion points to the following question: Is it possible to define a single empirical model to estimate frost damage of concrete due to both failure mechanisms? Apparently not, because the role of the pore size distribution (PSD) of the aggregate is completely different in both cases. There is no obvious link between PSD and frost damage whenever failure by expulsion of water into paste takes place, except for the likely association with the total porosity. The inclusion of coarse aggregates prone to both types of failure in the same regression analysis, may lead to a distorted relation between frost durability and PSD, to unrepresentative correlation coefficients, and to the occurrence of outliers or points which deviate significantly from the general trend of the data, if there exists any.

Two empirical correlations between freezing and thawing durability of concrete and the pore structure of its coarse aggregate fraction, have been reported in the literature.

Kaneuji, Winslow, and Dolch (11) determined an empirical correlation between frost durability of concrete, as it is measured by ASTM C666-A, and the pore structure of the coarse aggregates used in the concrete mix. The pore structure was characterized by two parameters: PV, mercury intruded volume of pores larger than  $45 \text{ \AA}$  and MD the corresponding median diameter of such pore volume. Thirteen vacuum saturated aggregate samples, whose absorption ranged from 0.89% to 14.55%, were used in that study; the following expression was obtained by multiple regression analysis

$$\text{EDF} = \frac{0.579}{\text{PV}} + 6.12 \text{ MD} + 3.04 \quad (1)$$

where EDF is an index related to the durability factor defined in ASTM C666-A.

Expression 1, combined with an extensive study of concrete pavements with varying extent of D-cracking, was further used to determine border values for accepting or rejecting coarse aggregates prone to D-cracking. A complete discussion of those findings is presented in reference (22).

A second empirical correlation equation was reported by Maage (23). This equation correlates a measure of frost

resistance of concrete and two parameters of the pore structure of concrete aggregates; it has the following form:

$$F = \frac{6.2}{PV} + 2.1 PO.03 \quad (2)$$

where:

F = frost resistance number

PV = intruded pore volume

PO.03 = pores with diameter bigger than  $0.03\mu$  in percent of PV

As can be observed in the previous approaches, an empirical expression correlating a measure of durability and pore structure is initially found; then, assuming a correspondence between laboratory results and field performance, pavements with varying extent of D-cracking are analyzed and rated according to the empirical equation. Using those results and the physical appearance of the pavements, corresponding border values are defined.

### II.3.2 Approach Used in This Study

Most of the research related to frost durability of concrete, as it is affected by coarse aggregates and their pore structure, has been oriented to identify aggregates potentially deleterious. This is just one aspect of the more general problem. Other aspects of the same problem, perhaps more important, are:

1. It is not enough to identify a good or poor aggregate on the basis of one or more of its physical properties. In order to make better decisions for an efficient use of varying quality aggregates, it is necessary to conventionally define how good a good aggregate is, as well as how poor a poor aggregate is, according to the extent of damage that it produces under field exposure. This may be accomplished by the development of a rating scale to assess the potential performance of concrete aggregates.
2. Once the quality level of an aggregate or production sample has been rated, the next question is what permissible amount can be used when it is combined with aggregates of different quality?

Two basic approaches have been applied to accomplish the objectives stated in this chapter. The first approach, presented in II.3.3, consisted of a comparative analysis of the pore size distribution of frost resistant and non-resistant argillaceous aggregates. Emphasis was placed on the detection of any distinctive characteristic of argillaceous aggregates; for that purpose data reported in reference (24) were used. In the second approach, presented in II.3.4, Discriminant Analysis was used to identify coarse aggregates giving rise to good and poor field performance of concrete pavements. The same methodology was used in II.3.5

to study the effect of different proportions of varying quality aggregates on frost durability. The second approach was based on the set of data reported in reference (22) and some data reported in (25).

### II.3.3 Comparative Analysis of Frost Resistant and Non-resistant Argillaceous Aggregates

Extensive laboratory testing has been conducted on varying quality aggregates used in the State of Indiana. In particular, argillaceous aggregates were recently studied by Shakoor (25), including the following laboratory determinations:

- Absorption
- Specific Gravity
- Insoluble Residue
- Unconfined Freeze-Thaw Losses
- Iowa pore Index
- Pore Size Distribution (PSD)
- etc.

Likewise, laboratory results of core samples taken from pavements deteriorated under field exposure were also reported in the same reference.

An inspection of these data can provide convenient response and explanatory variables, and further analysis of the same raw data may be performed using statistical techniques or other convenient methods. In this section, a comparative analysis of the pore structure of frost resistant

and non-resistant argillaceous aggregates was performed. As a result of this exploratory analysis, an apparent contrast between durable and non-durable aggregates was found. This contrast can be observed when the pore size distribution data are plotted as

$$\Delta V_j \text{ vs. } \log d_j$$

where:

$\Delta V_j$  = volume increment intruded by the j-th pressure increment

$d_j$  = lower limit of pore sizes intruded by the j-th pressure increment

Selected samples were taken from reference (24) for this comparative analysis, based on their unconfined freeze-thaw losses after 50 cycles (AASHTO T103, procedure A). Some of them were relatively durable and others were non-durable. These samples are listed in Table II.1; while in Table II.2, core samples taken from severely surface deteriorated pavements are shown.

Table II.1 Laboratory Results Reported in Reference (24)

Sample	Unconfined Freeze-Thaw Losses (%)	Absorption (%) (ASTM C 127)
L1	2.5	0.86
L3	7.9	2.50
L4	2.6	1.96
L5	1.6	1.83
K11	1.5	2.70
K12	3.6	2.45
T1	46.3	5.13
T5	61.0	4.86
K19	83.6	5.50
K20	80.7	6.75

Table II.2 Unsound Aggregates on the Basis of Field Performance, Reference (24)

Sample	Absorption (%)
I 265-C3	4.5
I 265-C5	4.5
US 24-SR115-C2	4.1
US 24-STN4-C8	4.3

A summary of  $\Delta V_j$  vs.  $\log d_j$  plots including all the samples listed in tables II.1 and II.2, is given in Figures II.3, 4, 5, and 6.

Figure II.3 shows the pore size distribution of six aggregate samples whose percent losses range from 1.5% to 3.6%, and only one sample with 7.9% losses. These are freeze-thaw resistant aggregates. Figure II.4 shows the pore size distribution of four aggregate samples whose percent losses range from 46.3% to 83.6%. These are frost non-resistant aggregates.

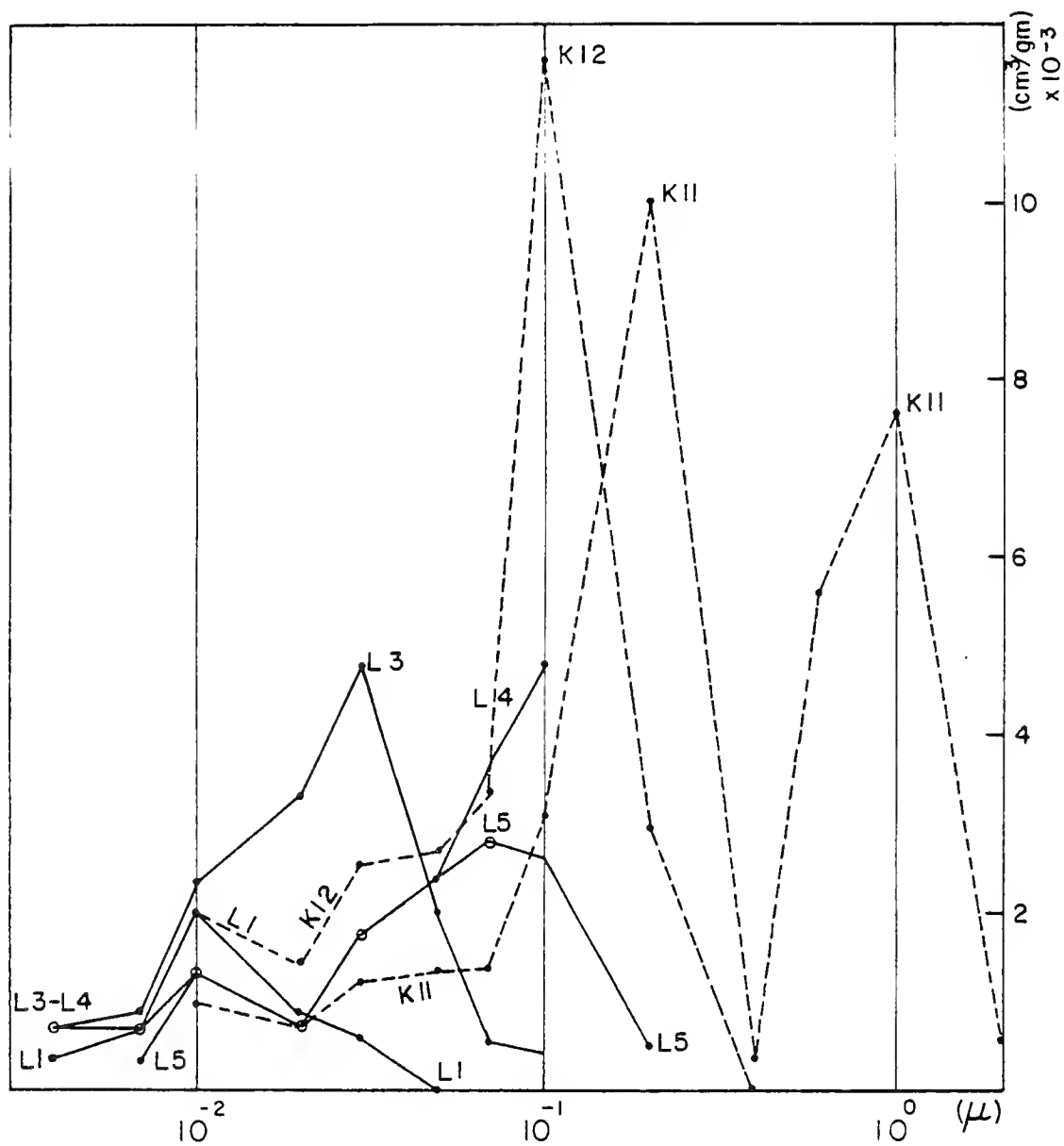


Figure II.3 Pore Size Distribution of Samples L1, L3, L4, L5, K11 and K12



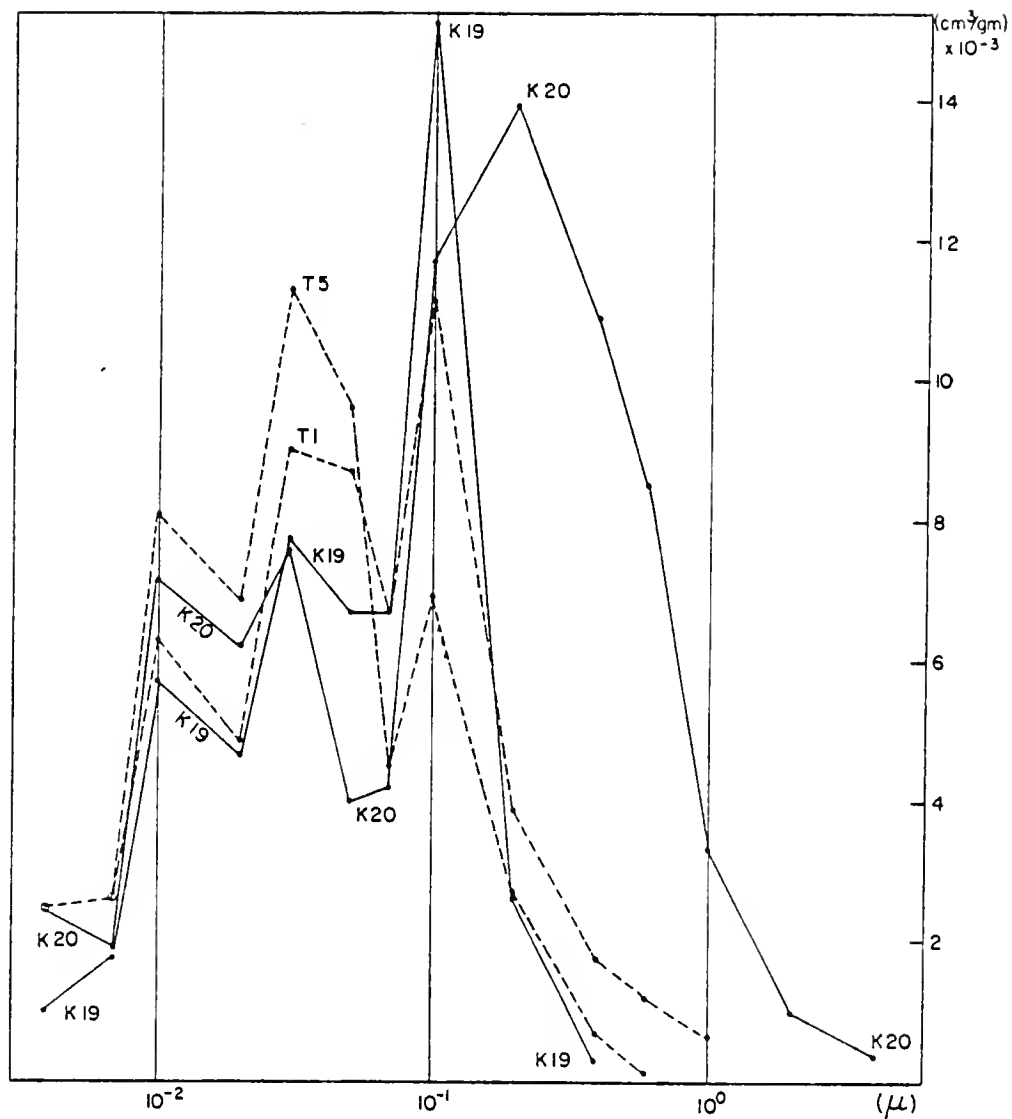


Figure II.4 Pore Size Distribution of Samples T1, T5, K19, and K20

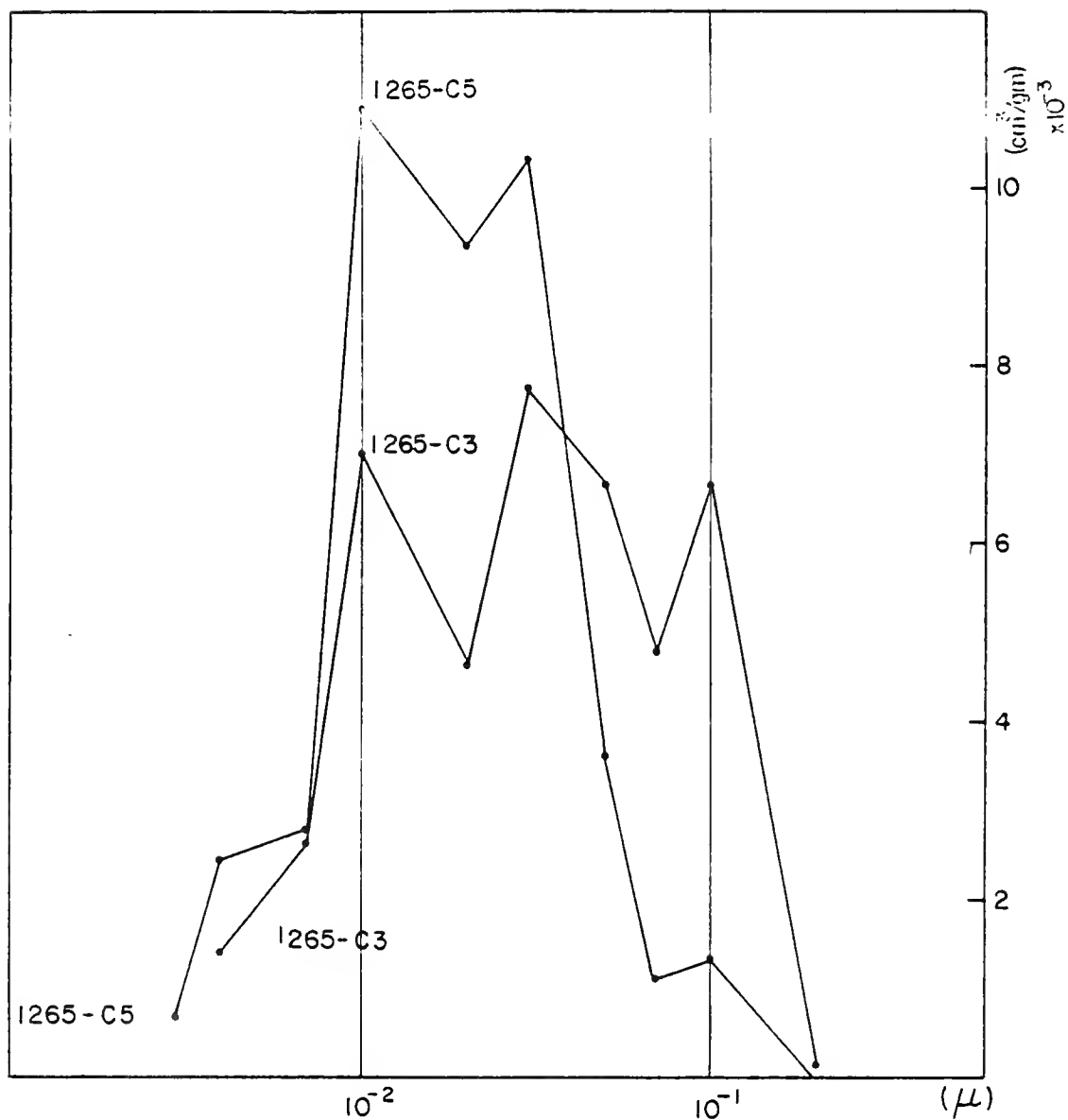


Figure II.5 Pore Size Distribution of Samples I265-C3 and I265-C5

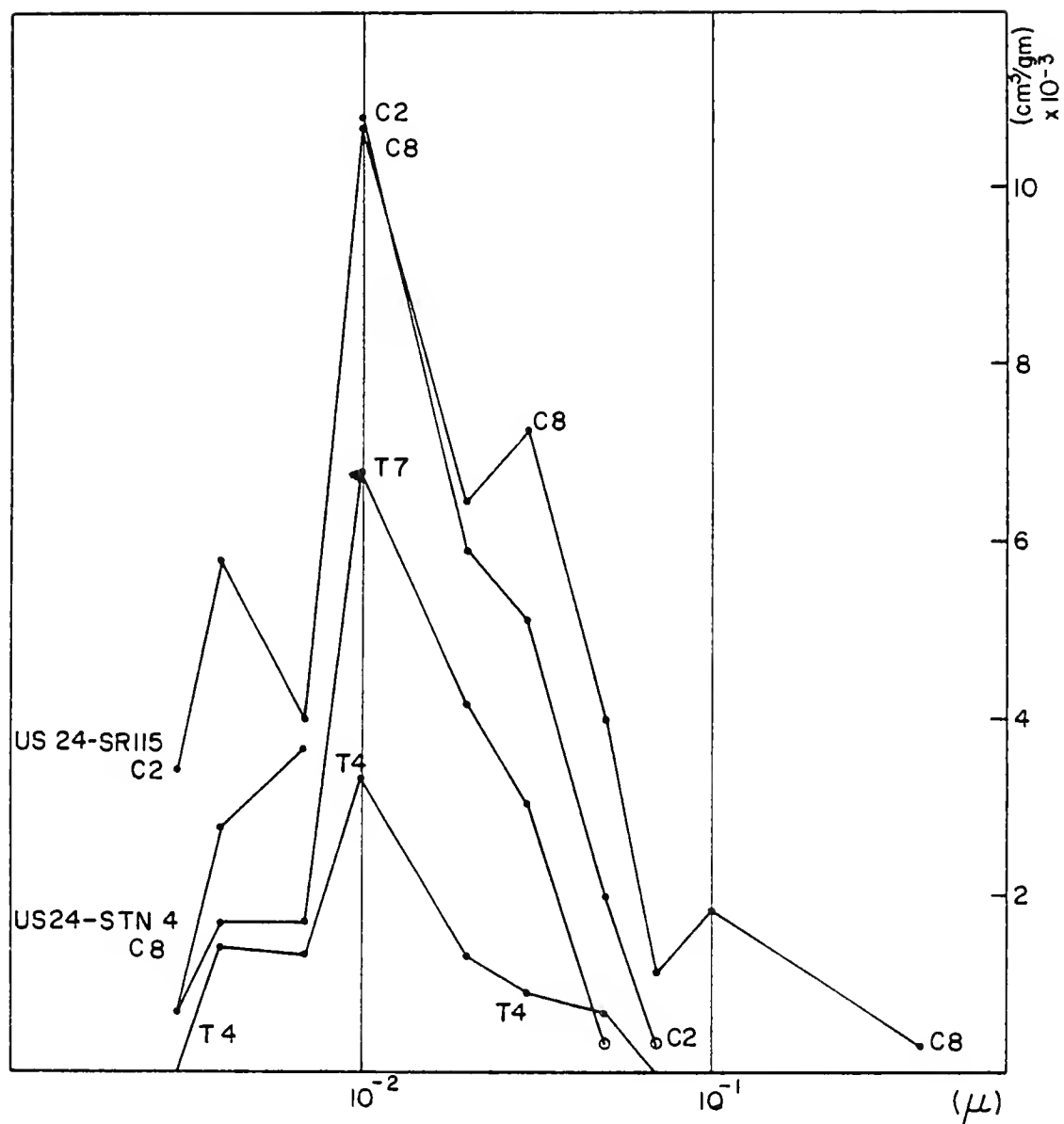


Figure II.6 Pore Size Distribution of Samples US24-SR115-C2 and US24-STN4-C8

The comparison between resistant and non-resistant aggregates indicates some distinctive characteristics of their pore structure. All the samples of argillaceous aggregates under consideration have most of their pore sizes smaller than about  $0.6\mu$ , except for K20. Both sets of samples, resistant and non-resistant, have characteristic peaks in the ranges from  $10^0$  to  $10^{-1}\mu$ , and from  $10^{-1}$  to  $10^{-2}\mu$ . However, a distinctive characteristic seems to be associated to the non-resistant samples: they have a considerable volume of pores smaller than about  $10^{-1}\mu$ ; particularly in the range between  $10^{-1}$  and  $10^{-2}\mu$ . It is also interesting to observe that there is a direct proportionality between (%) losses and the volume of pores previously indicated. This proportionality can be observed by inspecting samples K11, K12, and L3, which have approximately the same total porosity, but their respective proportions of pores in the range  $10^{-1}$  to  $10^{-2}\mu$  increases as it does their corresponding percent losses.

In Figures II.5 and II.6, the pore size distribution of aggregates that were severely deteriorated in situ are shown. The same pattern of intruded volumes observed for non-resistant samples is also noticed in these samples.

#### II.3.4 Discriminant Analysis

For the purpose of reducing several sources of uncertainty from the analysis, it is convenient to establish a direct correlation between the freezing and thawing

durability of concrete pavements and the pore structure of their composing coarse aggregates. Such correlation between in situ frost durability of pavements and pore structure of aggregates, implies that both variables must be systematically characterized and measured. In this discussion frost durability and pore structure are defined as the dependent and independent variables respectively.

Pore structure can be characterized by the pore size distribution (PSD) of the porous matrix, and measured by mercury porosimetry. Frost durability is an attribute not so easily quantified. A direct manifestation of frost durability of concrete pavements is their appearance and structural integrity over time, their extent of distress or deterioration. The extent of distress of pavements can be quantified in various ways; the specific method to be used always depends on the intended application of the results. Frequently, conventional measurements are defined and corresponding scales are constructed, which combined yield "durability indices".

The definition of a measure of frost durability, and its corresponding scale, is a very important step because it controls the type of manipulations and mathematical analysis that can be performed with the data set thus obtained. Campbell (26), Stevens (27), and Nunnally (28), give a classification of different measurement scales, their properties, and the kind of valid mathematical analyses that can

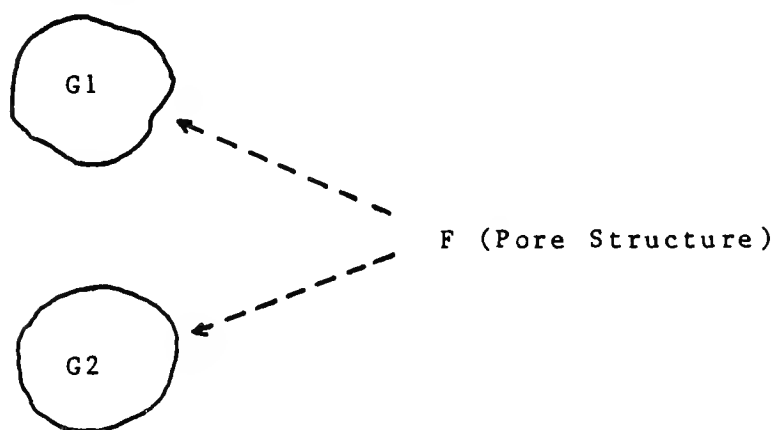
be applied to the data obtained in each case. Specific examples of scales to measure extent of deterioration are:

1. Portland Cement Association (PCA) scale for rating the extent of deterioration of concrete pavements due to D-cracking (29).
2. NYDOT scale for measurement of structural condition of concrete and bituminous pavements, regardless of the source of distress (30).

Both scales are visual and basically ordinal in the sense described by Stevens (27) and Nunnally (28).

The form of the correlation between two or more variables is commonly determined by multiple regression analysis; however, in order to apply this method, the dependent and independent variables must be quantitatively measured using an interval or a ratio scale. Most often this is not the case when the extent of D-cracking is evaluated in situ, and other methods like Discriminant Analysis may be used. Discriminant Analysis is a statistical technique useful for grouping several items on the basis of one or more quantitative characteristics or attributes (31, 32). It is also used for classifying single items into one of two or more pre-defined groups, based on quantitative attributes of those items. In the present study the later approach has been applied as follows. Assume two groups of pavements with different extent of D-cracking, G1 and G2, where the

pore structure of the composing coarse aggregates is known in each case. The first step of the analysis is to obtain a function  $F$  which can discriminate between  $G_1$  and  $G_2$  by using some measurement of the pore structure.



or

$$D = F [(PSD)] \quad (3)$$

where:

$G_1, G_2$  = groups of pavements classified according to extent of D-cracking

$F$  = Discriminant function

$(PSD)$  = an alternative characterization of the pore structure

$D$  = discriminant score which differentiates between both groups

The discriminant function  $F$  can be estimated from a selected sample of pavements whose perspective field performance and the  $PSD$  of its coarse aggregate fraction are known. After the discriminant function is obtained, the

potential extent of distress due to an aggregate with unknown field record can be estimated using expression (3).

In previous sections of this chapter, the correlation between frost durability and one or more parameters derived from the pore structure was discussed; in this section the correlation between frost durability and direct measures of the pore struction is intended. Such direct correlation simply implies that the cummulative PSD be broken in its component volumes associated with different ranges of intruded pore sizes. The basic idea behind this approach is not to lose the information that may be contained in the component volumes of the pore structure, by using summary measures of its PSD. Stating the analysis in this manner, the relative significance of the intruded volume in different ranges of pore sizes can be empirically investigated. The component volumes can be determined during the process of intrusion, or they can be obtained from the cummulative PSD as is shown in Figure II.7. After those computations, the PSD of any i-th piece of aggregate can be represented as follows:

$$(PSD)_i : \{\Delta V_{1i}\}, \{\Delta V_{2i}\}, \dots, \{\Delta V_{ni}\} = \{\Delta V_{ji}\}$$

where:

$$\{\Delta V_{ji}\} = \text{intruded volume in the } j\text{-th size range of the PSD of the } i\text{-th piece of aggregate}$$



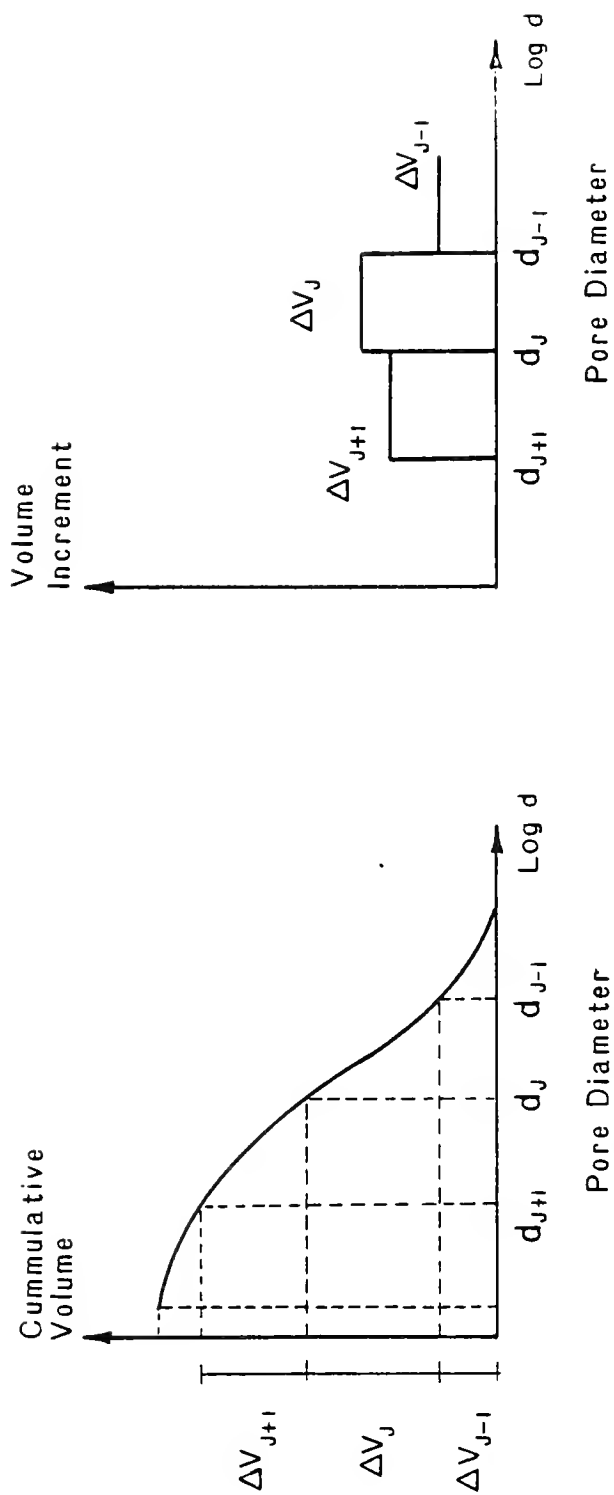


Figure II.7 Determination of Pore Volume Increments from the Cumulative Pore Size Distribution

Frequently concrete is made of coarse aggregates of different freeze-thaw resistance, included in different percentages in the mix. In order to take into consideration such differences of resistance and the respective proportions of those aggregates in the whole mix, it is necessary to postulate and define the equivalent pore size distribution concept. Assuming the existence of some critical pore sizes, the more each aggregate contributes to the total volume of those pores the less durable the concrete is expected to be, and vice versa. This assumption also implies that the relative influence of each aggregate is directly proportional to the percentage in which it occurs in the concrete mix.

The equivalent pore size distribution concept is a method of characterizing the entire coarse aggregate fraction of concrete. It is useful for analyzing and estimating the potential freezing and thawing durability of concrete by the use of equation (3). The definition of this concept is as follows. Assume a concrete mix whose coarse aggregate fraction can be classified according to  $m$  groups; the proportion of aggregates in the  $m$ -th group is  $P_m(\%)$  and the pore size distribution representative of that group is  $(PSD)_m$ , as is indicated in Table II.3

Table II.3 Coarse Aggregate Fractions in a Concrete Mix

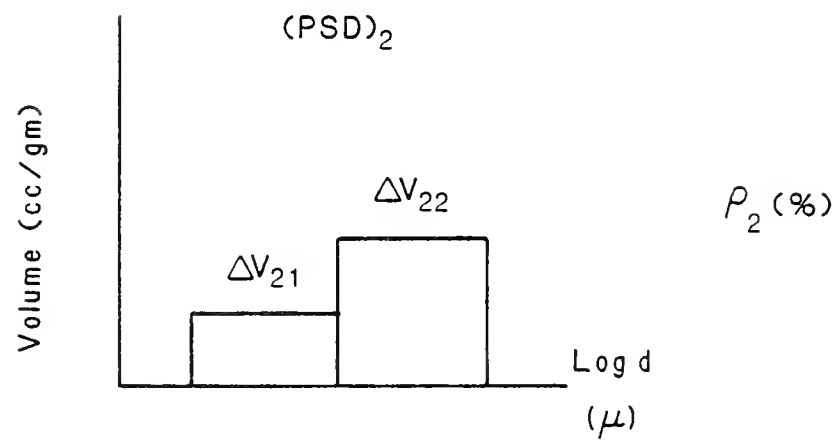
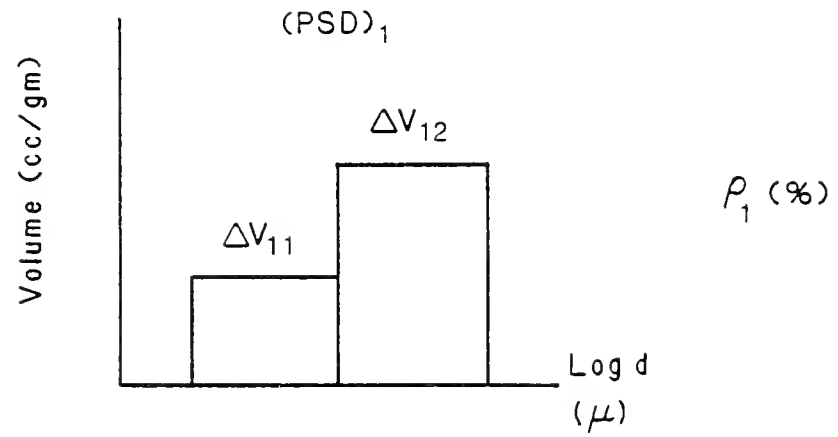
Megascopic Classification	(%)	PSD
1	$\rho_1$	$(PSD)_1$
2	$\rho_2$	$(PSD)_2$
.	.	.
.	.	.
.	.	.
m	$\rho_m$	$(PSD)_m$
$\Sigma 100\%$		

After each pore size distribution is re-expressed as described in Figure II.7, they can be arranged for further computations. In this section the computation of the equivalent PSD is illustrated with a simplified case of two different aggregates and their respective percentages  $\rho_1$  and  $\rho_2$ , and pore size distributions  $(PSD)_1$  and  $(PSD)_2$ . In addition, the number of pore size ranges in each PSD is reduced to two. After the basic expressions are derived, they are extended to the general case by induction.

From Figure II.8, adding the respective volume increments in each pore range of the two pore size distributions, and taking into consideration the aggregate percentages, yields

$$\Delta V_1 = \Delta V_{11} \rho_1 + \Delta V_{12} \rho_2 \quad (4)$$

$$\Delta V_2 = \Delta V_{21} \rho_1 + \Delta V_{22} \rho_2$$



$$\Delta V_1 = \Delta V_{11} P_1 + \Delta V_{21} P_2$$

$$\Delta V_2 = \Delta V_{12} P_1 + \Delta V_{22} P_2$$

Figure II.8 Determination of Equivalent Pore Size Distribution

where  $\Delta V_1$  and  $\Delta V_2$  are the equivalent volume of pores in the first and second pore size ranges respectively.

In general, assuming  $m$  aggregate fractions and the PSD's subdivided in  $n$  pore ranges, the equivalent pore volume in the  $j$ -th pore size range is given by

$$\Delta V_j = \sum_{L=1}^m \Delta V_{jL} \cdot \rho_L \quad (5)$$

$$j = 1, 2, \dots, n$$

From the later equation, the complete equivalent PSD could be represented by

$$\begin{aligned} \Delta V_1 &= \Delta V_{11} \rho_1 + \Delta V_{12} \rho_2 + \dots + \Delta V_{1m} \rho_m \\ \Delta V_2 &= \Delta V_{21} \rho_1 + \Delta V_{22} \rho_2 + \dots + \Delta V_{2m} \rho_m \\ &\vdots \quad \quad \quad \vdots \end{aligned}$$

$$\Delta V_n = \Delta V_{n1} \rho_1 + \Delta V_{n2} \rho_2 + \dots + \Delta V_{nm} \rho_m$$

which can be re-expressed as

$$\begin{array}{cccccc} \Delta V_1 & & \Delta V_{11} & \Delta V_{12} & \dots & \Delta V_{1m} & \rho_1 \\ \Delta V_2 & & \Delta V_{21} & \Delta V_{22} & \dots & \Delta V_{2m} & \rho_2 \\ \cdot & = & \cdot & \cdot & & \cdot & \cdot \\ \cdot & & \cdot & \cdot & & \cdot & \cdot \\ \cdot & & \cdot & \cdot & & \cdot & \cdot \\ \Delta V_n & & \Delta V_{n1} & \Delta V_{n2} & \dots & \Delta V_{nm} & \rho_m \end{array} \quad (6)$$

or simply

$$\{\Delta V_{jx1}\} = [\Delta V_{ji}] \{\rho_{ix1}\}$$

Notice that each column of the matrix  $[\Delta V_{ji}]$  represents the PSD associated with each aggregate classification included in the concrete mix; likewise, the proportion of each of those aggregate classifications is represented by  $\{\rho_{jx1}\}$ .

Assessing the potential field performance of concrete based on its equivalent PSD, as it is given by equation (6), requires that the discriminant function be estimated first. In this study the discriminant function was estimated using a set of data reported in reference (22); these data were gathered from a field survey of Indiana pavements which were in a wide state of distress. Such state of distress was rated according to an existing scale developed by the Portland Cement Association (PCA). Basically, this PCA scale is as follows

<u>PCA Scale</u>					
0	1	2	3	4	5
-----> Increasing deterioration					

It is an ordinal scale where 0 corresponds to excellent field performance, no D-cracking is observed at the time of inspection, and 5 corresponds to severe deterioration : extensive D-cracking and structural damage of the pavement. There is no quantitative relationship between any pair of scores in the scale. Lindgren gives detailed information related to each surveyed pavement in reference (22); some of the data included:

1. PCA rating

2. Age of the pavement

3. At least one core was taken for laboratory study

From each core, after it was longitudinally sliced and polished, the following information was obtained in the laboratory.

1. Macroscopical classification of each piece of coarse aggregate.

2. Proportion of each aggregate fraction classified according to 1.

3. Representative PSD of each fraction occurring in the core.

The total number of pavements surveyed by Lindgren was reduced to two selected groups; each group consisted of excellent and poorly performed pavements respectively. It was decided to use these two extremes of the scale because it is not known if intermediate groups might be in a transitory state toward further deterioration. The screening of data to get each group was based mostly on the PCA rating combined with the age of each pavement. The total number of pavements thus obtained was increased with the addition of other results reported by Kaneuji in reference (25). The set of data used for the estimation of the Discriminant Function is shown in Table II.4.

Table II.4 Selected Group of Pavements from  
References (22) and (25)

Group	Sample	PCA rating	Age (Yrs.)
I	A81	0	15
	B01	0	13
	C31	0	16
	C41	0	15
	C61	0	17
	C81	0	16
	C101	0	13
	H51	0.5	14
	J21	0	15
	N31	0	17
	T21	1.0	22
	N41	0	25
	O41	0	12
	P01	0	14
	P11	1.0	22
II	A001	3.5	3
	C01	4.5	20
	C53	4.5	17
	M11	3.5	14
	M31	5.0	26
	M51	3.5	29
	N01	4.0	26
	M21	2.5	20
	T51	2.5	22
	301*		
	Ke-1*		
	L03	3.0	39
	302*		
	695*		

\* Field samples reported by M. Kaneuji (25).

The entire range of pore sizes measurable by mercury porosimetry was subdivided in several pore size ranges, arbitrarily selected. These size ranges were:



Table II.5 Arbitrary Pore Size Ranges and Corresponding Limits

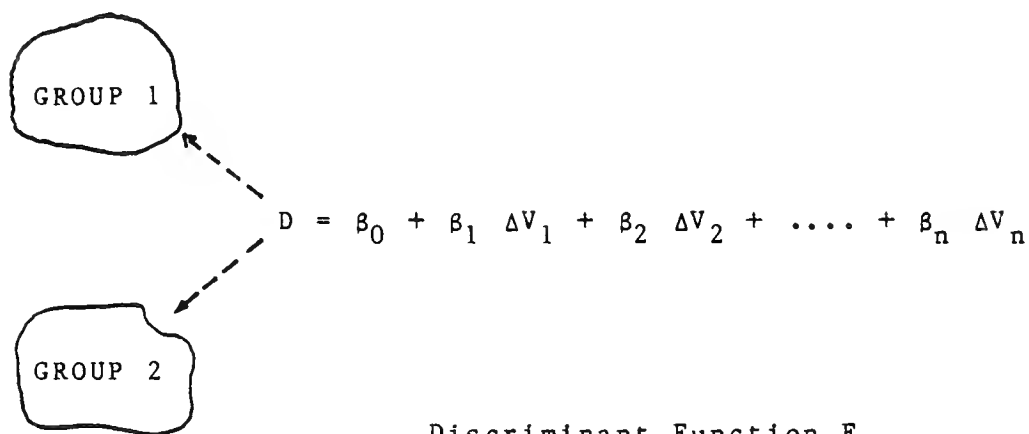
Pore size range No.	Limits ( $\mu$ )	Pore size range No.	Limits ( $\mu$ )	Pore size range No.	Limits ( $\mu$ )
01	$d > 10$	06	$0.4 \leq d < 0.6$	11	$.03 \leq d < .05$
02	$4 \leq d < 10$	07	$0.2 \leq d < 0.4$	12	$.02 \leq d < .03$
03	$2 \leq d < 4$	08	$0.1 \leq d < 0.2$	13	$.01 \leq d < .02$
04	$1 \leq d < 2$	09	$.07 \leq d < 0.1$	14	$.007 \leq d < .01$
05	$0.6 \leq d < 1$	10	$.05 \leq d < .07$	15	$.004 \leq d < .007$

using these pore size ranges and equation (6), the equivalent PSD of each pavement indicated in Table II.4 was computed. Then the best sets of pore size ranges were found with the computer program DISCR of the Library of Programs of the Purdue University Computing Center (PUCC). The best sets of 12, 10, 8, and 6 size ranges were computed in order to check the consistency of the present approach. Only the first set of size 12 is discussed in this section to illustrate the method of analysis.

In this analysis, the dependent variable is pavement performance, which is either excellent or poor, groups I and II respectively. The independent variable is the pore structure characterized by the equivalent PSD of each pavement, and reduced to the best set of 12 pore size ranges. The program DISCR yields the following subset of the best 12 size ranges:

{01, 02, 03, 04, 05, 06, 08, 09, 10, 11, 12, 15}

Discriminant analysis was performed in order to find the discriminant function which classifies each pavement in one of two groups



where:

$D$  = discriminant score

$\beta_j$  =  $j$ -th discriminant coefficient

$\Delta V_j$  = intruded volume in the  $j$ -th pore size range  
(  $\times 10^{-3}$  cc/gm)

The function F was found with the program DISCRIMINANT of the Statistical Package for Social Sciences implemented in the PUCC. As a result of the analysis, each pavement was grouped according to its discriminant score D as it is indicated in Figure II.9 and the discriminant function was

$$\begin{aligned}
 D = & 1.824 + 0.393 \Delta V_1 + 0.220 \Delta V_4 - 1.555 \Delta V_6 - 1.561 \Delta V_8 \\
 & + 5.176 \Delta V_9 - 2.678 \Delta V_{10} - 4.229 \Delta V_{11} \\
 & + 3.080 \Delta V_{12} + 2.276 \Delta V_{15}
 \end{aligned}
 \tag{7}$$



Figure II.9 Grouping of Pavements According to their Discriminant Scores

In Figure II.9 can be noticed that pavements with excellent field performance are grouped with positive discriminant scores, and pavements with poor performance are grouped with negative discriminant scores.

Some observations are pertinent in respect of these results:

1. 100% of the pavements rated as excellent were classified in the right group, Group I; 100% of the pavements rated as poor were classified in the right group, Group II. In Figure II.9 there is no overlap between the group of pavements with excellent and poor field performances. It means that the discriminant score  $D$ , quantified with equation (7), is an alternative manner to differentiate between both extreme performances. The larger the discriminant score ( $D \gg 0$ ), the more likely the pavement belongs to GROUP I; the smaller the discriminant score ( $D \ll 0$ ), the more likely the pavement belongs to GROUP II.
2. From the inspection of the empirical model represented by expression (7), two important characteristics can be detected.
  - a. There is an alternate change of signs, which may reflect the connectivity of the porous matrix, as internal flow occurs.

- b. The relative effect of the intruded volume in each pore size range, may be assessed by the sign and magnitude of its discriminant coefficient. For instance the relative abundance of pores larger than  $1\mu$ , reflected in  $\Delta V_1$  and  $\Delta V_4$  yields a positive discriminant score which corresponds to an excellent field performance.

In addition, the same unit intruded volume in  $\Delta V_6$  and  $\Delta V_8$ , and in  $\Delta V_{10}$  and  $\Delta V_{11}$ , is more detrimental in the later pore size ranges than in the former; this is reflected in the negative signs and the relative magnitude of their discriminant coefficients.

3. The usefulness of the Equivalent Pore Size Distribution, as a working concept for making inferences about actual concrete pavements, seems to be supported by the fact that it was able to discriminate between Groups I and II.
4. Only two groups of pavements with extreme performances, excellent and poor, have been included in this analysis. Before any other intermediate group of pavements is defined and included in a similar analysis, more theoretical work should be done to develop a rating scale and to understand the complex relation between frost durability and pore structure.

5. The same methodology previously described could be applied when the data set is composed by single pieces of aggregates whose field performance and PSD are known. In this case, the equivalent PSD given by equation (6) is reduced to the trivial solution when there is only one aggregate ( $m=1$ ) and  $\rho_1 = 100\%$ .

The applicability of expression (7) to identify coarse aggregates prone to D-cracking, was further analyzed using a selected number of rock samples thoroughly studied by Shakoor (24). Two sets of samples were selected. The first set corresponds to argillaceous aggregates with high percent losses due to unconfined freezing and thawing; because of such high losses, the aggregate samples are expected to be potential contributors to D-cracking.

The second set corresponds to pieces of failed aggregates taken from the top of concrete cores obtained from surface deteriorated pavements. Both sets are indicated in Table II.6.

Table II.6 Discriminant Scores of Aggregate Samples Studied by Shakoor (24)

Aggregate Sample	Losses <sup>*</sup> (%)	Discriminant <sup>**</sup> Score
Laboratory Samples		
T1	46.3	-23.97
T5	61.0	-33.50
K19	83.6	-21.47
K20	80.7	-28.20
Field Samples		
I265-C3		-17.34
I265-C5		-12.64
US 24-SR115-C2		6.04
US 24-STN4-C8		-10.08

\* After 50 unconfined freezing and thawing cycles

\*\* Computed by equation (7)

From the inspection of the data presented in Table II.6, it is found that all the aggregate samples potentially deleterious under freezing and thawing (T1, T5, K19, and K20) show a highly negative discriminant score. Likewise, all the field samples, except one, also show highly negative discriminant scores. Both data sets show a consistently negative discriminant score which, according to the analysis previously presented and from Figure II.9, is characteristic of aggregate samples prone to D-cracking. There is one exception in these results, sample US24-SR115-C2, which may be explained by the fact that all those field samples are involved in a surface type of failure. This type of failure is associated with the presence of deicing salts and at the present time it is not known if D-cracking will also take place in the future. The possible mechanisms of surface

failure are discussed in Chapter III of this study.

At this point, it should be recognized that expression (7) is an empirical model; as such, regardless of how well or how poorly it represents the occurring physical phenomenon, it is not expected to correctly identify the potential performance of aggregates 100% of the time. This is because of the large number of factors involved in D-cracking. However, the predicting power of the model can be improved by continuous maintenance, which means that the data used to derive the model should be periodically increased with additional samples. In addition, the assumptions behind the entire approach should also be verified or modified as the theoretical knowledge of the phenomenon improves.

It was mentioned at the beginning of this chapter that some discrepancies may exist between laboratory and field resistance of concrete to freezing and thawing. In this regard various possible causes were indicated. However, despite these possible differences, the relative performance of concrete aggregates can be estimated by laboratory tests.

Kaneuji (25) conducted several laboratory experiments dealing with the freeze-thaw resistance of concrete. He used various aggregate samples selected ad hoc, and their PSD was measured by mercury porosimetry. The relative frost resistance of concrete made of those aggregates, was deter-



mined by ASTM C666-A method and by a modified critical dilation test. Coarse aggregates performing extremely badly or extremely well in these tests are likely to exhibit the same pattern of performance under field exposure. Assuming that this is reasonably correct, such pattern of performance should also be reflected by the discriminant scores associated to each sample studied by Kaneuji.

Some of the results reported in reference (25) are shown in Table II.7, as well as the corresponding discriminant scores computed with equation (7).

According to the sign and magnitude of their discriminant scores, and from Figure II.9, concretes made of aggregates BR-3, Ke-1, H-1, BR-5, BR-1, and MB are expected to experience severe D-cracking. On the contrary, concretes made of aggregate samples BM-1 and F-2 are expected to show excellent performance. There is no clear cut classification for aggregates CC-1, McC, and K<sub>o</sub> because their discriminant scores are located neither in Group I nor in Group II, but in between. They may be assumed to give rise to intermediate performance. Finally, sample PC-1 was not properly classified according to its discriminant score and its expected performance.

Table II.7. Discriminant Scores of Aggregate  
Samples Studied by Kaneuji (25)

Sample	Absorption (%)	$\epsilon \times 10^{-6}$ *	NDF**	D***
BR-3	14.6	>500	8.9	-43.52
CC-1	11.8	131	36.0	+ 1.05
K <sub>e</sub> -1	10.1	197	19.6	- 3.76
H-1	9.3	500	3.5	-31.48
F-2	9.7	0	46.5	+ 1.98
McC	8.9	250	27.2	+ 0.18
BR-5	7.7	157	15.3	-14.95
BR-1	5.8	300	19.9	-47.53
PC-1	4.7	236	16.7	+13.0
MB	3.4	194	35.6	- 8.94
K <sub>o</sub>	2.5	283	31.8	+ 1.39
BM-1	2.9	0	78.1	+ 8.89

\* Critical dilation

\*\* Normalized durability factor

\*\*\* Discriminant score computed with equation (7)

### II.3.5 Permissible Amount of Deleterious Aggregates

The severity of freezing and thawing damage of concrete attributable to the coarse aggregate fraction, variates from nil, regardless of the number of freeze-thaw cycles, to almost complete desintegration in a few cycles. Both extreme responses are found whenever very good or very poor aggregates are used. Most often, the coarse aggregate fraction is composed by aggregates of varying quality which

produce concrete of intermediate frost resistance. Before this more general case is discussed, the analysis of a particular case is in order.

How does the freezing and thawing damage to concrete vary as the percentage of deleterious aggregates increases?

In 1948, Sweet performed several experiments related to this question (13). Aggregates with known field performance were used in his experiments; the physical properties of some of them are given in Table II.8.

Table II.8 Data Reported in Reference (13)

Aggregate Sample	Field Performance	Vacuum Absorption (%)	Percent Losses
67-2S	Good	0.8	4.7
82-1G	Bad	2.6	27.2
35-2S ch**	Bad	6.2	63.7
9-1S	Bad	8.3	8.5

\* After 50 unconfined freeze-thaw cycles \*\* Chert aggregate

Each bad aggregate source was combined with the good aggregate in different percentages ranging from 0% to 100%. With each of these combinations of aggregates, prismatic concrete specimens were fabricated and subjected to freezing and thawing cycles. The number of cycles to get a 30% loss in dynamic modulus of the testing specimens is shown in Figure II.10, against the corresponding percentages of bad aggregates. From this figure, and the results presented in Table II.8, the following observations can be made:

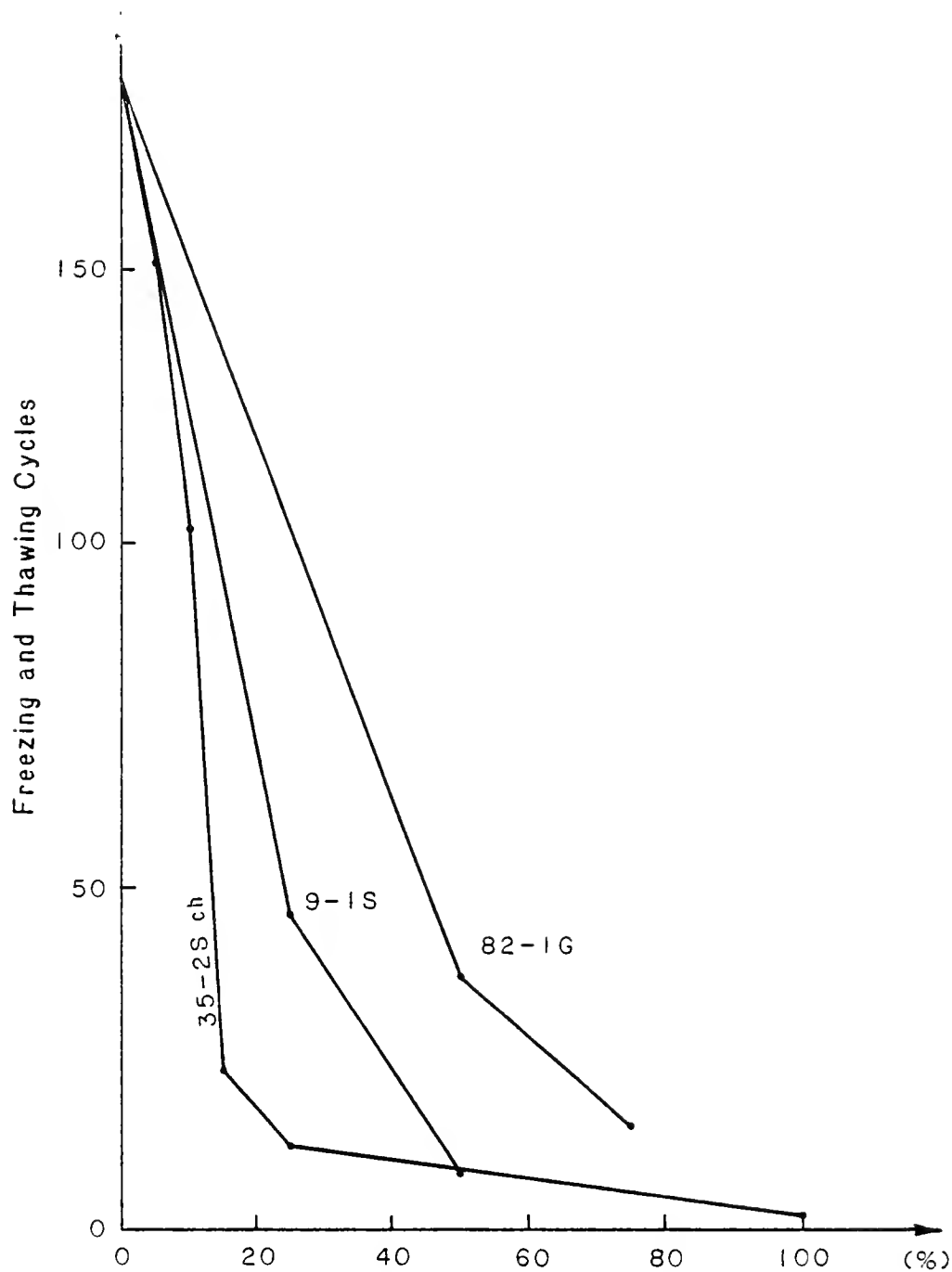


Figure II.10 Freeze-Thaw Resistance Versus (%) of Varying Quality Aggregates

1. Aggregates 82-1G and 35-2S ch are likely to contribute to failure of the prismatic testing specimens by the critical distance mechanism. The later aggregate source seems to be less frost resistant than the former. The third bad aggregate is relatively frost resistant and it seems to contribute to failure by the expulsion of water into the surrounding paste mechanism.
2. From the general trend observed in Figure II.10, it appears that coarse aggregates which fail by the critical distance mechanism are more detrimental to concrete, than those aggregates which produce failure by expulsion into paste.
3. The permissible amount of deleterious aggregates obviously depends on the tolerable level of damage. Assuming two arbitrary levels corresponding to a 30% loss of dynamic modulus at 100 and 50 freeze-thaw cycles, results in the following estimated permissible percentages.

Table II.9 Permissible Percentages of Deleterious Aggregates

Number of Cycles	Aggregate Sample	Percentage (%)
100	35-2S ch	10
	9-1S	15
	82-1G	26
50	35-2S ch	13
	9-1S	25
	82-1G	45

The most important thing to be noticed in Table II.9 is the order of magnitude of the permissible percentages, and how they variate as a function of the more likely failure mechanism. Two data sets are particularly important for comparative purposes. Whenever the failure mechanism involved is critical distance, as in aggregate 35-2S ch, the permissible percentage seems to be very small; it is about 10%. This value is also supported by data reported by Walker et al (33). For aggregate 9-1S, which produces failure by the expulsion mechanism, the permissible percentage is about 15% for 100 cycles and 25% for 50 cycles. This aggregate has a very high absorption, 8.3%. In contrast to 35-2S ch, aggregate 82-1G also is likely to fail by critical distance, but its absorption is only 2.6%. Its permissible amount for 100 cycles is about 26%.

From these data it appears that, except for extremely bad sources, the permissible amount of deleterious aggregates for 100 cycles is about 15% to 26% of all the aggregates in the concrete mix. However, the validity of these limiting values is questioned according to the following discussion.

Permissible percentages obtained from standard freezing and thawing tests, using small beams as testing specimens, may not be entirely valid or extrapolated to actual structural prototypes because of the geometrical considerations involved. Assume a standard prismatic testing specimen as

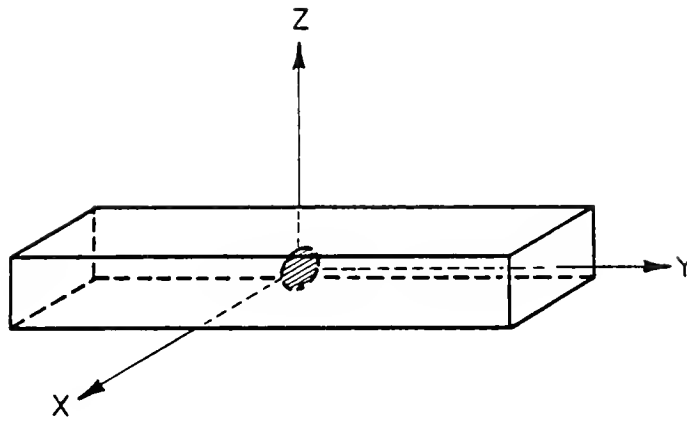


Figure II.11 Deleterious Aggregate in the Center of Test Specimen

it is shown in Figure II.11.

A single piece of aggregate experiencing internal failure by the critical distance mechanism, can give rise to tensile strains along the X, Y, and Z axis shown in Figure II.11. This state of strains and the corresponding tensile stresses, may be so severe that a single piece may produce the structural failure of the specimen as a whole. It is important to recognize that the relative severity of damage produced by such a single aggregate piece in a test specimen will be much more destructive than that produced in a corresponding volume of concrete in a pavement slab. Therefore, the permissible amounts determined from small test specimens should be taken as lower limiting values of the actual percent giving rise to the same level of damage in a pavement slab. How much these values differ from each other is not known; however, any value determined using small beams is on the conservative side.

In section B, a discriminant function was obtained from two groups of pavements with excellent and poor field performance, Groups I and II respectively. The discriminant function was given by expression (7). It was also found that both groups of pavements could be differentiated according to their discriminants scores, as indicated in Figure II.9. From that figure, pavements with excellent field performance have discriminant scores  $D > +1.8$  and pavements with poor field performance have scores  $D < -2.0$ .



For the present purposes, it will be conventionally assumed that  $D > +1.5$  implies excellent performance and  $D < -1.5$  implies poor performance. On the basis of these limiting values, it is possible to define three regions along the discriminant axis. Regions I, II, and III, each region representing poor, intermediate, and excellent performances respectively, Figure II.12.

Any concrete is expected to be composed by aggregate fractions which can be classified within each region in the corresponding proportions Q, I, and P. Figure II.12. These proportions obviously sum up to 100%.

$$Q + I + P = 100\% \quad (8)$$

where:

Q = percent of aggregates whose discriminant score is  
 $D < -1.5$

I = percent of aggregates whose discriminant score is  
 $-1.5 < D < +1.5$

P = percent of aggregates whose discriminant score is  
 $D > +1.5$

For concrete pavements with excellent performance, P is expected to be larger than Q, while it should be the opposite for poorly performing pavements. In order to verify this statement, all the pavements listed in Table II.4 were further analyzed. Expression (7) was used to compute the discriminant score of each aggregate fraction included in a

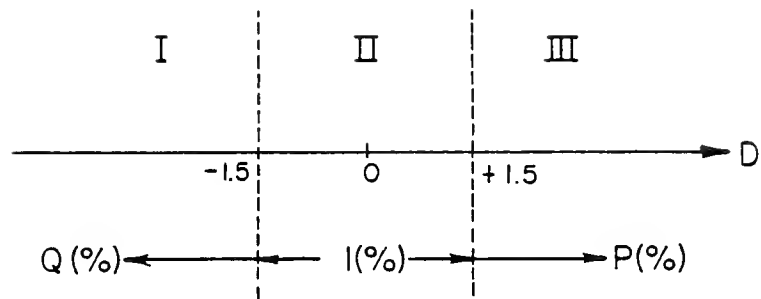


Figure II.12 Conventional Subdivision of the Discriminant Score Axis

pavement, then the percentages Q, I, and P were computed. These operations were repeated for each pavement included in Groups I and II, and the results are shown in Tables II.10 and II.11. The overall mean values of P, I, and Q are also shown in the same tables. It was found that, for Group I the relative proportion P (%) of those aggregates designated as excellent predominated over those designated as poor Q (%) and intermediate I (%). An inverse pattern was observed for Group II.

The main objective of this section is to determine on a quantitative basis, how "poor" and "excellent", and perhaps "intermediate", percentages combine to give rise to excellent and poor performances.

This problem may be restated in the following question: Is it possible to differentiate between Groups I and II, on the basis of the percentages Q, I, and P of each pavement? This is a typical problem for which Discriminant Analysis can be used. The dependent variable is given by Group I and Group II, and the independent or explanatory variables are Q, I, and P. After the analysis was performed using the data listed in Tables II.10 and 11, the following discriminant function was determined.

$$D' = 1.00 - 5.07 Q + 1.68 P \quad (9)$$

where:

$D'$  = discriminant score

P, Q, = they were defined before

Table II.10 Pavements in GROUP I

Core	Q(%)	I(%)	P(%)
A81	10.0	10.0	80.0
B01	0.0	50.0	50.0
C41	20.0	20.0	60.0
C61	16.0	22.0	62.0
C81	17.0	6.0	77.0
C101	34.0	8.0	58.0
H51	0.0	0.0	100.0
J21	0.0	7.0	93.0
N31	0.0	0.0	100.0
T21	29.0	35.0	38.0
N41	30.0	10.0	60.0
O41	13.0	0.0	87.0
P01	0.0	9.0	91.0
P11	23.0	27.5	49.5
	13.7%	14.5%	71.8%

Table II.11 Pavements in GROUP II

Core	Q(%)	I(%)	P(%)
A001	53.0	2.0	45.0
C01	50.0	50.0	0.0
C53	70.5	0.0	29.5
M11	76.0	12.0	12.0
M31	44.0	29.0	27.0
M51	32.0	20.0	48.0
N01	36.0	17.0	47.0
M21	63.0	22.0	14.0
T51	65.0	0.0	35.0
L03	47.0	7.0	46.0
MK301	50.0	50.0	0.0
Ke-1	66.6	0.0	33.3
MK302	100.0	0.0	0.0
MK695	66.6	0.0	33.3
	58.6%	15.0%	26.4%

Other results of this discriminant analysis were:

- a. The intermediate percentage I (%) was not statistically significant
  - b. 96.4% of all the pavements were correctly classified in their right group by expression (9)
  - c.  $D'=0$  was the border value between both extreme performances,
- and

$$\begin{aligned} D' < 0 & \text{ implies poor performance} \\ D' > 0 & \text{ implies excellent performance} \end{aligned} \quad (10)$$

It must be stressed that these findings are applicable to differentiate between two extreme performances; no intermediate performance can be assessed by the present approach.

Using the results of the discriminant analysis indicated before it is possible to perform the following algebraic manipulations. Assuming  $D'=0$ , the border value between extreme performances, and substituting in expression (9) yields

$$5.07 Q - 1.68 P - 1.00 = 0 \quad (11)$$

In addition, from physical considerations it is known that:

$$\begin{aligned} Q & > 0 \\ P & > 0 \end{aligned} \quad (12)$$

and re-expressing equation (8) as an inequality, given that I (%) was not statistically significant, results in

$$Q + P < 100\% \quad (13)$$

Finally, the graphical representation of inequalities (12) and (13) defines a triangular region in a  $Q - P$  plane, as it is indicated in Figure II.13. This region can be further divided in two sub-regions by equation (11), which represents the bi-dimensional boundary between excellent and poor performances of concrete pavements, according to inequalities (10). Equation (11) and the corresponding subregions are also indicated in Figure II.13.

Figure II.13 represents an alternative manner for dealing with the acceptance-rejecting problem whenever coarse aggregates of varying frost resistance are blended. In order to illustrate the potential application of the previous findings, assume a quarry composed by several ledges as shown in Figure II.14. The total thickness of the quarry ( $H_T$ ), and the thickness of each ledge are known ( $h_1, \dots, h_j, \dots, h_n$ ). Therefore, the proportion of aggregates from each ledge in a production sample can be estimated by

$$P_i(\%) = \frac{h_i}{H_T} \times 100 \quad (14)$$

where  $i = 1, 2, \dots, n$

In addition, the discriminant scores of each ledge ( $D_1, \dots, D_j, \dots, D_n$ ) can be computed with equation (7); finally, the percentages  $Q$ ,  $I$ , and  $P$  can be computed as defined for equation (8). With these values and Figure II.13, it is possible to locate any quarry in the  $Q-P$  plane in order to make

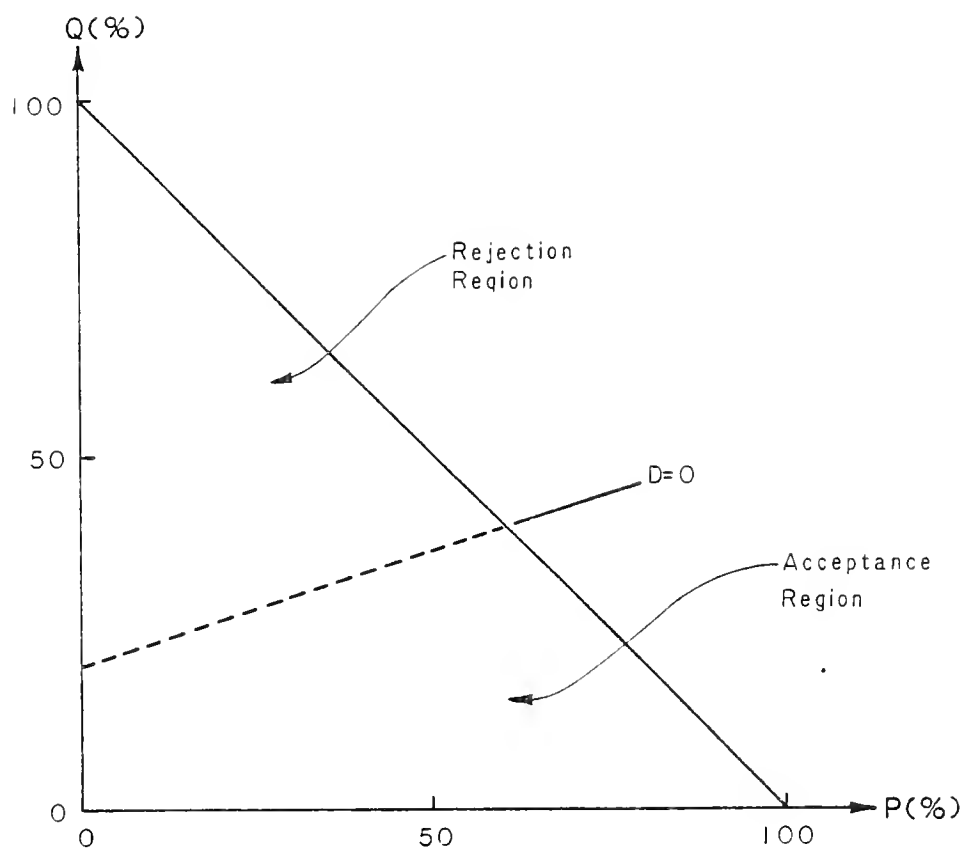


Figure II.13 Acceptance and Rejection Regions in  $Q$ - $P$  Plane

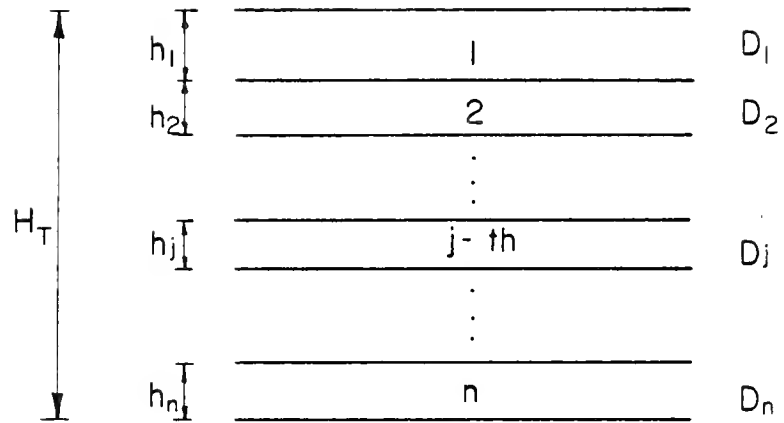


Figure II.14 Quarry Composed by  $n$  Ledges



the decision of accepting or rejecting the production sample according its potential contribution to D-cracking.

It should be recognized that such decision is based on the possible combinations of (Q, P) values which give rise to two extreme responses: excellent and poor field performances. No intermediate performance can be assessed by the present approach, because only two groups of pavements with known extreme performance were used in the analysis.

The present findings suggest the following observations.

1. The arbitrary three-way classification of coarse aggregates in Q, P, and I proportions depending on their discriminant scores, was necessary because of the lack of a proper rating scale at the present time.
2. There is no unique allowable percentage Q of deleterious aggregates. In any particular situation, the permissible amount of deleterious aggregates is variable and it depends on the proportions of intermediate and excellent aggregates in the mix.
3. It was found that further subdivision of regions I, II, and III in Figure II.12, resulted in a discriminant function which correctly classified 100% of the pavements in groups I and II. This discriminant function, similar to equation (9), yielded a three dimensional

acceptance-rejection diagram; however, because of the exploratory nature of the present approach, the more simple case in the Q-P plane was discussed.

4. All the pavements included in Groups I and II, listed in Tables II.10 and II.11, were located in the Q-P plane as it is shown in Figure II.15. The grouping of the pavements in separated clusters is to be noticed; the boarder line between both groups is given by equation (9).

#### II.4 Summary of Chapter II

The significance of the pore structure of coarse aggregates in the freezing and thawing durability of concrete has been analyzed. The measurement of frost durability, the characterization of pore structure, and their possible correlation to identify concrete aggregates that are potentially deleterious have been discussed.

A comparative analysis of argillaceous aggregates of varying frost resistance was performed by the inspection of their  $\Delta V_j$  vs.  $\log d_j$  plots. It was found that the argillaceous aggregates under study have an abundance of pores in the range from  $10^{-1}$  to  $10^{-2} \mu$ , and the unconfined freezing and thawing losses appeared to be directly proportional to such volume of pores.

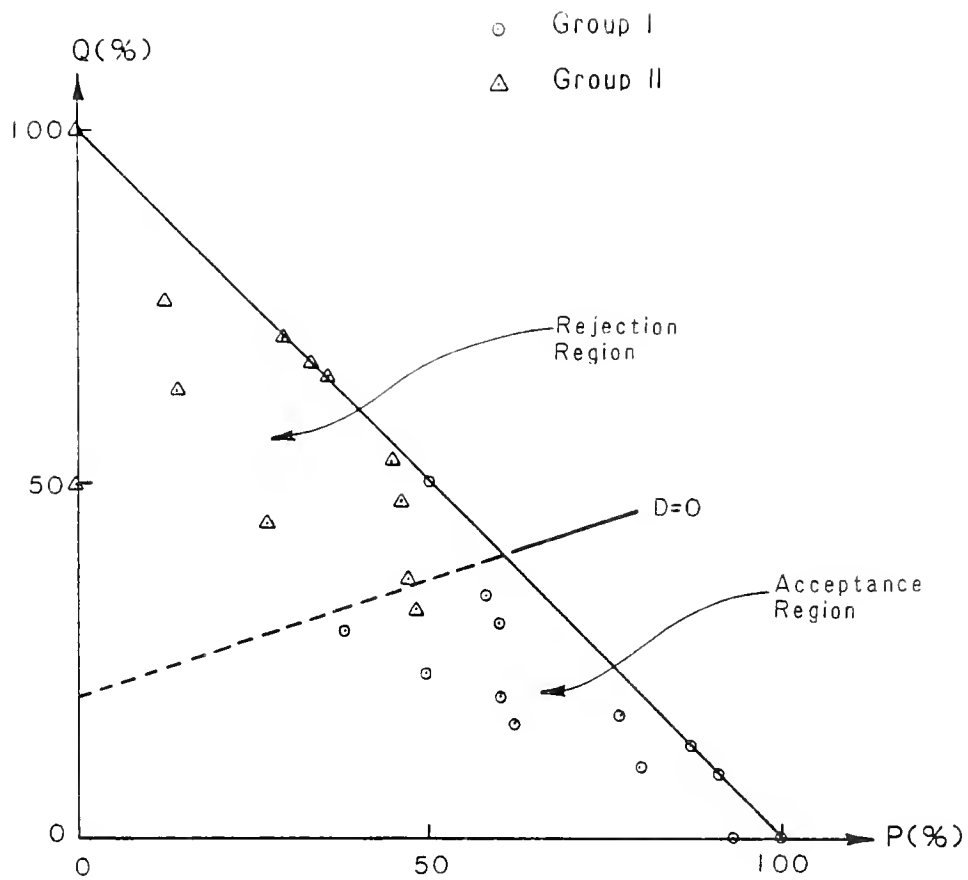


Figure II.15 Location of Groups I and II of Pavements in Q-P Plane

An alternative approach to identify potentially deleterious aggregates has been presented in this chapter. This alternative approach is based on the actual field performance of concrete pavements and direct measurements of the pore structure. Discriminant Analysis was used to correlate freezing and thawing durability and pore size distribution, and a discriminating function was obtained. The predicting power of the discriminant function was verified using laboratory and field results, and reasonable agreement was found between actual and predicted performances. Positive discriminant scores  $D > 1.5$  are associated with excellent field performance, while negative discriminant scores  $D < -1.5$  are associated with poor field performance. Some recommendations for periodical revision of the predicting model have also been presented.

The permissible amount of frost non-resistant aggregates in concrete pavements has also been studied. Border Limiting percentages for the acceptance or rejection of concrete aggregates, have been defined from the analysis of the varying quality fractions occurring in field core samples. The findings of this analysis were summarized in an acceptance - rejection diagram, which is defined by the percentage of aggregates whose discriminant score is  $D < -1.5$  and the percentage of aggregates whose discriminant score is  $D > +1.5$ .

## CHAPTER III

### SURFACE DETERIORATION

#### III.1 Introduction

##### III.1.1 Statement of the Problem

Surface deterioration of concrete pavements exposed to freezing and thawing may take several forms. Pop-outs and scaling are the most frequent. The former is associated with internal failure of coarse aggregates, typically cherts, close to the surface of the pavement, while the latter involves failure of the cement paste.

A problem of severe surface deterioration of some concrete and bituminous pavements in Indiana has been recently observed after the pavements have been in operation for only one to two years. In all the surveyed cases, inspection showed that the failure plane occurred through a coarse aggregate particle, and there was no apparent damage originating in the surrounding cement paste. Construction records indicate that the concrete was air entrained, which suggests that the paste was reasonably well protected

against freezing and thawing action; but by no means is protection provided for the coarse aggregate by air entrainment. The same pattern of surface failure was observed in different locations, but it was particularly accentuated in a cross over open early to traffic and exposed to large amounts of deicers.

In some cases the intense surface damage made necessary an overlay to improve the riding quality of the pavements. In other cases, for bituminous pavements, the structural integrity was seriously affected.

An extensive previous research included collecting field core samples of selected pavements, and sampling of the corresponding quarries that supplied the coarse aggregate. The results of petrographic analyses and the determination of physical properties of those samples are given in reference (24). The findings reported in that reference indicate that the aggregates involved in this type of failure are highly argillaceous; the clay mineral was classified as Illite, and it was uniformly distributed in the aggregate matrix. In addition, one possible failure mechanism for these argillaceous rocks was discussed in the same reference.

### III.1.2 Significance of the Problem

The continuous depletion of aggregate sources with adequate field performance, as well as cost considerations,

stresses the need for a more efficient use of varying quality aggregates. An efficient use implies that the aggregate quality should match, as closely as possible, the quality level specified for its intended use; such quality level depends on the type of structure and structural member, and its interaction with the exposure conditions. Whenever the quality of the aggregate exceeds that required, a waste of resources occurs; on the contrary, if the quality of the aggregate is less than that required, a functional or structural failure may take place.

In order to make a better use of coarse aggregates, it is necessary to study how the aggregate is related to various types of failures. The argillaceous aggregates involved in the present study give rise to severe surface deterioration of concrete and bituminous pavements. However, at the present time, it is not known if the aggregate performance is acceptable in deeper layers of the pavement. Likewise, it is not known whether or not, and to what extent, D-cracking will take place in the future. It is important to identify the primary causes of this surface problem in order to formulate some recommendations for the future use of these and other similar aggregates.

### III.1.3 Statement of Objectives

Unconfined freezing and thawing losses of these argillaceous aggregates, saturated with water and with 5% NaCl

salt solution, are presented in reference (24). The percent losses of some of those argillaceous aggregates are listed in Table III.2. From the inspection of those results, the relative severity of freeze-thaw cycles in the presence of salt solution is obvious. On the basis of these results and the reported field performance, a contributing effect of osmotic pressure to the failure of these argillaceous aggregates is postulated in this study.

The main objectives of this part of the research were as follows:

1. One purpose of this study was to determine the existence of any osmotic effect and its possible influence as a contributing cause of surface deterioration.
2. A second purpose was to compare and analyse the response mechanisms due to freezing of two rock specimens vacuum saturated with distilled water and salt solution respectively.

### III.2 Literature Review

Because of the possible association between the present problem and deicer scaling, the discussion of the latter seems appropriate.

Scaling results when: "Concrete mortar of poor quality will crumble away with repeated freezing and thawing cycles, gradually exposing the coarse aggregate particles" (34).



Increasing scaling of concrete pavements has resulted as a consequence of the profuse use of deicing chemicals in recent years. The combined influence of freezing in the presence of deicers and poor construction practices seriously affect the durability of concrete. Excessively wet concrete, over-finishing, and improper curing usually result in poor properties of the outermost zone of the pavement, which is also subjected to the most detrimental factors.

In 1956, Verbeck and Klieger (35) reported significant results concerning the problem of "salt" scaling of concrete. Some of those findings are summarized as follows:

1. Solution concentrations of the order of 2 to 4 weight percent produce the highest rate of scaling.
2. It seems that the mechanism of surface scaling is physical rather than chemical.

In addition, the benefits of air entrained to improve the resistance of concrete to freezing and thawing in the presence of deicing chemicals are also reported in reference (36).

Other research workers have found the same results. However, there is some disagreement with respect of the mechanisms involved in the salt scaling of concrete. Cordon (34) presented a detailed discussion of several theories and mechanisms advanced to explain salt scaling. Experimental

determinations and further observations reported lately seem to support more than one hypothesis (37,38,39,40). Some of the various hypotheses proposed to explain the failure mechanism(s), attribute salt scaling to:

1. Crystallization pressure.
2. Chemical Reactions.
3. Osmotic and hydraulic pressures.
4. Thermal gradients.

The first two were not found to be significant during experimental observations (39,41), and the osmotic pressure hypothesis has been discarded on the basis of numerical calculations (41). From the interpretation of his experimental results, Snyder (42) suggested that thermal gradients in combination with hydraulic pressure are the most significant causes of salt scaling.

Rosli and Harnik (38) found that the temperature shock produced by the application of deicing salts on surface and the consequent temperature gradient, may give rise to internal tensile stresses as high as the tensile strength of the surface layer of concrete pavements.

Harnik, Meier, and Rosli (40) concluded that the negative effects of the application of deicing salts on concrete are due to:

1. A higher degree of saturation of the concrete surface.
2. The temperature shock or thermal gradient.
3. Supercooling of pore water, which causes high hydraulic pressure once freezing starts.

Some of the hypotheses previously discussed have been rejected because of experimental evidence, others because of qualitative analyses, and some others, such as osmotic pressure, have been rejected on the basis of numerical calculations.

It seems unlikely that concrete scaling is due to a single cause; on the contrary, it seems reasonable to assume that two or more mechanisms simultaneously take place, while their relative importance is controlled by the characteristics of the concrete and its components, and the environment. Coarse aggregate may take an important role in surface deterioration, regardless of the benefits of air entrained in the surrounding mortar. Such appears to be the case for the argillaceous aggregates considered in this study. Its poor field performance and up to 99% losses in unconfined freezing and thawing in the presence of 5% weight NaCl solution, strongly suggest the existence of one or more additional disruptive mechanisms.

In the following sections, the relative importance of one possible mechanism is postulated; specifically, the

build up of osmotic pressure that eventually exceeds the tensile strength of the coarse aggregate. In this regard, in 1955, Powers (8) stated:

"Experimental work has not yet revealed the relative importance of osmotic pressure. It need not be a major mechanism in ordinary freezing and thawing tests, for all the effects of freezing have been observed when freezable water contains only a trace of alkali. However, osmotic pressure may be a major factor in "Salt scaling". When the normal salute content is augmented in regions near the surface of the pavement by salts applied for ice removal, osmotic pressure in partially frozen capillaries may be the dominant source of stress. This is an inference, not yet checked experimentally."

### III.3 Experimental Work

In order to accomplish the objectives of this study, two laboratory experiments were designed. They are described, and their results are discussed in the following sections.

#### III.3.1 Determination of Osmotic Effect

By definition, "Osmosis is the phenomenon whereby solvent permeates a semipermeable membrane separating two solutions of different concentrations. A net flow of solvent occurs from the less to the more concentrated solution" (43). A semipermeable membrane is one that permits the flow of solvent but not the flow of solute. From the previous definition it is apparent that two conditions must be

satisfied in order for osmotic pressure to take place: first, the barrier material must be capable of acting as a semipermeable membrane, and second a concentration gradient should exist through the membrane.

Experiments performed by Verbeck and Gramlich, dealing with the alkali-aggregate reaction, supported the idea that cement paste is capable of acting as semipermeable membrane (44). Likewise, the limiting expression for quantifying the magnitude of osmotic pressure was also reasonably confirmed in the same investigation. By analogy with liquid flow through porous media of unit thickness, osmotic pressure may be taken as the driving pressure giving rise to such flow. For dilute solutions, osmotic pressure can be computed as follows:

$$\pi = RTC/M \qquad 15$$

where:

$\pi$  = osmotic pressure

R = gas constant

T = absolute temperature ( $^{\circ}\text{K}$ )

C = concentration gradient, in grams/l

M = molecular weight of solute

#### Materials and Apparatus

Three rock samples designated as P, G, and CC-1, were used for these determinations. The first material, sample P, was sampled from a quarry that provided aggregate for

some of the surface deteriorated pavements under investigation. It is a highly argillaceous limestone. The other samples were included for the purpose of studying the possible dependence of the osmotic phenomenon on different pore size distributions. The pore size distribution of each material was determined by mercury porosimetry, and their respective results are given in Appendix A.

Sodium chloride was used as solute in a 5% weight concentration in distilled water; this concentration was selected to be consistent with previous laboratory studies conducted by Shakoor (24), and the Indiana Department of Highways (45).

For the purpose of determining whether or not each selected material was able to perform as a semipermeable membrane, it was necessary to design a testing device. Such a device should contain the concentrated solution inside, the testing specimen in one end, and a volume measuring pipette in the other end. The equipment and dimensions are shown in Figure III.1.

#### Specimen Preparation

Cores 1 3/8" diameter were taken from each rock sample, and several slices 5 mm thick were cut from them using a diamond saw. These slices were subsequently ground on each side until they were 1.5 to 4 mm thick. The actual thicknesses of three testing specimens taken from samples P,

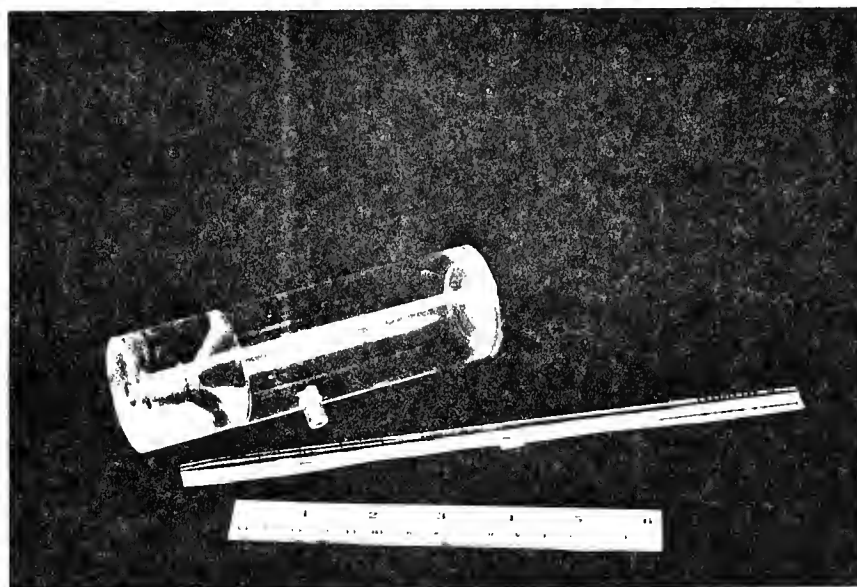


Figure III.1 Apparatus Used for the Determination of the Osmotic Phenomenon

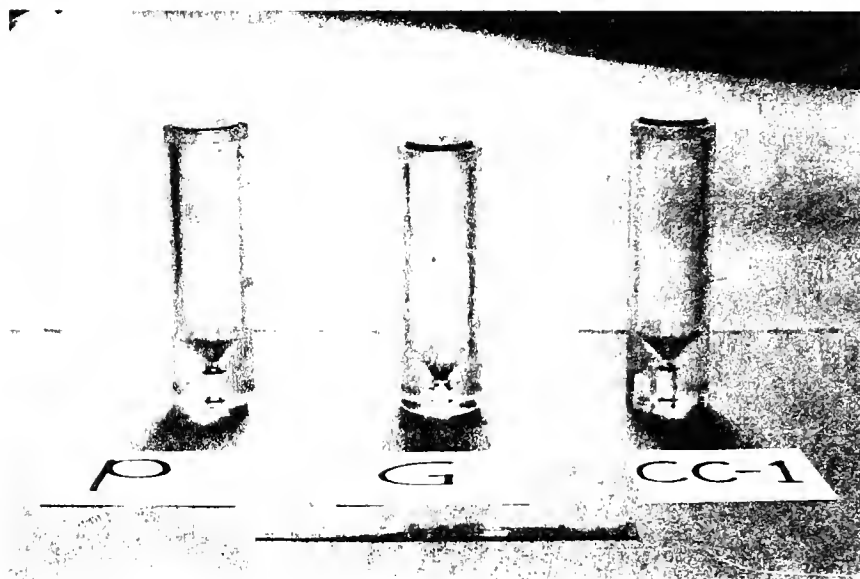


Figure III.2 Test Specimens Bonded to Acrylic Tubes





Figure III.3 Test in Progress

G, and CC-1 were 1.60, 3.93, and 1.70 mm respectively. All the slices were oven dried at  $105^{\circ}\text{C}$  for 24 hr. and, after cooling to room temperature in a desiccator, each specimen was bonded with epoxy cement to one end of the tube, as shown in Figure III.2. After curing the resin for 24 hrs., the specimen was de-aerated for 2 hr and vacuum saturated with salt solution for 2 more hr. The vacuum pump was then turned off and the specimen was allowed to saturate for one week under atmospheric pressure.

The testing procedure consisted of completely filling the acrylic tube with salt solution, and fixing tightly the pipette in its position. No air bubbles were left in the tube. Then the whole apparatus was put in contact with distilled water; the initial pipette reading was taken, and the flow of water through the specimen was monitored by recording pipette readings and elapsed time. A running test is shown in Figure III.3.

#### Analysis and Interpretation of Results

The experiment was repeated using each of the three selected samples. The osmotic phenomenon was observed in only one case, sample P, which is a highly argillaceous aggregate with very fine capillary pores. The experimental results taken during nine days, volume of solvent permeating toward the more concentrated solution and corresponding elapsed time, are plotted in Figure III.4. In this plot,

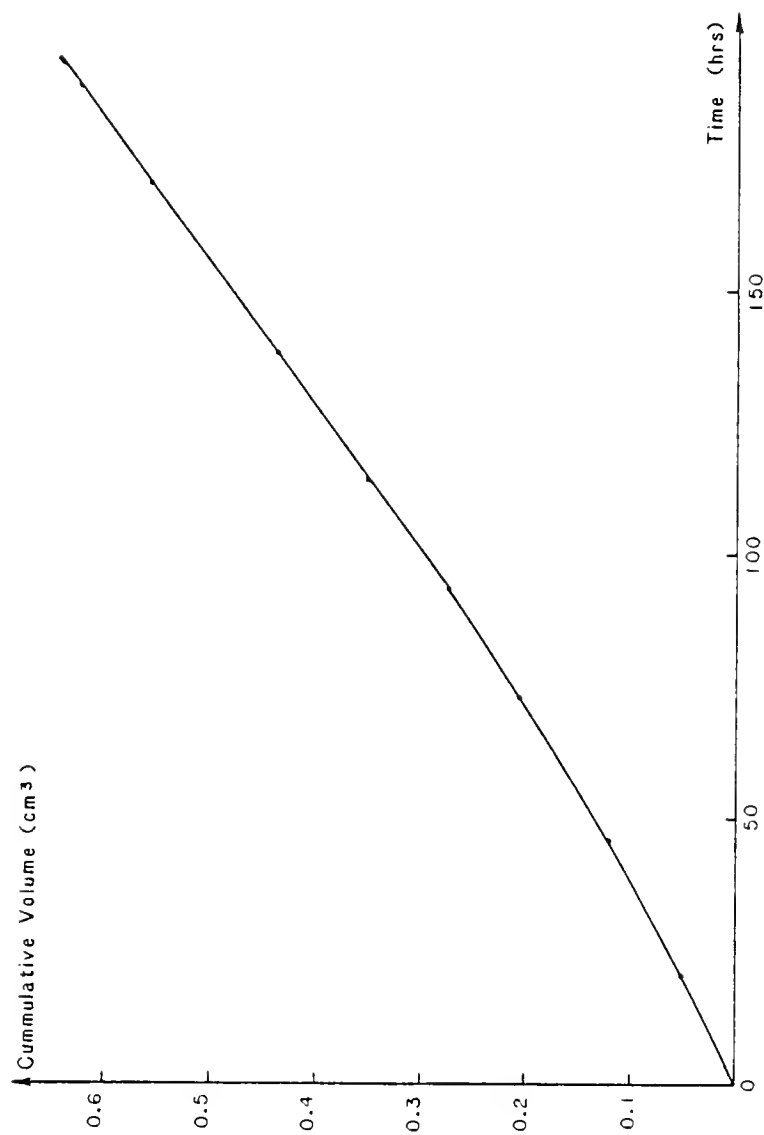


Figure III.4 Volume of Solvent Permeating Toward Concentrated Solution, Against Time

there is an initial transitory period where the response is non-linear, and later the response approaches a straight line which represents the steady state condition of the phenomenon.

The fact that osmotic pressure was observed in only one case suggests that, for that sample (P), an additional detrimental mechanism may arise during freezing and thawing if a salt concentration gradient exists. However, it is not known how important the effect of osmotic pressure is with respect to the hydraulic pressure mechanism. For the other two samples, G and CC-1, there would be no such additional disruptive pressure.

The different responses observed between samples P, and G and CC-1, can be explained as follows. Several processes may take place through membranes and filters, i.e. Ultrafiltration, Dialysis, Osmosis, Reverse Osmosis, etc. According to Kesting (43), the occurrence of each process is associated with membranes with characteristic ranges of pore sizes; for instance, osmosis occurs if the barrier material has pore sizes in the range from 6 angstroms to  $0.06\mu\text{m}$  approximately. From the pore size distribution data given in Appendix A, Table III.1 was computed.

From these results, it is evident that osmosis occurs whenever there is a significant amount of pore sizes smaller than about  $0.06\mu\text{m}$ , which is the limiting value proposed by

Kesting. Based on these findings, further analysis of the results presented in reference (24) was performed.

Table III.1 Percentage of Pore Sizes Smaller than  $0.06\ \mu\text{m}$

Sample	$\Delta V(\%)^*$
P	85.0
G	6.0
CC-1	1.0

\* Volume of pores smaller than  $0.06\ \mu\text{m}$  diameter, expressed as percent of the total intruded volume.

Two data sets are particularly important. First, those cases in which the presence of 5% weight NaCl solution made very severe the freezing and thawing action in comparison with the use of pure water. Some of those laboratory results are indicated in Table III.2. Except for one example, the percent losses in pure water after 50 unconfined freeze-thaw cycles were less than 4%; the same aggregates in the presence of salt solution showed losses up to 50%. For these samples, the volume of pores smaller than  $0.06\ \mu\text{m}$  diameter  $\Delta V(\%)$  was computed and it was found to be a significant fraction of the entire pore size distribution.

The second data set corresponds to cores taken from surface deteriorated pavements. From the top of each core, pieces of aggregates that experienced failure were obtained for mercury porosimetry determinations. The fraction of pores smaller than  $0.06\ \mu$  is also indicated in Table III.2.

Table III.2 Percentage of Pore Sizes Smaller than  
0.06 $\mu$ m. Shakoor's data (24)

Laboratory Results			
Sample	F&T Loss (%)** in water	F&T Loss (%)** 5% salt	$\Delta V(\%)^*$
T4	3.50	37.30	91.9
T7	3.68	47.37	90.0
K5	40.48	99.67	87.7
L2	3.53	43.23	76.4
L4	2.60	49.97	38.2
L5	1.56	36.25	38.5
L6	3.77	34.01	78.8
Field Cores			
I265-C2			36.1
I265-C3			59.9
I265-C5			85.0
US 24-SR115-C2			88.6
US 24-STN2-C3			76.2
US 24-STN2-C4			72.0
US 24-STN3-C6			79.1
US 24-STN4-C7			79.5
US 24-STN4-C8			77.9

\* Volume of pores smaller than 0.06 $\mu$ m diameter, expressed as percent of the total intruded volume.

\*\* F&T losses after 50 cycles.

In all cases a significant proportion of such capillary pores was found.

The results presented in Table III.2, in connection with those presented in Table III.1, seem to support the occurrence of an osmotic effect in laboratory and field conditions. In both cases, the increased severity of the freezing and thawing action in presence of salt solution was evident.

### III.3.1 Significance of Osmotic Effect

Multiple studies have validated the importance of the hydraulic pressure hypothesis as a disruptive mechanism during freezing and thawing. However, the study of the relative importance of the osmotic pressure mechanism remains as a fruitful area for research.

#### Experimental Designs

In order to determine the relative significance of osmotic pressure in the freezing and thawing failure of the argillaceous aggregates under study, two additional experiments were performed. The first experiment consisted of freezing two testing specimens vacuum saturated with distilled water and salt solution respectively. The second experiment consisted of monitoring the state of strains during freezing of a test specimen vacuum saturated with salt solution. Sample P and 5% weight NaCl salt solution were consistently used in both experiments. All the test specimens were taken 1/2" apart from each other from a single rock sample.

The first experiment consisted of freezing two identical cylindrical specimens 2 inches long and 1 1/8 inches in diameter saturated with distilled water and salt solution respectively. The cooling rate was 4 to 5° C/hr. Readings of volume changes due to frozen water and corresponding temperatures were simultaneously taken, as described in the next chapter. The results of this experiment are presented

in Figure III.5.

The second experiment was designed to quantify any possible contribution of osmotic pressure to the state of strains already produced by hydraulic pressure after an initial freezing stage. Everything was the same as in the first experiment, except for the strain gages bonded to the test specimen before it was vacuum saturated with salt solution. The location of the strain gages and the bonding and recording procedures are described in Appendix B. This experiment was conducted in two stages. In the first stage, the temperature was steadily dropped at a rate of 4 to 5 degree C/hr until initial freezing occurred; then, after an additional temperature drop, further cooling was stopped at about  $-14^{\circ}$  C. In the second stage, the specimen reached the uniform temperature of the freezing chamber, and it was kept in that condition for several hours. During all the stages, simultaneous readings of the state of strains and temperatures were recorded. The results are presented in Figures III.6, III.7 and III.8.

#### Analysis and Interpretation of Results

The most important features of the first experiment are summarized in Table III.3.

Absorption values were larger whenever salt solutions were used. This was consistently found in the present investigation using other samples, and it has also been previously



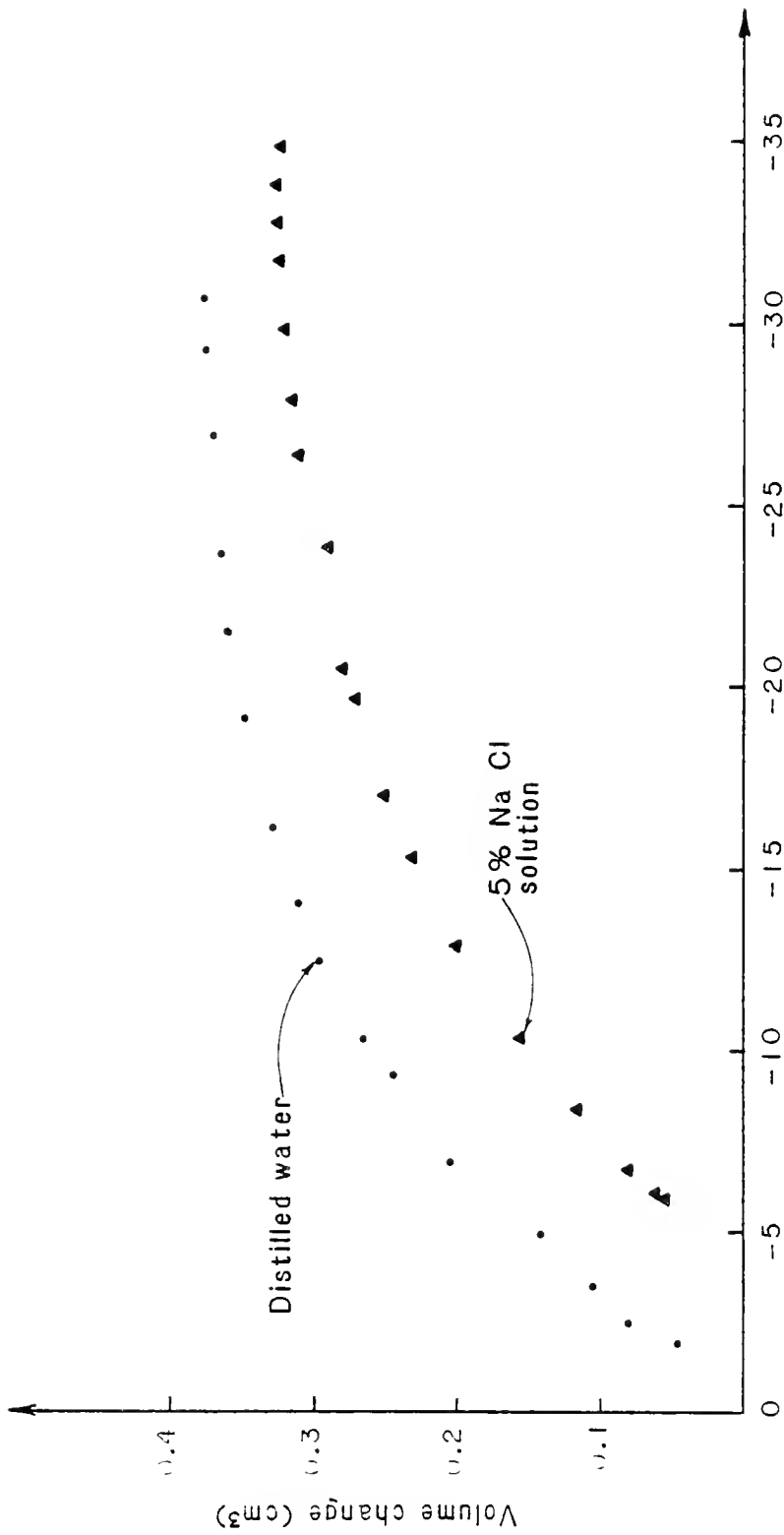


Figure III.5 Volume Increase Observed in Rock Specimens Saturated with Water and Salt Solution Respectively

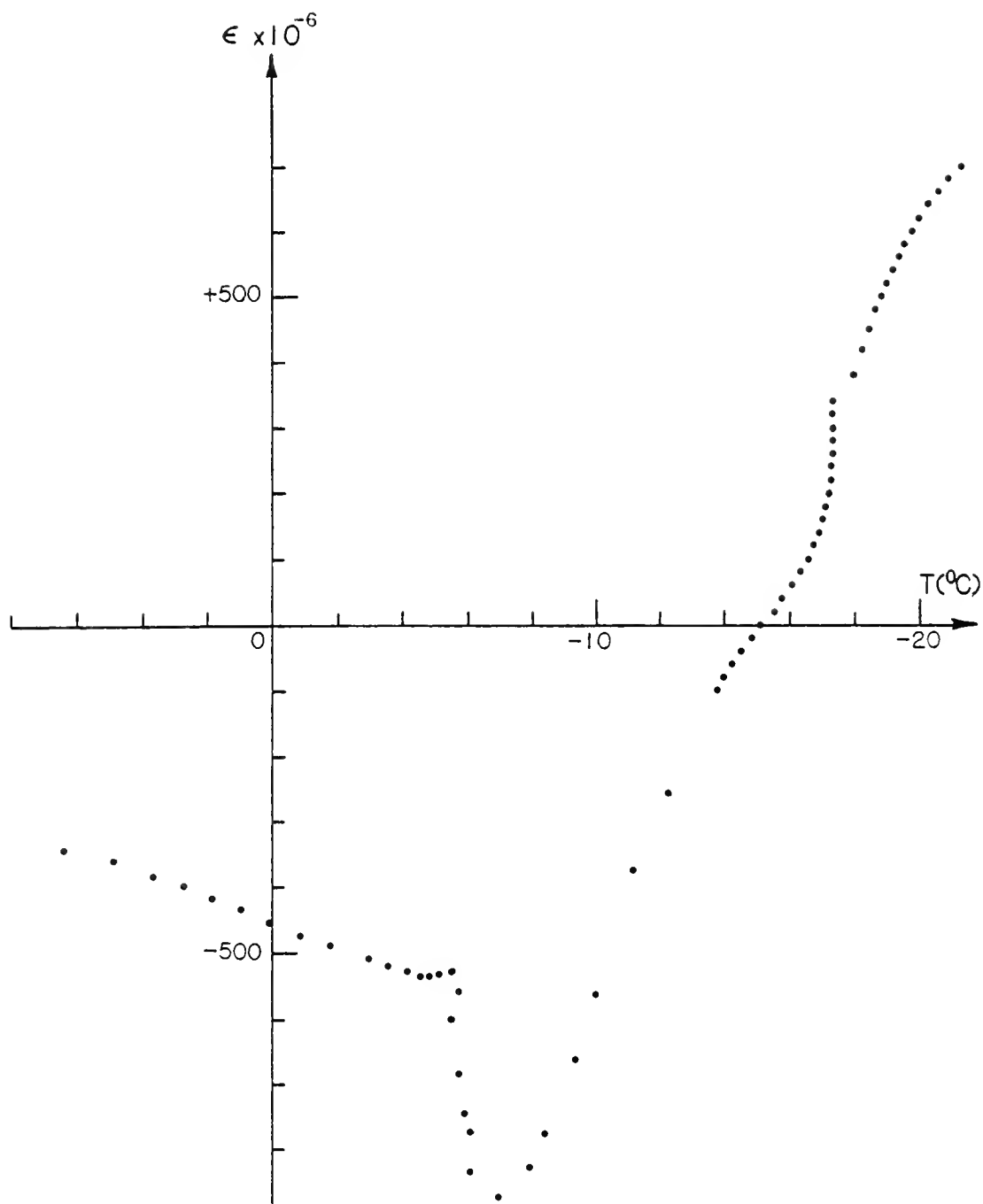


Figure III.6 Strain Readings During the Two Stages of the Experiment

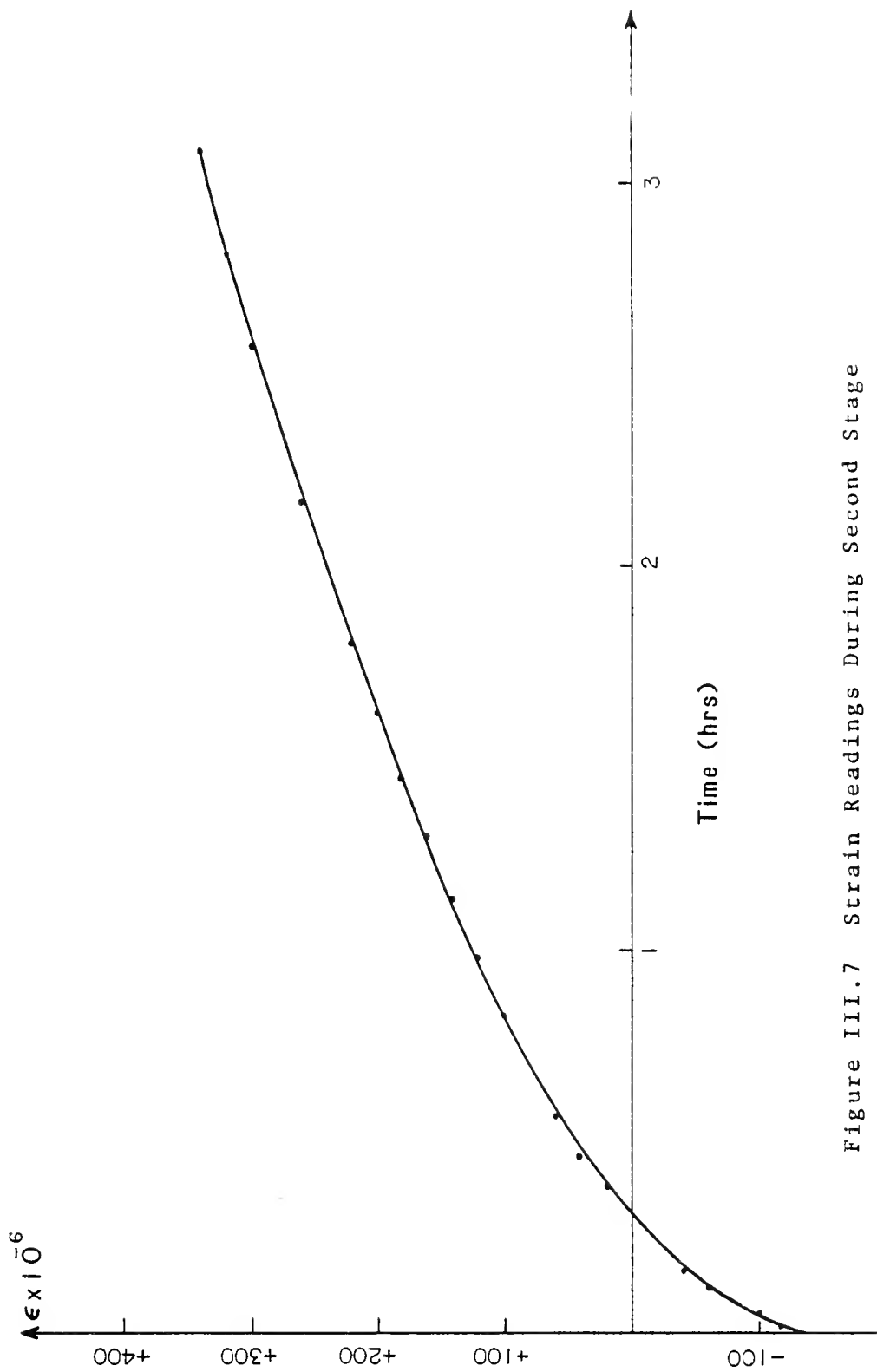


Figure III.7 Strain Readings During Second Stage

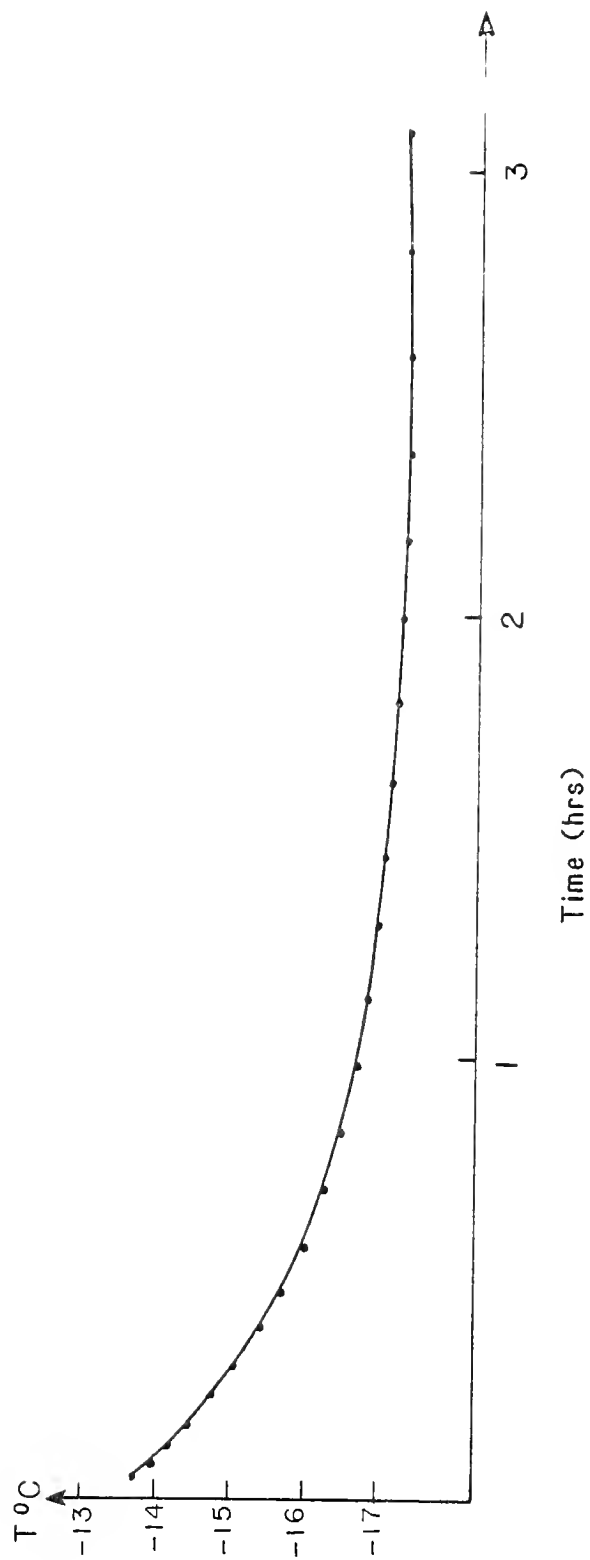


Figure III.8 Temperature Readings During Second Stage

Table III.3 Data Obtained from the Freezing of Rock Specimens Saturated with Water and 5% NaCl Salt Solution Respectively

Parameter	Water Saturation	Salt Saturation
Absorption	4.43%	4.81%
Beginning of freezing	-1.9°C	-5.8°C
Total volume of absorbed water	5.83cm <sup>3</sup>	6.05cm <sup>3</sup>
Initial volume of frozen water	0.44cm <sup>3</sup>	0.60cm <sup>3</sup>
Total volume of frozen water	4.19cm <sup>3</sup>	3.60cm <sup>3</sup>
	at -30.8°C	at -31.8°C

reported (37,40). As was expected, freezing of water began at a lower temperature in the presence of NaCl solution, and the total volume of frozen water was smaller than that corresponding to saturation with distilled water. This is explained by the fact that, as freezing of water continues, the concentration of the unfrozen solution simultaneously increases until a value is reached for which no further freezing of water is possible. For the salt used in this experiment, NaCl, such concentration and the corresponding freezing temperature are 23.3% and -21°C respectively (46).

Presumably, the hygroscopicity of NaCl and the lowering of the relative vapor pressure contribute to obtain larger absorption values. Several authors, Fagerlund, Rosli, Litvan, etc., attribute the severity of freezing and thawing in salt solutions to the resulting higher degrees of saturation. The smaller the internal pore space available to accommodate the expanding volume of water, the higher the

internal pressure in the pore structure may be.

Supercooling of water has also been suggested as another negative effect of deicing salts. Harnik et al (40) stated that whenever supercooling occurs, large amounts of suddenly frozen water should be expected once freezing starts. Consequently, large hydraulic pressure could be generated, and the freezing process would become more detrimental.

According to the present findings obtained from both experiments, the following discussion seems pertinent. The general tendency observed in the plots of volume change due to frozen water against temperature looks similar for both specimens, except for the translated origin when the specimen was saturated with salt solution. No significant difference in the initial volume of frozen water was observed between both cases, despite the difference in supercooling effect (Table III.3 and Figure III.5). In addition, the freezing rate of water, observed by recording displaced volume of mercury versus time, was larger for the specimen saturated with distilled water in comparison with the freezing rate observed in the specimen saturated with salt solution.

After freezing and thawing once, both specimens were inspected and circumferential cracking was observed at the middle height of the cylinder saturated with salt solution.

No cracking was apparent on the specimen saturated with water. Such different response cannot be explained by the hydraulic pressure mechanism alone, because in the case of the more deteriorated specimen the total volume of frozen water was smaller, no negative effect of supercooling was observed in respect of large volumes of suddenly frozen water, and finally the freezing rate was consistently smaller. Therefore, it seems reasonable to postulate the existence of a second detrimental mechanism.

The results of the second experiment provide direct evidence to support the hypothesis that, for the argillaceous aggregates under consideration, there exists an additional osmotic effect that contributes to the surface failure mechanism. The state of strains recorded during the two stages of the second experiment is shown in Figure III.6. The state of strains after the temperature of the freezing chamber was kept constant is shown in Figure III.7. The relative significance of the osmotic pressure is supported by the steady increase of tensile strains while the temperature of the specimen remains practically constant, Figure III.8.

For a temperature change of approximately  $2^{\circ}\text{C}$  (from  $-15^{\circ}\text{C}$  to  $-17.3^{\circ}\text{C}$ ) the strain increment was more than  $300 \times 10^{-6}$  in/in in a less than three hour period. This strain increment by itself, even assuming that no strains are due to hydraulic pressures, may be large enough to

produce failure. It should be pointed out that such strains had been larger if the test had lasted longer.

The response of the testing specimen in the second experiment shows an interesting characteristic: the NaCl solution saturated specimen becomes an osmotic cell by itself once freezing starts. It means that, after a selective water freezing occurs, there is an increment in the solution concentration of some of the unfrozen capillaries left throughout all the specimen. This, and the internal flow taking place due to the volume displaced by the freezing water, seems to give rise to concentration gradients within the specimen. As a consequence of such concentration gradients, an osmotic pressure starts to build up inside the specimen. It should also be recognized that osmotic pressure and hydraulic pressure are simultaneously present once freezing starts; but, after the temperature remains constant, the effect of the former predominate over the effect of the latter.

#### III.4 Summary of Chapter III

The occurrence of the osmotic phenomenon in the argillaceous aggregates under consideration has been discussed and experimentally verified. Likewise, the significance of osmotic pressure as a contributing factor to aggregate failure has also been experimentally verified.



On the basis of the findings presented in this chapter, the following recommendations are presented:

1. The simple testing procedure used to detect the ability of coarse aggregates to perform as semipermeable membranes may be used to identify coarse aggregates prone to surface deterioration in the presence of deicers. This test could be used instead of more elaborate procedures involving unconfined freezing and thawing.
2. Quantitative estimations using the Poisseuille equation, and the results presented in Chapter IV, show that high hydraulic pressures can be generated in a porous matrix whenever there is a significant volume of pores smaller than  $0.06\mu$ . Therefore, the same simple test might be used to identify and reject coarse aggregates giving rise to D-cracking by the internal failure mechanism. Further analysis and experimentation using selected samples is desirable in this respect.

CHAPTER IV  
FREEZING-POINT DEPRESSION  
AND ITS INFLUENCE ON FROST ACTION IN ROCKS

IV.1 Introduction

IV.1.1 Statement of the Problem

Bulk water normally freezes at 0 degree C, and after freezing occurs its original volume increases approximately 9%. Under certain conditions, water may freeze at lower temperature, but still a corresponding volume increase is reported to take place (48). Damage of saturated porous building materials arises whenever freezing and other critical physical properties are simultaneously present. In order for failure not to occur, the volume increment resulting during freezing needs to be accommodated in internal empty cavities or it should be readily expelled to the surface of the freezing sample. One physical property highly influential on this processes is the pore structure, which can be characterized by the pore size distribution (PSD) of the material, as it is determined by mercury porosimetry.

Frost damage has been studied in connection with the freezing rate of water and the permeability of porous materials, and the latter has been taken as a fixed property of the pore structure (6). The relationship between the freezing phenomenon and capillary pore size has also been studied and significant conclusions pertinent to frost damage are reported in reference (19). In this investigation, it was intended to study the relationship between the freezing of water in "saturated" rock samples and their PSD. Likewise, the possible effects of this relationship on frost damage are qualitatively discussed and quantitatively analyzed through an example.

#### IV.1.2 Significance of the Problem

Water held in a porous matrix does not freeze at  $0^{\circ}$  C. This is supported by the fact that water within materials of large pore sizes freezes at temperatures lower than, but close to zero centigrade. Likewise, water within materials with fine pores freezes at much lower temperatures. Common building materials have a range of pore sizes from several microns to a few angstroms; therefore, it should be expected that freezing occurs at a corresponding range of temperatures below  $0^{\circ}$  C.

Because of the dependence between freezing point of water and capillary pore size, several important implications on possible mechanisms of frost damage should be

expected. First, the maximum amount of ice formed should be dependent on the minimum applied temperature; experimental results support this fact (9, 10). Second given that natural building materials may have a wide range of pore sizes, several "freezing points" result as the temperature drops. This has the following direct effects, which should be taken into consideration in the study of frost damage mechanisms:

1. As the temperature drops, the permeability of the porous matrix progressively decreases, which implies that the use of any permeability value measured at room temperature ( $K_0$ ), may be applicable only at the beginning of the freezing process. This is due to changes in the effective porosity. This change, in addition to an increasing viscosity of water, directly affect the hydraulic pressure generated during freezing.

The importance of the previous statement is suggested by the fact that it is not always the initial state of strains after freezing which produces failure, but a subsequent cumulative state of strain, increasing as the temperature decreases. Consequently any theoretical model including  $K_0$  in the prediction of failure may or may not be appropriate, depending on the magnitude of the initial strain.

2. Given that ice formation is controlled by PSD and cooling rate, the rate of ice front propagation is also expected to depend on PSD. Because of this dependence, it seems unlikely that there is a unique value of ice rate propagation, even if the cooling rate is assumed to be constant. Further discussion is presented in the end of this chapter.

Some consequences of the relationship between freezing point and capillary pore size have been discussed. Its study is important because the theoretical modeling of the freezing process and its consequences must be involved, to some extent, with the relationship between freezing point depression and PSD. Furthermore, the determination of such a relationship may provide sound basis for improved specifications and testing procedures, as well as a better insight for the interpretation of experimental results dealing with frost damage.

#### IV.1.3 Statement of Objectives

In this part of the study it is intended to accomplish the following objectives:

1. To determine the freezing point of water as a function of pore size, and to determine the applicability of previous equations derived for that purpose.

2. It is intended to discuss quantitatively the implications of the experimental findings of this study in relation to frost damage.

#### IV.2 Literature Review

Regarding the freezing phenomenon of water, Chalmers pointed out: "Strictly speaking, zero degrees is the equilibrium temperature: the point at which ice and water can remain in contact with one another indefinitely, neither increasing at the expense of the other" (49).

Under certain circumstances, water freezes at temperatures lower than  $0^{\circ}$  C. Some common causes are:

1. Presence of dissolved substances i.e. salts, hydroxides, etc.
2. Restriction of capillary size.
3. Supercooling.

An example of the first cause is given by a 5% weight NaCl concentration in water, which reduces the freezing point to about  $-2.5^{\circ}$  C, and at the saturation concentration, 20%, the freezing point of water is reduced to about  $-23^{\circ}$  C. The first and second causes yield the same effect, both contribute to lowering the vapor pressure of water. In this respect, Powers (9) stated:

"A given reduction in vapor pressure signifies the same reduction in freezing point, regardless of the mechanism by which the reduction is effected".

It is important to mention that ice and water can remain in contact with one another indefinitely at the reduced temperature. This is the equilibrium crystallization temperature of the system.

The third cause, supercooling, is defined as follows: "When a substance is cooled below the equilibrium temperature, it is said to be "supercooled" or "undercooled" (50). Supercooling of water is possible only in the absence of ice; if ice is present, water can not be cooled below its equilibrium temperature. Supercooled water crystallizes rapidly if it is placed in contact with an ice crystal of a proper size; this fact indicates that supercooled water is in a metastable state.

Supercooling of water proceeds until the first ice crystal nucleus is formed. This formation may result by two processes: homogeneous nucleation and heterogenous nucleation. Homogeneous nucleation takes place at temperatures around  $-40^{\circ}\text{C}$ , which is the minimum temperature for the spontaneous formation of the first crystal nucleus. However, such a process occurs only in pure water. The presence of solid impurities in water is the main cause of heterogeneous nucleation. This process consists of the build up of ice crystals around impurities, or even on the wall of the

container. Room dust has the ability to cause nucleation at about  $-5^{\circ}\text{C}$  (51).

The freezing point depression of water in capillary pores has been studied theoretically and experimentally by many investigators.

In 1932, from thermodynamic considerations and taking account of the influence of capillary tension, Kubelka (52) derived the following equation which relates freezing point depression to capillary radius.

$$\Delta T = \frac{2 \sigma_{L-g} V_f T_o}{\Delta H} \frac{1}{r} \quad 16$$

where

- $\Delta T$  = freezing point depression
- $\sigma_{L-g}$  = surface tension of fluid (Liquid-air)
- $V_f$  = molar volume of liquid
- $\Delta H$  = latent heat of fusion of liquid
- $T_o$  = freezing temperature of bulk liquid
- $r$  = capillary radius

From the equilibrium of a spherical crystal in its own melt, Sill and Skapski (53), 1956, derived the following equation

$$\Delta T = \frac{2 \sigma_{S-L} T_o}{\rho_s \Delta H} \frac{1}{r} \quad 17$$

where

- $\sigma_{S-L}$  = solid-liquid interfacial tension
- $\rho_s$  = density of the solid phase



$r$  = crystal radius

All other symbols have the same meaning as before.

Other expressions have also been reported, and they are essentially of the same form as (16) and (17). For instance, if there is no complete saturation, equations (16) and (17) are slightly modified by the addition of one term. Blachere and Young (54) added one term to equation (17) for taking into consideration the effect of liquid-vapor interfaces. Williams (55) also added another term to equation (17) in order to include the effect of solid-vapor interfaces. Expressions (16) and (17) only differ in the assumed value of surface tension,  $\sigma_{L-g}$  or  $\sigma_{S-L}$ . The use of the former yields greater freezing point depressions since  $\sigma_{L-g} < \sigma_{S-L}$ .

Based on the experiments performed by Powers and Brown-yard (9), which support  $\sigma_{L-g}$  instead of  $\sigma_{S-L}$ , Fagerlund (56) used  $\sigma_{L-g}$  in his derivations and he arrived to the following semi-empirical expression applicable in the range  $-50^{\circ}\text{C} < \Delta T < 0$

$$r = \frac{1}{8.061\Delta T - 6.12 \times 10^{-2} (\Delta T)^2 + 2 \times 10^{-4} (\Delta T)^3} \quad 18$$

where:

$r$  = capillary radius (microns)

$\Delta T$  = freezing point depression ( $^{\circ}\text{C}$ )

Experimental studies have been conducted to verify the applicability of theoretical derivations. Blachere and

Young (54) used samples of porous glass powder of different mean capillary pore sizes, and differential thermal analysis was used to detect the freezing temperature during cooling. They found reasonable agreement between their experimental results and a modified equation (17). Fagerlund used the experimental results reported by Williams (55), and he found that equations (16), (17), and (18) lie close to the experimental observations.

In the present study, no attempt is made to discuss the assumptions behind the expressions and their limitations. However, a few practical observations are pertinent. Equations (16), (17) and (18) are based on properties of water whose magnitude may not be accurate as temperature and capillary pore size decreases, i.e. surface tension, latent heat of fusion, density, etc. Likewise, the semi-empirical expression (18) was compared with experimental results obtained at temperatures from  $-0.2$  to about  $-2^{\circ}\text{C}$ , which makes uncertain any extrapolation beyond this range. Field temperatures and those used in laboratory studies of frost damage normally are lower than  $-2^{\circ}\text{C}$ .

#### IV.3 Experimental Work

An experiment was designed to determine the freezing point of water in a saturated rock sample. The experiment is based on the fact that water increases its volume once it freezes, and this volume change can be recorded using a

dilatometric flask. It is assumed that the test specimen is completely saturated at the beginning of the test; the validity of such assumption can be reasonably verified from the actual experimental results.

#### IV.3.1 Conceptual Approach

The determination of the relationship between freezing point and capillary pore size is based upon the following conceptual approach. Assume a rock sample of unit dry weight whose physical properties are known, i.e. absorption, specific gravity, pore size distribution, etc. After this sample is saturated with water, and the volume of empty pores is negligible, a volume of water  $V_w$  will be filling its pore structure. This volume of water is absorbed in a range of capillary pore sizes of the relative proportions represented by the PSD of the porous matrix, Figure IV.1.(b).

As the temperature drops below zero centigrade degrees, water progressively freezes in first the larger, and then the smaller pores. As a consequence of this freezing, a cumulative volume increase  $\Delta V_j$  results, which corresponds either to water expelled to the surface of the sample, where it freezes, or to ice formed inside the sample. From the observed volume increment  $\Delta V_j$  at any temperature  $T_j$ , Figure IV.1.(a), it is possible to compute the corresponding volume of frozen water  $V_j$ ; then, from Figure IV.1.(b), it is also

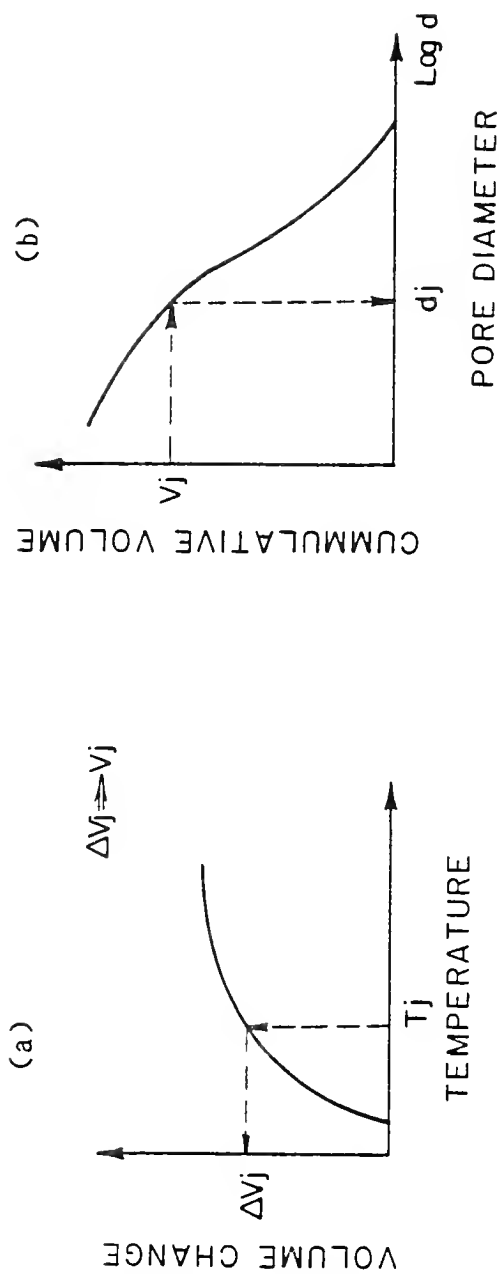


Figure IV.1 Pore Size Distribution and Corresponding Volume Changes as Water Freezes

(a) Cumulative Volume Increase Against Temperature

(b) Cumulative Pore Size Distribution

possible to determine the smallest pore diameter in which the water has become frozen.

Once a convenient number of data points  $(d_j, T_j)$  have been obtained, a statistical regression analysis can be performed in order to define the nature of the relationship between pore size and freezing point depression.

#### IV.3.2 Experimental Determinations

##### Materials and Apparatus

Two rock samples were used in this experiment, samples designated as P and G; their physical properties are indicated in Appendix A.

The equipment consisted of:

- A. Freezing chamber, Thermotron Model SM-8C, where temperatures as low as  $-60^{\circ}$  C can be applied. The cooling rate was manually controlled at about 4 to  $5^{\circ}$  C/hr.
- B. Three thermistors, previously calibrated, were used for temperature readings at the center and at the surface of the dummy specimen. The third thermistor was used for taking the temperature of the chamber close to the test specimen.
- C. A dilatometer, constructed by joining a  $1\text{ cm}^3$  pipette, with  $1/100\text{ cm}^3$  subdivision, to the cap of a standard weighing bottle of  $45\text{ cm}^3$  capacity, Figure IV.2.

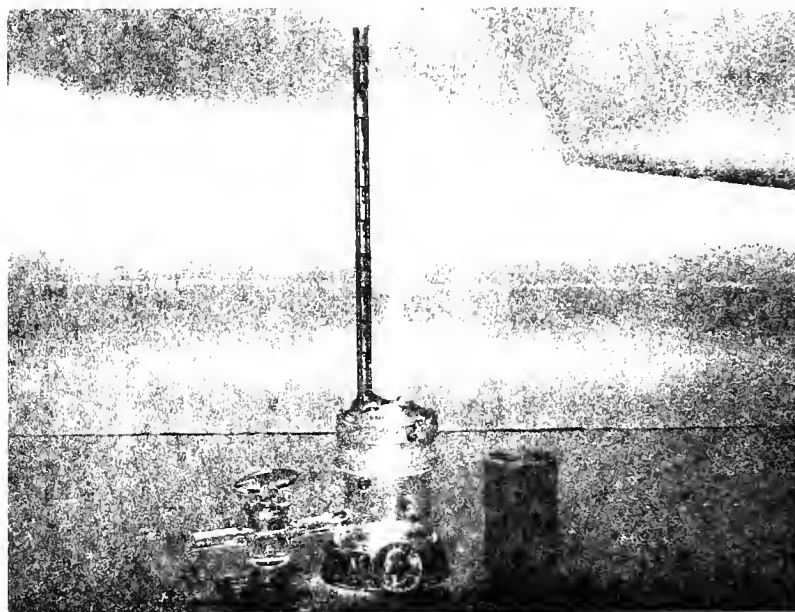


Figure IV.2 Dilatometer

### Test Specimens and Conditioning

Two cylindrical test specimens, 1 3/8" diameter and 2" height, were obtained from each sample P and G using a diamond bit. One specimen was used for taking the temperature readings and the other for taking the corresponding readings of volume change. Both specimens were oven dried for 24 hrs at 105° C, and then they were vacuum saturated with distilled water. Once the specimens were vacuum saturated, they were left immersed in water for at least two weeks before testing.

It was decided to measure temperature changes using a dummy specimen, conditioned exactly as the active specimen, in order to avoid undesirable disturbances during the recording of volume changes. Temperature was measured at the center and at the surface of the dummy specimen; the temperature difference was always smaller than about 1.5°C, and the mean value was used in subsequent computations. Figure IV.3. The sample continuity was restored by filling the 3/16" perforation with rock powder obtained from the same sample. The water content of this filling powder was fixed equal to that of the surrounding material.

### Testing Procedure

After conditioning two specimens of the same sample as described, both were weighed saturated and surface dry (SSD), three times each to detect and to average any

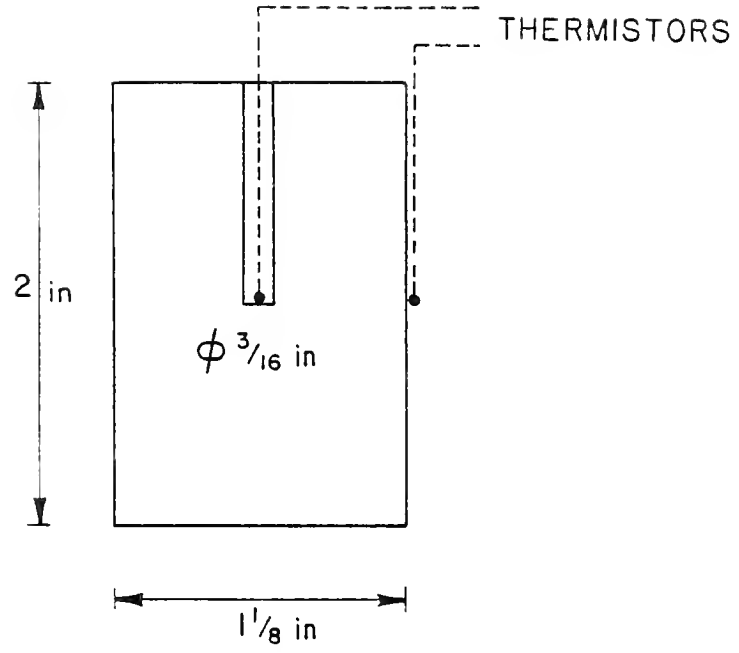


Figure IV.3 Dummy Specimen for Temperature Measurements



possible weight variation when the specimens were brought to SSD condition. Then the specimen was immediately placed in the dilatometer flask, which was then filled with mercury from the lower part in order to force the inside air upward as filling proceeded. It was carefully checked that no air bubbles were left inside of the flask and the pipette, Figure IV.4. Once the thermistors were in place, the same process was repeated with the dummy specimen.

Both flasks were put inside of the freezing chamber at room temperature and initial readings were taken, starting at about  $8^{\circ}\text{C}$ , the cooling rate was manually controlled at about 4 to  $5^{\circ}\text{C/hr}$  and simultaneous readings of volume change, temperature, and time were taken.

## Results

### Analysis and Interpretation

The experimental results are shown in Figure IV.5. The discussion and interpretation of these results are presented in the following section.

Pipette readings against temperature in the range  $+10^{\circ}\text{C}$  to about  $-30^{\circ}\text{C}$  are shown in Figure IV.5. Three characteristic responses of the testing specimen can be identified in this graph. First there is a volumetric contraction between  $+10^{\circ}\text{C}$  and about  $-2^{\circ}\text{C}$ , which is linearly dependent on temperature and can be represented as follows:

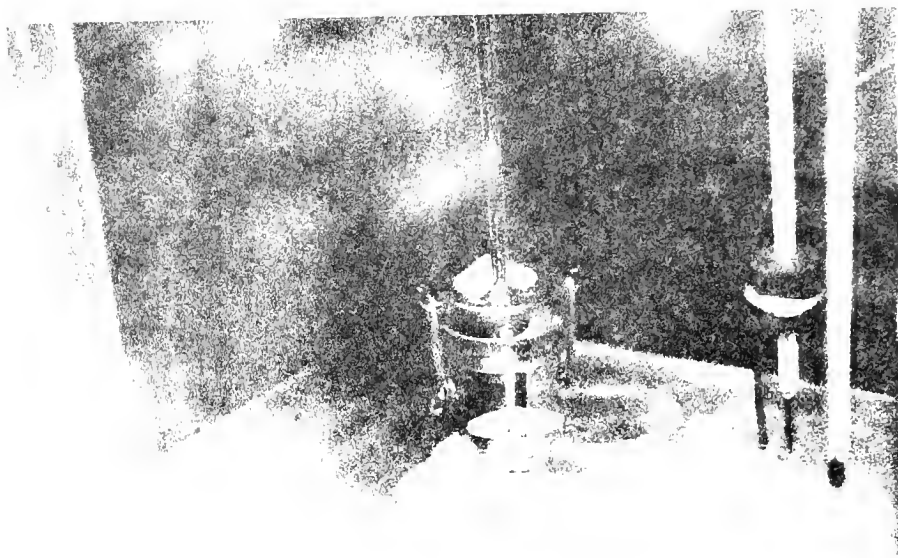


Figure IV.4 Test Specimen in Dilatometer Filled with Mercury

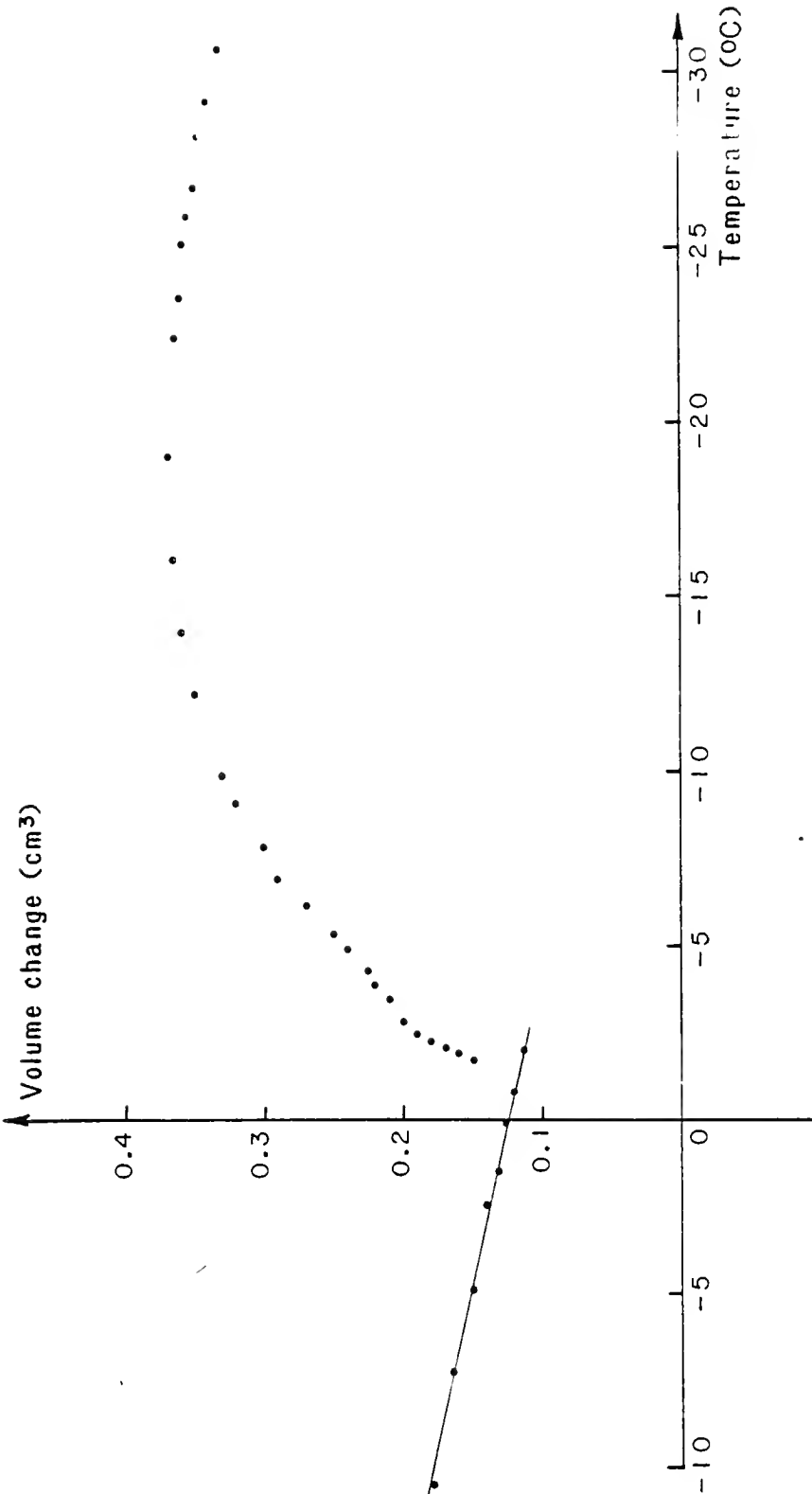


Figure IV.5 Pipette Readings Against Mean Temperature

$$\Delta V_T = (\alpha_m + \alpha_{Hg} + \alpha_g) \Delta T \quad 19$$

where

$\Delta V_T$  = total volumetric thermal contraction  
corresponding to temperature change  $\Delta T$ .

$\alpha$  = volumetric coefficient of thermal  
contraction

m, Hg, g = subindices representing testing material,  
mercury, and glass flask

Second, starting at the initial freezing point of capillary water at about  $-2^{\circ}\text{C}$  and down to about  $-30^{\circ}\text{C}$ , a deviation from the straight line response is observed. The difference between the observed value and the projection of the straight line is directly proportional to the volume of frozen water, approximately. Finally, the third characteristic response is observed when the whole system starts contracting; this is because all the freezable water has been frozen at that minimum temperature.

From Figure IV.1.(a), it is possible to compute the cumulative amount of frozen water  $V_j$ , at any temperature  $T_j$ ; then, from the cumulative PSD representing the total amount of water absorbed in the testing specimen, it is possible to determine the pore size  $d_j$  up to which water has been progressively frozen. Figures IV.1.a and b.

This operation of going from  $T_j$  to  $V_j$  and from  $V_j$  to  $d_j$ , as described, was repeated for each temperature reading made in the experiment. Finally a data set of 31 points  $(T_j, d_j)$  was

obtained for further analysis, Table IV.1. It was suspected that a few points at the beginning of the temperature range would be rejected; this is because of the sudden changes of volume and temperature occurring at the beginning of freezing, which makes it difficult to take accurate readings. The identification and rejection of such points was left for the statistical analysis.

Table IV.1 Experimental Readings During  
Freezing of Rock Specimen

Temperature	Volume Increase	Diameter
(°C)	( $\times 10^{-1}$ C.C.)	(microns)
-1.9	0.48	0.45
-2.1	0.58	0.16
-2.3	0.70	0.077
-2.5	0.80	0.062
-2.9	0.92	0.051
-3.5	1.05	0.045
-4.0	1.18	0.040
-4.3	1.25	0.037
-5.0	1.43	0.030
-5.4	1.56	0.028
-6.2	1.81	0.024
-6.9	2.05	0.020
-7.8	2.20	0.019
-8.2	2.26	0.0187
-9.1	2.45	0.0176
-9.9	2.60	0.0167
-10.4	2.66	0.0163
-12.2	2.93	0.0147
-14.0	3.12	0.0136
-16.1	3.29	0.0125
-19.1	3.49	0.0113
-21.5	3.62	0.0106
-22.6	3.63	0.0105
-23.6	3.66	0.0103
-25.2	3.74	0.0099
-26.0	3.73	0.0099
-26.8	3.73	0.0099
-28.3	3.77	0.0098
-29.3	3.75	0.0098
-30.8	3.77	0.0097

The statistical analysis consisted of empirical model building using the  $(T_j, d_j)$  data set. Three statistical models were derived from the data set. They were sequentially derived and adjusted until the basic assumptions of regression analysis were met, and the physical phenomenon was properly represented. The first form of the model, adopted from equations (16) and (17), was obtained after the logarithmic transformation of the data set. The second model was studied because of the "lack of fit" of the first, and its form was assumed after inspecting the logarithmic plot of the data. The form of the third model was derived because of the physical inconsistency of the second model at  $T = 0^\circ\text{C}$ , this inconsistency was eliminated after forcing the regression analysis through the origin. All three models are included in Table IV.2.

Table IV.2 Empirical Models of the Freezing Process in a Porous Matrix

Model	Empirical Model	$R^{2*}$
I	$d \cdot T^{-0.7439} = -0.9815$	0.961
II	$1/d = -4.2545 + 8.7601T - 0.2542T^2 + 0.2729 \times 10^{-2}T^3$	0.997
III	$1/d = 7.6656T - 0.1824T^2 + 0.1370 \times 10^{-2}T^3$	0.999

where:

$d$  = pore diameter, microns

$T$  = freezing point depression,  $^\circ\text{C}$

\*  $R^2$  = coefficient of determination

As can be observed, all three analyses strongly confirm that a continuous relationship between  $T_j$  and  $d_j$  exists, at least in the temperature range under consideration. However, despite the high value of the correlation coefficient in each case, the pattern of residuals invalidates Model I, and physical consideration of the phenomenon invalidate model II. Finally, the third model was selected because no model violations were detected by inspecting the plot of residuals, and the physical conditions of the phenomenon were satisfied. It should be noticed that by forcing the regression analysis through the origin, the magnitude of  $R^2$  is expected to be different from that previously obtained and shown in Table IV.2. Despite such a difference, the agreement between predicted and observed values is excellent.

The predicting power of the expression obtained in this study was verified against the experimental results obtained by Williams and discussed by Fagerlund in Figure 1, p. 216, of his paper (56). For the same purpose, the experimental results obtained by Blatchere and Young, Figure 1, p. 307, reference (54), were also used. In both cases the agreement between the experimental results and the values estimated using the third model is excellent.

Dolch (57) derived an equation which relates melting point of water to capillary radius. This equation is given as follows:

$$d.T = 2.34 \times 10^{-1}$$

20

where

$d$  = capillary pore size, microns

$T$  = melting point,  $^{\circ}\text{C}$

This expression yields almost identical results to the semi-empirical expression proposed by Fagerlund (56). In Figure IV.6, both expressions and the empirical model derived from the data in this study are shown.

#### Implications with Respect to Frost Damage

According to the hydraulic pressure hypothesis, the magnitude of the hydraulic pressure generated in a saturated porous sample during freezing is given by (6)

$$P_{\max} = \frac{0.09 V_i L}{27.7 K} \quad 21$$

where

$P_{\max}$  = maximum hydraulic pressure, psi

$L$  = dimension of aggregate in direction of freezing, in.

$K$  = permeability coefficient of aggregate, cm/sec

$V_i$  = rate of freezing of water, cm/sec

It has been already discussed how the permeability coefficient decreases as the temperature drops. Further consideration is given in this section to the second important parameter  $V_i$ , the rate of freezing of water. In computations reported in the literature related to frost damage, freezing rates of 1 in/hr and 2.5 in/hr have been used (6,



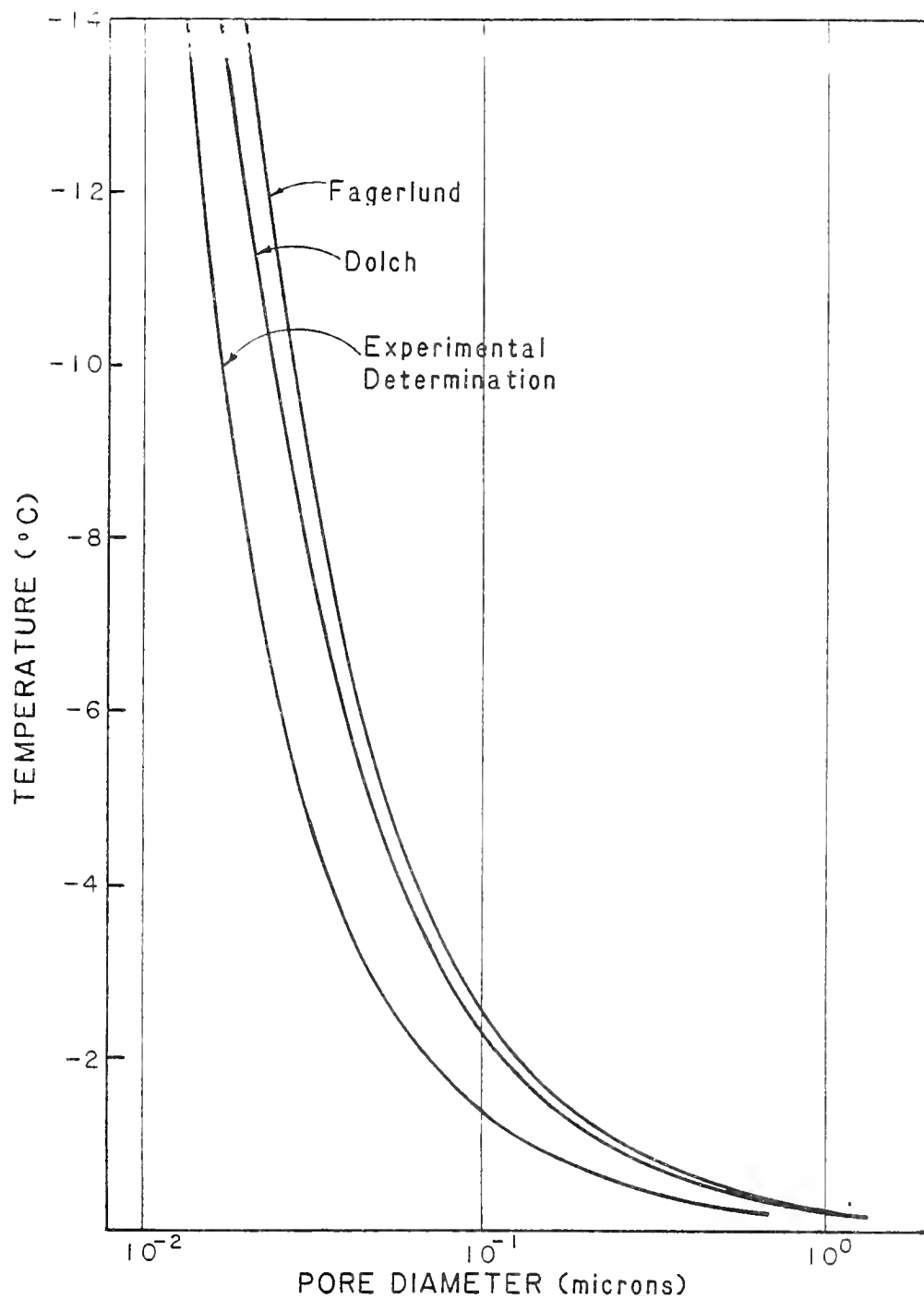


Figure IV.6 Freezing Point of Water as a Function of Pore Diameter

19). It was postulated in the beginning of this chapter that  $V_1$  was expected to be dependent on the pore size distribution of the porous matrix; the purpose of this discussion is to illustrate, quantitatively, such dependence.

Assume two imaginary saturated rock samples of identical geometry and physical properties, which are frozen at a uniform cooling rate  $H_0$  ( $^{\circ}\text{C/hr}$ ). They have the same porosity, but their respective PSD are different, they are translated respective to each other as it is shown in Figure IV.7.

Assuming that the minimum temperature is low enough for all the water to become frozen in both samples, the total discharge from each sample is given by

$$\begin{array}{ll} \text{SAMPLE 1} & \text{SAMPLE 2} \\ Q_1 = \frac{0.09 V_T}{t_{1f} - t_{1i}} & Q_2 = \frac{0.09 V_T}{t_{2f} - t_{2i}} \end{array}$$

where:

$Q_1, Q_2$	= discharge (cc/hr)
$V_T$	= volume of absorbed water
$t_{1i}, t_{2i}$	= time at which freezing starts
$t_{1f}, t_{2f}$	= time at which freezing ends
$(t_{1f} - t_{1i}), (t_{2f} - t_{2i})$	= time increment in which all water becomes frozen

The temperature at any time is given by  $T = H_0 t$ , and the

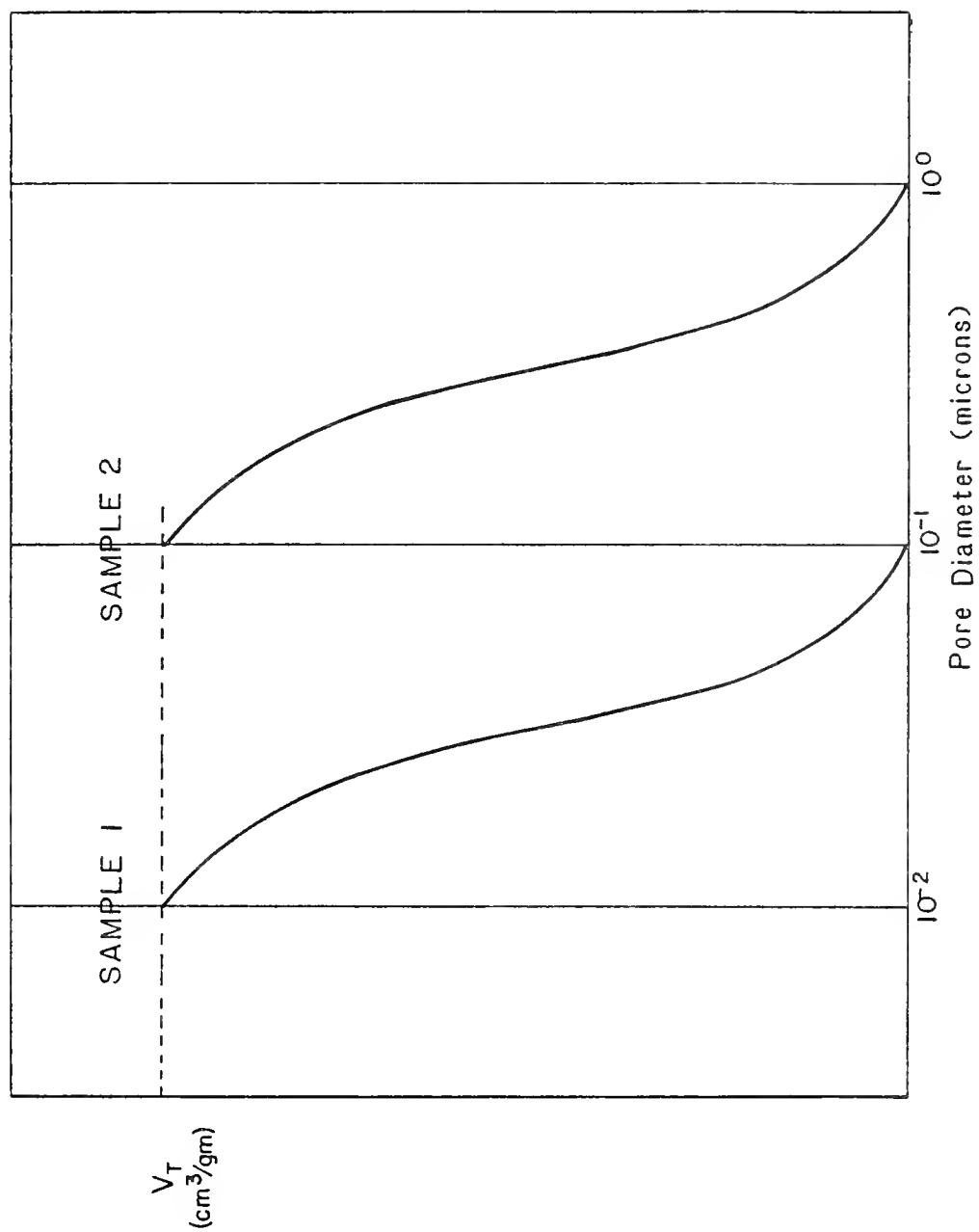


Figure IV.7 Arbitrary Pore Size Distribution

discharge is also given by  $Q = V \cdot A$ , where  $V$  is discharge velocity and  $A$  is the total discharge area. Substituting these values in equations (22) yields

$$V_1 = \frac{0.09V_T}{T_{1f}-T_{1i}} \frac{H_o}{A} \quad \text{and} \quad V_2 = \frac{0.09V_T}{T_{2f}-T_{2i}} \frac{H_o}{A}$$

consequently

$$\frac{V_1}{V_2} = \frac{T_{2f}-T_{2i}}{T_{1f}-T_{1i}} \quad 23$$

The specific temperature values indicated in equation (23) can be computed for each PSD shown in Figure IV.7, using the third empirical expression given in Table IV.2. Finally, after substituting values

$$\frac{V_1}{V_2} = \frac{1}{20.2}$$

This simple example illustrates how the rate of water expulsion or discharge, and consequently the rate of freezing of water, depends on the PSD of the porous matrix. It is also evident that two opposite effects are taking place as freezing of water progresses. First, the rate of ice propagation and water expulsion decreases; which, taken by itself, should generate lower hydraulic pressures. However, this may not happen because the effective permeability is also reduced. Whether or not the simultaneous occurrence of both effects cancels each other is not known. A simplified approach to answer this question is desirable.

## Observations

Sample G was left out of the analysis for the following reasons:

- A. Owing to its PSD with a big proportion of relatively large pores, a large volume of water was suddenly frozen at the beginning of freezing. Freezing and the corresponding volume increase were so fast, that it was not possible to take readings of volume changes as was done for sample P.
- B. Because of the phase change of water to ice, a considerable amount of heat was released which suddenly increased the temperature of the system. This temperature change may give rise to misleading temperature readings, which could invalidate the entire experiment.

Sample P did not show the first problem because it was mostly composed by relatively small capillary pores. In addition, the initial amount of frozen water was small enough that no large increment of temperature occurred. Despite such small values of initially frozen water and temperature increment, the first two readings appeared as outliers in the plot of residuals of the regression analysis. For that reason, they were rejected and excluded from further statistical analyses.

The total volume of frozen water in sample P at

$-30.8^{\circ}\text{C}$ , was equal to  $V_f = 4.19 \text{ cm}^3$ . Given that the total volume of vacuum absorbed water was  $V_T = 5.83 \text{ cm}^3$ , it means that  $V_{uf} = 1.64 \text{ cm}^3$  remained as unfrozen water at such minimum temperature. Three possible reasons are advanced to explain this findings. First, the minimum temperature applied,  $-30.8^{\circ}\text{C}$ , was not low enough to freeze the water absorbed in the finer capillaries. Second, the degree of saturation was less than 100%; therefore, part of the volume change was accommodated in the empty pores of the test specimen. The third reason is suggested by the inspection of Figure IV.5. In that figure, it appears that the last two or three points lie on a straight line which is parallel to the straight line representing the first stage of the freezing process. This may be indicative that all the freezable water has been frozen, and the volume  $V_{uf} = 1.64 \text{ cm}^3$  corresponds to unfreezable water, regardless of the minimum applied temperature.

It is possible that more than one of the previous reasons are involved in these results. However, the following discussion is presented in support of the third.

It is recognized that the properties of water adsorbed on a solid surface are different from those of bulk water (58). In particular the freezing point of water is substantially depressed, and for layers of water molecules close to the surface of the adsorbent, freezing may not occur at all. Powers and Brownyard (9) conducted several experiments in

order to estimate the thickness of the layer of unfreezable water adsorbed on cement paste; they found this thickness to be 7 to 10 Angstroms.

In this study, the thickness of unfrozen water was computed as follows:

$$t = \frac{V_{uf}}{S_A \cdot W_d} \quad 24$$

where

$V_{uf}$  = volume of unfrozen water  
 $S_A$  = specific surface area  
 $W_d$  = dry weight of testing specimen

In the present experiment, the specific surface of sample P is  $S_A = 15.5 \text{ m}^2/\text{gm}$ , as computed from the mercury intrusion data. Finally, after substituting values in equation (24) results that  $t = 8.4$  Angstroms. The reasonable agreement between this value and those values determined by Powers and Brownyard, seems to support the significance of the third reason to explain the volume of unfrozen water.

#### IV.4 Consideration About Frost Action in Connection with Rate of Ice Formation and Pore Structure

The rate of ice formation relative to a pore structure has been discussed based upon phenomenological considerations. In order to have a better insight of the mechanism of frost action in rocks, as it is influenced by the rate of

ice formation and pore structure, it is necessary to develop a quantitative approach relating these parameters.

In this section a simplified approach of the relationship between frost action, rate of ice formation, and pore structure is presented. The purpose of this approach is to estimate the magnitude of limiting pore diameters which are likely to control the occurrence of frost damage in porous building materials. After these values are estimated, significant general conclusions with respect to frost susceptibility can be drawn.

Because of its importance in the present analysis, the magnitude of the rate of ice propagation or rate of ice growth is discussed first. The rate of ice formation in bulk water is different from the rate of ice formation in small capillaries. Small capillaries give rise to freezing point depressions as was already discussed in this chapter; however, beyond a certain pore diameter such influence becomes negligible and water freezes close to  $0^{\circ}\text{C}$ . In this situation, the rate of ice formation in a saturated porous matrix is expected to occur as it does in bulk water.

In bulk water, the free growth of ice crystals has been reported to occur at a certain rate which depends on the extent of supercooling. Hillig and Thurnbull (59) conducted their experiments using glass tubes, and they found the rate to be



$$U_i = (0.158 \pm 0.009) \Delta T^{1.69 \pm 0.03} \text{ cm/sec} \quad 25$$

where

$\Delta T$  = extent of supercooling ( $^{\circ}\text{C}$ )

From experimental measurements Lindemeyer, Orrok, Jackson, and Chalmers (61) found that the rate of ice formation is not uniquely dependent on  $\Delta T$ , but "... the velocity depends upon whether the ice is growing freely in water or on a solid surface, and on the properties (presumably thermal diffusivity) of the solid". Given that the thermal diffusivities of glass and concrete are approximately the same, the rate of ice formation in both materials is expected to be within the same order of magnitude. Data reported by Helmuth (61), obtained with saturated cement paste samples, show reasonable agreement with the values predicted by equation (25). These data are used in subsequent computations in this section.

Owing to the relatively large pore diameters of most rocks, and the likely presence of surface ice on concrete structures such as pavements, a large extent of supercooling is not expected to take place. Assuming  $\Delta T = -2.7^{\circ}\text{C}$  implies, from Helmuth's determination, that the rate of ice propagation is  $U_i = 0.51 \text{ cm/sec}$ . This value is used in the following simplified analysis of the freezing process in rock samples.

### Basic Assumptions

1. Internal hydraulic pressure results due to viscous forces opposing the movement of water out of a test specimen.
2. Flow of water during freezing is unidirectional. This condition can be satisfied by fixing the geometry of the test specimen.
3. The porous matrix is characterized by a parallel model of tortuous tubes of uniform and single diameter  $d$ , and porosity  $\eta_o$ .

In Figure IV.8 is shown a testing specimen whose physical properties are known. The equilibrium conditions at failure due to freezing action can be stated as follows.

$$\Sigma F_z = 0: \quad \sigma_u A_T = \Delta P_H a_v \quad 26$$

where

$$\begin{aligned} \sigma_u &= \text{ultimate tensile strength} \\ \Delta P_H &= \text{hydraulic pressure at the center of the specimen} \\ A_T &= \text{gross area} \\ a_v &= \text{area of voids} \\ &= \eta_o A_T \\ \eta_o &= \text{porosity} \end{aligned} \quad (27)$$

According to the Poiseuille equation, assuming round pores and taking a tortuous flow into consideration, the

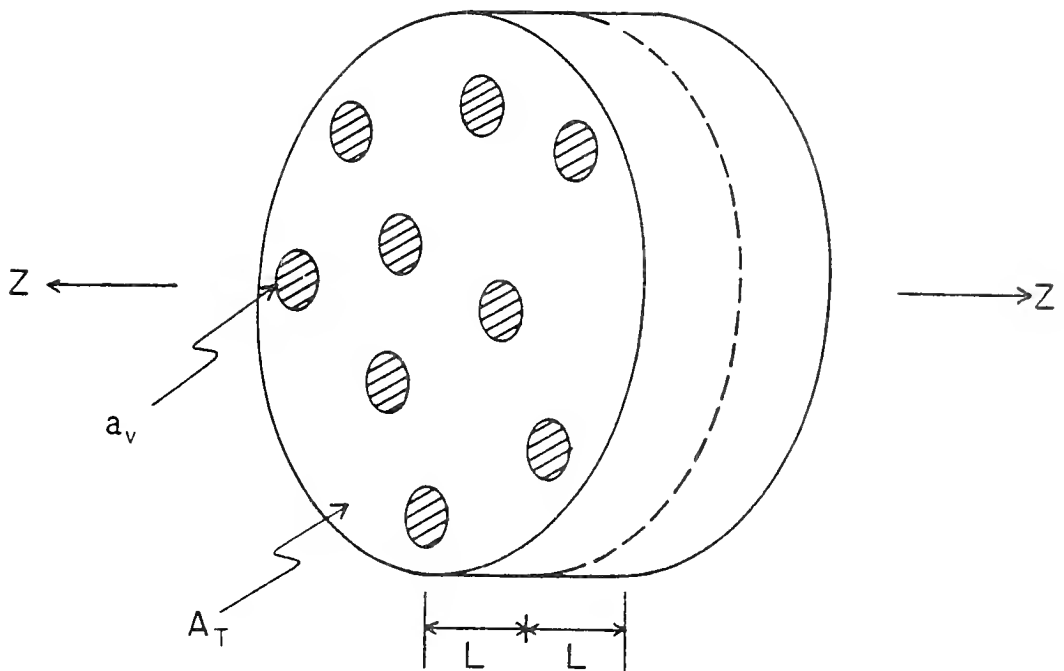


Figure IV.8 Rock Test Specimen

internal hydraulic pressure at the center of the specimen is:

$$\Delta P_H = \frac{32\mu K_t L U_i}{d_{cr}^2 10} \quad 28$$

where

- $\mu$  = viscosity
- $K_t$  = tortuosity factor
- $U_i$  = rate of ice formation
- $d_{cr}$  = critical pore diameter
- $L$  = half the thickness of the sample

Substituting (27) and (28) into (26) yields

$$\sigma_u A_T = \frac{32\mu K_t L}{d_{cr}^2} \cdot \frac{U_i}{10} \eta_o A_T$$

and finally

$$d_{cr}^2 = \frac{32\mu L U_i}{10\sigma_u} \eta_o K_t \quad 29$$

A preliminary parametric study or sensitivity analysis of the freezing process can be performed using equation (29). According to the purpose of this section, a limiting value  $d_{cr}$  was computed using the following values:

$$U_i = 0.51 \text{ cm/sec} \quad (\text{from reference 61})$$

$$\mu = 4 \times 10^{-5} \frac{\text{lb-sec}}{\text{ft}^2} \quad (\text{from reference 62})$$

$$\eta_o = 0.15, K_t = 5, \sigma_u = 1000 \text{ psi}$$

the viscosity value corresponds to  $-2^\circ\text{C}$ ; the last three values were estimated and are assumed to be reasonably

valid.

After computations, it is found that

$$d_{cr} = 1.15 \times 10^{-5} \sqrt{\bar{L}} \text{ (in)} \quad 30$$

Typical  $L$  values which occur in most practical situations are:  $1/4"$ ,  $3/8"$ ,  $1/2"$ , and  $3/4"$ , after substituting these values in equation (30) yields the following pore diameters:  $0.15\mu$ ,  $0.18\mu$ ,  $0.21\mu$ , and  $0.25\mu$ , respectively.

The freezing process giving rise to internal hydraulic pressures and corresponding tensile strains, is more complex than the ideal situation previously analyzed. In order to resemble reality more closely, a second approach is desirable; however, from the results of the more simplified case important inferences can be drawn regarding any rock sample. Assuming that the pore size distribution is known, then

- A. The range of sizes of the critical pore diameter, as it was analyzed, is small; for practical considerations a working value equal to  $0.2\mu$  may be used.
- B. A significant volume of pores whose diameter is smaller or equal than about  $0.2\mu$ , can be expected to give rise to high internal hydraulic pressures and severe deterioration by the critical distance mechanism.
- C. If the total volume of pores is composed by pore diameters larger than about  $2\mu$ , insignificant hydraulic

pressure of about 10 psi or less should develop. Under this condition, no failure of the testing specimen takes place by the critical distance mechanism. It should be noticed that  $d_u = 2\mu$  is the upper limiting diameter postulated in Chapter II.

- D. If the diameter of the total volume of pores is within the range from  $0.2\mu$  to  $2\mu$ , failure may occur depending on the total cumulative tensile strain that can be developed during freezing. This cumulative tensile strain depends on the entire pore size distribution.

For the sake of simplicity a parallel model and tortuous flow have been assumed; it has also been tacitly assumed that after freezing occurs, the ultimate strength  $\sigma_u$  is reached at once. Common building materials have a wide range of pore sizes, and the ultimate strength is reached sequentially as the temperature drops and the cumulative tensile strain tends toward the ultimate strain.

Despite the simplifying assumptions behind the present approach, the validity of the main concepts involved in the derivations are expected to give the reasonable order of magnitude to the results. The magnitude of the limiting diameter  $d_u$ , as it was defined and discussed in Chapter II, was found to be  $d_u = 2\mu\text{m}$  which is in reasonable agreement with the set of values obtained by Sweet (13), Blanks (14), Walker and Hsie (15), and Polach (16). In any case, the

present findings should be taken as working results that can be useful for further analyses of frost action in porous materials, as well as for reinterpretation of laboratory and field observations.

Based on the findings and discussions of this chapter, it is possible to identify three regions in the normal range of pore sizes of most building materials. These regions can be conventionally defined by taking into consideration the failure mechanisms postulated by Verbeck and Landgren (19). Assuming three rock samples of equal porosity and different pore size distributions, such as it is shown in Figure IV.9, they are likely to exhibit the responses indicated in Table IV.3.

Table IV.3 Potential Failure as it Depends on Pore Size Distribution (PSD)

PSD	Potential Type of Failure
I	Failure by the critical distance mechanism is the more likely to occur.
II	Additional theoretical analysis is required in order to make a reasonable prediction respect of the likelihood of failure.
III	Failure of surrounding matrix may occur by the expulsion mechanism.

Typical examples of building materials with well known frost susceptibility whose PSD is located in range I of Figure IV.9 are hardened cement pastes 28 days old and water

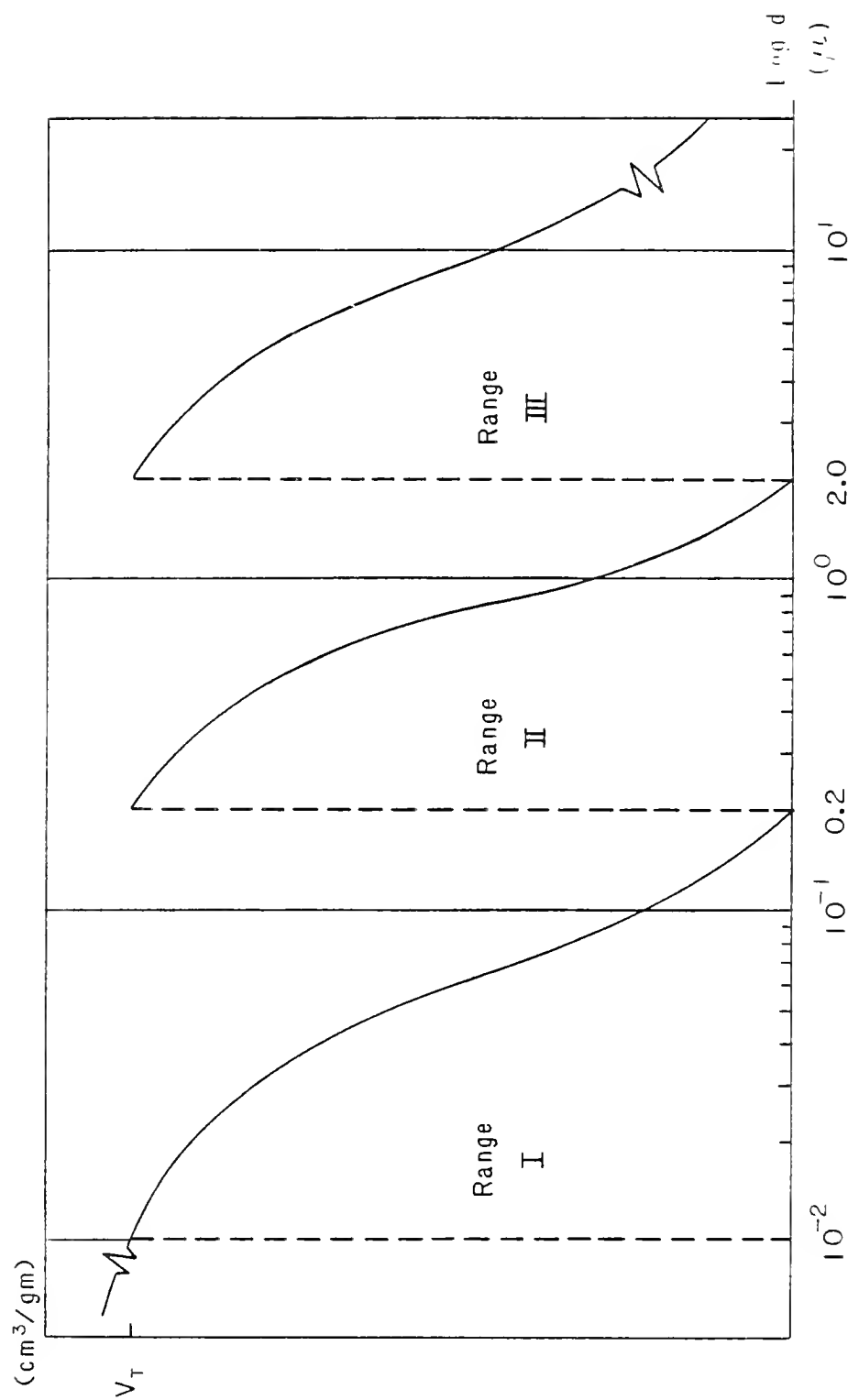


Figure IV.9 Rock Samples with Equal Porosity and Different Pore Size Distribution



cement ratio 0.60, reference (63). By the contrary, materials whose pore structure is mostly composed by large pores located in range III are slag aggregates, reference (22).

Most of the time concrete aggregates exhibit a wide range of pore sizes, and their pore structure is composed by different proportions of pores corresponding to the three ranges. In these cases, a significant volume of pores in ranges I and II is characteristic of frost non-resistant aggregates; by the contrary, insignificant volumes of pores in ranges I and II, and abundance of pores in range III are characteristic of frost resistant aggregates. The previous statement is supported by a close inspection of the results reported in reference (25), which are indicated in Table IV.4. Further evidence can be obtained analysing the PSD of the argillaceous aggregates studied by Shakoor (24).

Table IV.4 Volume of Pores in Ranges I, II, and III of Samples Taken from Reference (25)

Sample	$\epsilon \times 10^{-6}$ *	NDF**	$(\Delta V_I + \Delta V_{II})^{***}$	$\Delta V_{III}^{***}$
BR-3	>500	8.9	104.5	18.5
CC-1	131	36.0	4.9	105.7
K <sub>e</sub> -1	197	19.6	35.2	50.2
H-1	500	3.5	79.8	2.1
F-2	0	46.5	8.8	87.3
M <sub>c</sub> C	250	27.2	10.5	
BR-5	157	15.3		
BR-1	300	19.9		
PC-1	236	16.7	28.8	0.7
MB	194	35.6	23.7	7.0
K <sub>o</sub>	283	31.8	18.9	0.5
BM-1	0	78.1	3.0	0.6

\* Critical dilation, in/in

\*\* Normalized durability factor

\*\*\*  $\Delta V_i$  = intruded volume in the i-th range of pore sizes ( $\times 10^{-3}$  cc/gm)

CHAPTER V  
LABORATORY FROST SUSCEPTIBILITY  
OF BITUMINOUS SPECIMENS

V.1 Introduction

V.1.1 Statement of the Problem

The use of argillaceous aggregates in several bituminous pavements in Indiana has been very detrimental for their serviceability and structural integrity. It has been found that some of these bituminous pavements experienced serious damage within a period of one to two years. The extent of damage made resurfacing necessary in some cases. Shakoor (24) described one typical failure that took place as follows:

"Aggregate from Ledge 6 of quarry L, the upper few feet of which are quite argillaceous, was used in this road. Again, there was a rapid break up of this aggregate and the broken particles continued to come loose. Pitting of the pavement surface was the dominant mode of failure."

In addition, the same author pointed out that the application of deicing salts played an important role in such a type of failure.

It is important to conduct further studies of this problem because of the depletion of excellent aggregate sources, which stresses the need for using aggregate sources including varying percentages of deleterious materials, i.e. argillaceous aggregates.

#### V.1.2 Statement of Objectives

The fact that bituminous pavements were the most affected by the argillaceous aggregates under consideration suggested the following approach. It was decided to study the problem under laboratory conditions first, and then, based on those findings, to propose some recommendations for additional studies under actual field exposure. The laboratory study was guided by two questions

1. What are the most influential factors in the type of failure taking place?
2. Is it possible to use small percentages of argillaceous aggregates in surface layers of bituminous pavements, without having excessive deterioration?

In order to obtain alternative answers to those questions, the following objectives were stated in this part of the study:

1. To investigate the relative effect of asphalt content and percent of deleterious aggregates on the frost resistance of bituminous specimens.

2. To propose some recommendations for future studies of the problem under field exposure.

## V.2 Experimental Work

An experimental study was designed to determine the relative effect of asphalt content (A) and percentage of deleterious aggregates (P) on the frost resistance of bituminous specimens. It was suspected that the larger the asphalt content the more protected unsound aggregates are to become water-saturated. Based on practical considerations, two levels of asphalt content were included in this experiment: 4% and 6%. The relative effect of different percentages of "poor", "marginal", and "good" aggregates on frost resistance is more difficult to study. For instance, considering the following questions

1. How much "poor" and "good" aggregates can be safely combined in order to obtain an acceptable frost resistance?
2. How much "marginal" and "good" aggregates can be safely combined in order to obtain an acceptable frost resistance?

there are no answers to these questions. The difficulty for dealing with this problem results because, at the present time, there is not a proper rating scale to quantify the adjectives "poor", "marginal", etc. based on specific

aggregate properties. Despite the present situation, it is possible to restate the problem to obtain useful Limiting Values by combining two aggregates with well known durability history. One with excellent frost resistance and another with poor frost durability, such as a highly argillaceous aggregate.

#### V.2.1 Statistical Design and Analysis of the Experiment

In this section a completely randomized experiment is presented to investigate the significance of asphalt content, percent of deleterious aggregates, and number of freeze-thaw cycles on the resistance of bituminous specimens. The factors, factor levels, and response variables under consideration were as follows

Factors	Factor Levels
Asphalt Content (A)	4%, 6%
Deleterious Aggregates % (P)	0, 30%, 50%, 70%
No. of F & T Cycles (N)	50, 73

treatment combinations =  $2 \times 4 \times 2$

test specimens =  $16 \times 2$

#### Response Variables

Marshall Test (MT)

Pulse Velocity Test (PV)

The mathematical model for this completely randomized design is given by

$$Y_{ijk} = \mu + A_i + P_j + AP_{ij} + N_k + AN_{ik} + NP_{jk} + ANP_{ijk} + \epsilon_{(ijk)L} \quad 22$$

$$i = 1, 2 \quad j = 1, 2, 3, 4 \quad k = 1, 2 \quad L = 1, 2$$

where

$Y_{ijkL}$  = the response from the L-th specimen made of i-th asphalt content, the j-th percent of deleterious aggregates and tested at the k-th number of F & T cycles

$\mu$  = overall mean

$A_i$  = effect of the i-th asphalt content  
(fixed)

$P_j$  = effect of the j-th aggregate percent  
(fixed)

$AP_{ij}$  = effect of the interaction of the i-th asphalt content with the j-th aggregate percent

$N_k$  = effect of the k-th number of cycles  
(fixed)

$AN_{ik}$  = effect of the interaction of the i-th asphalt content with the k-th number of cycles

$NP_{jk}$  = effect of the interaction of the j-th aggregate percent with the k-th number of cycles

- $ANP_{ijk}$  = effect of the interaction of the i-th asphalt content with the j-th aggregate percent and the k-th number of cycles
- $\epsilon_{(ijk)L}$  = random error of the L-th specimen in the combination of the i-th asphalt content, with the j-th aggregate percent, with the k-th number of cycles.

The analysis of variance corresponding to the previous model is given in Table V.1.

Table V.1 ANOVA Using Equation (22)

Source	d.f.	EMS
Asphalt Content ( $A_i$ )	1	$\sigma^2 + 16\phi(A)$
Unsound Aggregate % ( $P_j$ )	3	$\sigma^2 + 8\phi(P)$
$AP_{ij}$	3	$\sigma^2 + 8\phi(AP)$
Number of Cycles ( $N_k$ )	1	$\sigma^2 + 16\phi(N)$
$AN_{ik}$	1	$\sigma^2 + 8\phi(AN)$
$NP_{jk}$	3	$\sigma^2 + 4\phi(NP)$
$ANP_{ijk}$	3	$\sigma^2 + 2\phi(ANP)$
Experimental Error	16	$\sigma^2$
Total	31	

From the inspection of the ANOVA table, it is observed that the statistical significance of all main effects and



factor interactions is tested using the error term.

#### V.2.2 Materials and Test Specimens

Two aggregate samples were used for making the test specimens used in this experiment. One aggregate sample was highly resistant to freezing and thawing action. The second aggregate sample was obtained from a single argillaceous ledge of very poor resistance to freezing and thawing. The physical properties of this Ledge were thoroughly studied by Shakoor, and it was identified as Ledge 5 of Quarry K, in reference (24).

Large pieces of rock were obtained from Ledge 5, and they were crushed and sieved in the laboratory for the purpose of getting the proper aggregate gradation. Such aggregate gradation corresponds to a surface mixture Type II, No. 9 as it is designated in the Standard Specifications of the State of Indiana (65). Given that the smaller sizes are not expected to be influential in the frost damage, only the two larger sizes of the entire gradation were taken into consideration in this study. For instance, a combination of 70% argillaceous aggregates and 30% excellent aggregates means that 70% of the total weight of 1/2" and 3/8" sizes is argillaceous, and the other 30% is frost resistant. The same frost resistant aggregate of the remaining sizes was used in all the test specimens.

Asphalt AC-20 was used in all the mixes in 4% and 6% contents as it was indicated in the experimental design. The test specimens were of the standard size corresponding to the Marshall Test, 4 in. diameter and 2-1/2 in height. All the specimens were made according to the standard designation ASTM D 1559. The order in which the specimens were fabricated was completely at random.

#### V.2.3 Conditioning and Testing of Specimens

Three days after the specimens were made, they were immersed in water for 48 hours before the application of freezing and thawing cycles. The typical freeze-thaw cycle applied in this experiment was according to the standard procedure ASTM C666-A. The extent of deterioration at different number of cycles was monitored by pulse velocity measurements. As the internal cracking of the test specimen increases, the time that an impulse takes to go through the specimen also increases. The readings from this testing procedure are given in microseconds, and the details for performing the test are discussed in the standard ASTM D 2845. The order in which the specimens were tested was completely at random.

#### V.2.4 Experimental Results

Stability values were determined first after 50 freezing and thawing cycles, and then at 73 cycles some specimens were severely deteriorated. Stability values were

determined as it is indicated in ASTM Designation D 1559, except for the testing which was performed at room temperature.

The experimental results corresponding to stability values and pulse velocity determination for all the test specimens are shown in Table V.2 and Table V.3 respectively. In Table V.3 the percent change in pulse velocity respect to the initial pulse velocity reading of each specimen are shown. Such percent was computed as follows

$$P_n = \frac{PV_n - PV_o}{PV_o} \times 100$$

where

$PV_o$  = initial pulse velocity reading ( $\mu$  sec)

$PV_n$  = pulse velocity after n freeze-thaw cycles  
( $\mu$  sec)

Table V.2 Stability Values (Lbs.)

		No. of Cycles			
		50		73	
		Asphalt Content	Asphalt Content	Asphalt Content	Asphalt Content
		4%	6%	4%	6%
Deleterious Aggregates	0%	8718	8383	8051	7945
		7304	8689	7862	7528
	30%	7712	7859	8454	7945
		7816	7970	7820	8209
	50%	8453	7454	6402	7825
		6454	7616	6950	7637
	70%	7648	8106	5610	7323
		7433	7760	6297	7030

Table V.3 Pulse Velocity Determinations (% change)

		No. of Cycles			
		50		73	
		Asphalt 4%	Content 6%	Asphalt 4%	Content 6%
Deleterious Aggregates	0%	11.0	3.6	5.1	6.0
		6.5	5.7	0.0	6.4
	30%	9.8	7.6	13.1	0
		20.0	6.3	7.6	12.2
	50%	26.1	9.8	32.5	5.0
		8.2	13.3	5.4	20.0
	70%	12.3	4.1	70.0	14.1
		28.0	2.6	39.2	3.0

Table V.4 ANOVA for Data Shown in Table V.2

Source	d.f.	S.S.	M.S.	F
$A_i$	1	1'241,888	1'241,888	5.04*
$P_j$	3	4'897,172	1'632,391	6.62**
$AP_{ij}$	3	760,839	253,613	1.03
$N_k$	1	1'311,390	1'311,390	5.32*
$AN_{ik}$	1	90,951	90,951	0.37
$NP_{jk}$	3	2'107,882	702,627	
$ANP_{ijk}$	3	1'024,090	341,363	1.39
Error	16	3'943,335	246,458	
Total	31	15'377,548		

\*Significant at the 5% level.

\*\*Significant at the 1% level.

Table V.5 ANOVA for Data Shown in Table V.3

Source	d.f.	S.S.	M.S.	F
$A_i$	1	958.1	958.1	10.4**
$P_j$	3	1,172.8	390.9	4.2*
$AP_{ij}$	3	1,164.1	388.0	4.2*
$N_k$	1	130.8	130.8	1.4
$AN_{ik}$	1	43.5	43.5	0.47
$NP_{jk}$	3	684.4	228.1	2.48
$ANP_{ijk}$	3	421.5	140.5	1.52
Error	16	1,474.2	92.1	
Total	31	6,049.4		

---

\*Significant at the 5% level.

\*\*Significant at the 1% level.

### V.3 Analysis and Interpretation of Results

In order to test the statistical significance of each of the factors under consideration, i.e. asphalt content (A), percent of deleterious aggregates (P), and number of freeze-thaw cycles (N), an analysis of variance was performed. The results of the analysis using the stability values are shown in Table V.4; in Table V.5 the results of the analysis of pulse velocity determinations are shown.

The analysis of variance performed with the stability values suggests the following observations:

1. All the main factors were found statistically significant at least at the  $\alpha = 0.05$  level of significance; by the contrary, second order and third order interactions were not found significant. Asphalt content (A) had a significant effect on the frost resistance of the test specimens, at the  $\alpha = 0.05$  level of significance. The percent of deleterious aggregate was found the most significant on the frost resistance of the bituminous specimens, at the  $\alpha = 0.01$  significance level. Finally, the frost resistance of the test specimens at 50 freezing and thawing cycles was significantly different from their frost resistance after 73 cycles.
2. Further details of the effects of A, P, and N on the frost resistance of the test specimens, can be observed in Figure V.1. Particularly important are
  - a. After the application of 50 freezing and thawing cycles, no significant damage was inspected on any of the test specimens, regardless of the asphalt content and the percent of deleterious aggregates. After 73 cycles, a varying extent of deterioration could be inspected including a few specimens almost disintegrated. The application of freezing and thawing cycles was stopped at 73 cycles.
  - b. After 73 freezing and thawing cycles were applied, deleterious aggregates in percentages smaller than

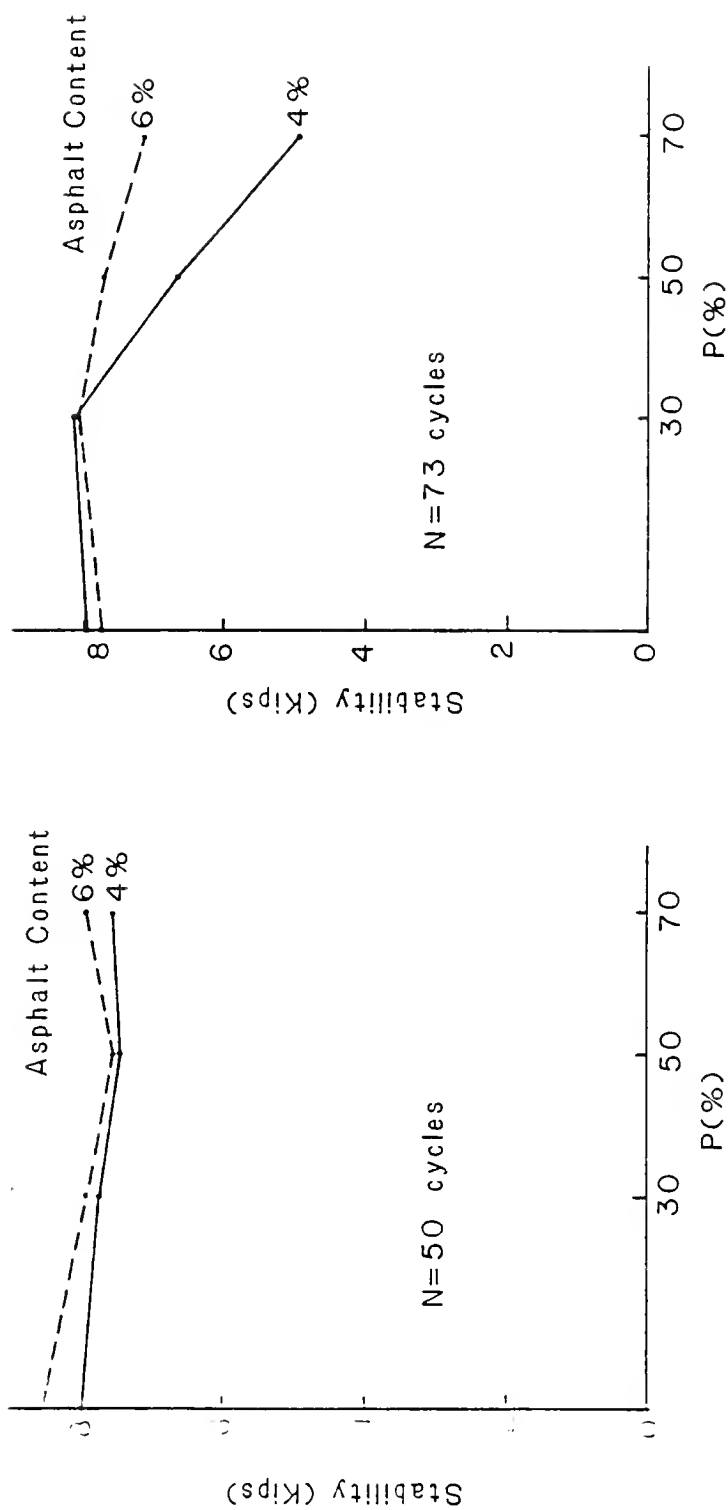


Figure V.1 Marshall Tests Results

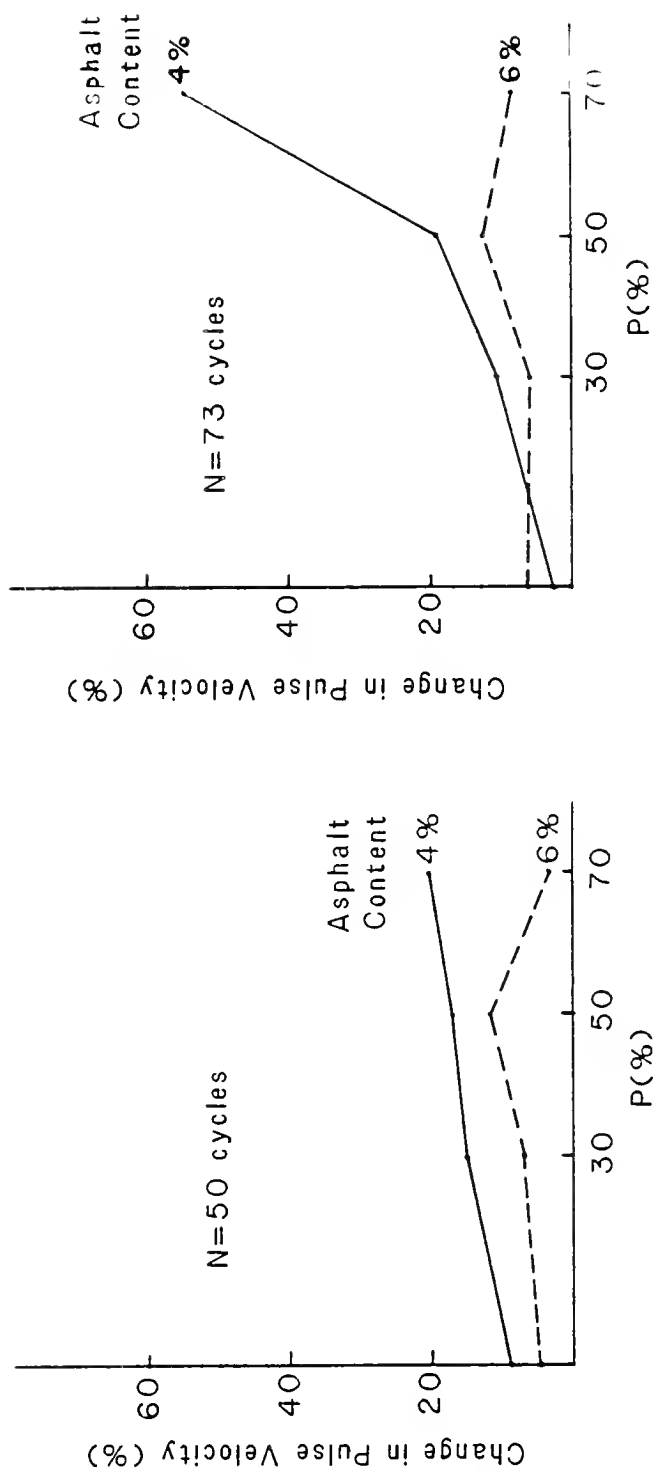


Figure V.2 Pulse Velocity Results. First Experiment



30% did not have any effect on the frost resistance of the test specimens regardless of the asphalt content. By the contrary, the asphalt content had a significant effect on frost resistance whenever the percent of deleterious aggregates was 50% and 70%. The larger the asphalt content the more frost resistant the specimens were. In Figure V.1 the relative effect of 6% and 4% asphalt content on frost resistance can be observed. For 4% asphalt content a severe reduction in frost resistance occurred.

A second analysis of variance was performed with the pulse velocity determinations. From the results shown in Table V.5 and in Figure V.2, the following observations are pertinent.

1. Two main factors, A and P, and one second order interaction AP, were found statistically significant at least at the  $\alpha = 0.05$  level of significance.
2. Except for some minor discrepancies, it seems that the same observations can be made from the analyses of stability values and pulse velocity determinations. However, the ability of the pulse velocity test to detect frost damage is apparent only after deterioration is self evident.

#### V.4 Recommendations for Further Studies Under Field Exposure

The laboratory experiment previously described provides limiting working values which can be used in the design of field test sections. In addition to verify and improve the laboratory findings, field test sections can be designed to investigate the effects of deicers and actual field exposure on the frost resistance of bituminous pavements. Likewise, the effect that deleterious aggregates in deeper layers have on the frost resistance of pavements can also be investigated.

The fact that at the present there is no adequate scale for rating varying frost resistant aggregates, imposes serious limitations to any experimental design to study the frost resistance of bituminous mixes in the field. However, if the usefulness of limiting values is recognized some practical recommendations may result from a field test section.

## CHAPTER VI

### SUMMARY AND CONCLUSIONS

#### VI.1 Summary

In this investigation the disruptive effects of coarse aggregates in concrete and bituminous pavements exposed to freezing and thawing action have been studied. For this purpose, two main approaches were used: Statistical Analysis of observational data and the Experimental Method. The particular problems of identifying frost non-resistant aggregates, and the determination of permissible amounts to be used when they are combined with sound aggregates were also discussed.

Argillaceous aggregates that give rise to severe surface deterioration of concrete pavements, and to almost complete failure of bituminous pavements were also investigated. Their typical pore size distribution was found to include a significant fraction of pores smaller than  $0.06\mu$  diameter. Such a fraction of pores is responsible for the generation of high osmotic pressures in the presence of deicers and freezing conditions. Osmotic pressure was identified as a significant source of deterioration whenever

these argillaceous aggregates are used in concrete and bituminous pavements exposed to deicers.

A simplified analysis of frost action in rocks provided results to identify three ranges of pore diameters, which are associated with the main failure mechanisms recognized at the present. These results are in agreement with the values that other authors determined by different approaches.

The tensile and compressive strengths of portland cement concrete are larger than those of bituminous concrete; this fact makes bituminous concrete potentially less resistant to the deleterious action of frost susceptible aggregates. In addition, the increased rigidity of bituminous concrete due to temperature drops, makes it more sensitive to the internal cracking of coarse aggregates. These differences between concrete and bituminous mixes seem to be responsible for a poor response of the latter, whenever argillaceous aggregates are used. This poor response is accentuated by the action of deicing salts on the surface layer; however, in interior layers not exposed to deicer, the same argillaceous aggregates can be expected to perform better.

The identification of frost susceptible aggregates has been a major concern for long time, and for that purpose several of their physical properties have been studied.

Sometimes, using one or more physical properties, the performance of an aggregate by itself or its performance in concrete have been predicted accurately, but at other times the predictions have been inaccurate. Lack of consistency has been the major problem of most of the recommended procedures.

According to what has been discussed in the context of this investigation, particularly in chapters II, III, and IV, the following physical properties are proper for further consideration:

1. Absorption
2. Adsorption.
3. Osmotic phenomenon.
4. Pore structure.

All these physical properties, except osmosis, have been used in the past to identify aggregates susceptible to freezing and thawing. Water absorption has been the simplest test to assess the potential frost susceptibility of concrete aggregates; however its predictions are highly inconsistent and unreliable. Such inconsistency can be alternatively explained according to Figure III.9. For instance, assume a concrete aggregate whose absorption is 2%, for most standards this aggregate may be accepted; however, such an aggregate can give rise to completely

different responses to frost action depending on its pore structure. If its pore size distribution is located in range III, the aggregate is likely to be harmless; on the contrary, if it is located in range I it is likely to be highly deleterious.

In order to take account of the inconsistency of the absorption test, an alternative procedure was recommended by the PCA including the adsorption of the aggregate. Using the vacuum absorption and the magnitude of the adsorption at 92% relative humidity, an acceptance-rejection border line was empirically defined. Despite this modification, the consistency between predictions and actual performance remains questionable. At 92% relative humidity the only pore sizes filled with water are those smaller than about  $0.03\mu$ . Freezing of the entire volume of water in these pores is most unlikely, because very low temperatures are required. Therefore, only a fraction of that volume of water is capable of producing damage by the critical distance mechanism. Assuming a minimum field temperature of  $-20^{\circ}\text{C}$ , all the water in pore sizes smaller than about  $0.01\mu$  would remain unfrozen. Consequently, the only volume of freezeable water is that fraction between about  $0.01\mu$  and  $0.03\mu$ , whose magnitude is unknown and confounded with the total adsorption value. Another disadvantage of this procedure is that most of the critical pore sizes, as it was discussed in Chapter III, are not taken into consideration by the

adsorption determinations. These are some reasons why the PCA test is likely to give inconsistent results regarding the performance of concrete aggregates exposed to frost action.

The complexity of the freezing and thawing action in rocks makes unlikely the correct classification of aggregates 100% of the time. However, if the results of experimental studies and theoretical analyses are combined, it is possible that aggregates of unknown performance will be correctly classified with acceptable frequency.

In this section, before the main conclusions are indicated, a sequential procedure is offered for the acceptance or rejection of aggregates with unknown performance under freezing and thawing action. The procedure is based on the findings of this investigation and on well known facts concerning frost action. First, the postulation of two failure mechanisms makes it necessary to recognize the existence of two permissible absorption values instead of one:

- A. There is one permissible absorption value whenever failure is expected to occur by the critical distance mechanism. From theoretical considerations, Verbeck and Landgren found

$$W_{EA} = 0.3\%$$

which was computed from the volume change that can be permitted by elastic accommodation.

B. Another permissible absorption value should be applied if failure is likely to occur by the expulsion into the paste mechanism. Assuming a concrete mix with 1" maximum size and 5% entrained air, such value is approximately

$$W_{EX} = 4.0\%$$

Second, according to the theory of capillary condensation, it is possible to estimate the volume of pores in which water is unlikely to freeze and to estimate the volume of pores within the most critical size range between  $0.01\mu$  and  $0.2\mu$ . These volumes of pores can be estimated by measuring absorbed water at 75% and 97% relative humidities. After these values, as well as the total absorption, are known better inferences can be drawn about the susceptibility of coarse aggregates to freezing and thawing.

A possible decision making process for accepting or rejecting aggregates with unknown performance would start with these two simple tests. If no strong conclusion can be made using such test results, then the osmotic pressure test can be done in order to reinforce any preliminary conclusion and to provide additional information about the effect of deicers on the aggregate. Finally, if still no decision can be made, a mercury porosimetry test is desirable to obtain the entire pore size distribution and thereby the discriminant score of the aggregate. After the discriminant score is computed, as it was described in Chapter II, the



aggregate can be classified. A decision making sequence is presented in Figure VI.1; the symbology used in that figure is defined as follows:

$W_T$  = aggregate absorption (%)

$W_{75}$  = percent adsorption at 75% relative humidity  
( $d < 0.01\mu$ )

$W_{97}$  = percent adsorption at 97% relative humidity  
( $d < 0.1\mu$ )

$W_F$  = freezable water content (%) at  $20^{\circ} \text{C}$   
 $= W_T - W_{75}$

$\Delta W_n$  = water content (%) in critical size range  
 $= W_T - W_{75}$

$W_{EA}$  = 0.3%

$W_{EX}$  = 4%

$\Omega$  = to be estimated by further research

$D$  = discriminant core

## VI.2 Conclusions

The discussions and conclusions corresponding to each part of this investigation were presented at the end of each chapter, and for that reason they are not repeated in this section; however, taking all the findings together, the following major conclusions seem pertinent.

1. Direct measurements of the details of pore structure, instead of summary parameters, seem to correlate better with alternative indices of frost susceptibility.

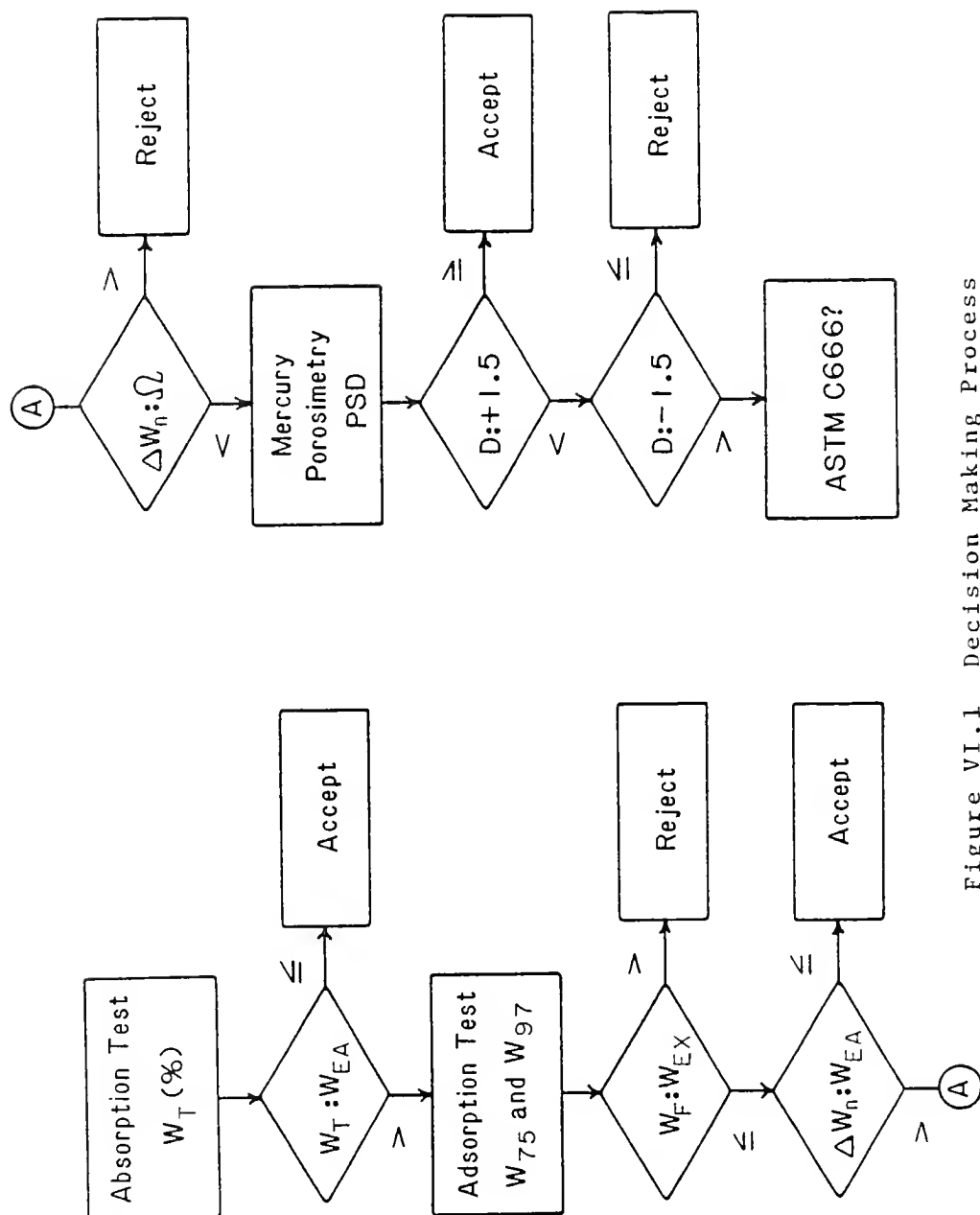


Figure VI.1 Decision Making Process

2. Rock samples with a significant volume of pore sizes smaller or equal than about  $0.06\mu$  are able to act as semipermeable membranes and osmosis can take place. In the presence of deicers, the argillaceous aggregates under investigation are capable of developing osmotic pressures which give rise to surface failure of concrete and bituminous pavements.
3. Based on phenomenological considerations and empirical results, it was found that freezing rate is not an absolute quantity, but it depends on pore structure. Such influence is more accentuated as the capillary pore size decreases.

## REFERENCES

## REFERENCES

1. Rhoades, R. and Mielenz, R.C., "Petrography of Concrete Aggregates, Proceedings, American Concrete Institute Journal, No. 6, Vol. 42, 1946, p. 581.
2. Lewis, D.W., Dolch, W.L., and Woods, K.B., "Porosity Determinations and the Significance of Pore Characteristics of Aggregates," Proceedings, American Society for Testing and Materials, Vol. 53, 1953, p. 449.
3. Dolch, W.L., "Permeability and Absorptivity of Indiana Limestone Coarse Aggregates," Ph.D. Thesis, Purdue University, 1956.
4. Dolch, W.L., "Studies of Limestone Aggregate by Fluid-Flow Methods, Proceedings, American Society for Testing and Materials, Vol. 59, 1959, p. 1204.
5. Dolch, W.L., "Porosity", Chapter 37, ASTM STP 169B, American Society for Testing and Materials, 1980, p. 646.
6. Powers, T.C., "A Working Hypothesis for Further Studies of Frost Resistance of Concrete," Proceedings, American Concrete Institute Journal, Vol. 41, 1945, p. 245.
7. Powers, T.C. and Helmuth, R.A., "Theory of Volume Changes in Hardened Portland Cement Paste During Freezing," Proceedings, Highway Research Board, Vol. 32, 1953, p. 285.
8. Powers, T. C., "Basic Considerations Pertaining to Freezing and Thawing Tests," Proceedings, American Society for Testing and Materials, Vol. 55, 1955, p. 1132.
9. Powers, T.C. and Brownyard, T.L., "Studies of the Physical Properties of Hardened Portland Cement Paste," Proceedings, American Concrete Institute Journal, Part 8, Vol. 43, 1947, p. 933.
10. le Sage de Fontenay, C. and Sellevold, E.J., "Ice Formation in Hardened Cement Paste-I. Mature Water-

- Saturated Pastes," Durability of Building Materials and Components, ASTM STP 691, American Society for Testing and Materials, 1980, pp. 425-438.
11. Kaneuji, M., Winslow, D.N., and Dolch, W.L., "The Relationship Between and Aggregate's Pore Size Distribution and its Freeze-Thaw Durability in Concrete," Cement and Concrete Research, Vol. 10, 1980, pp. 433-441.
  12. Litvan, G.G., "Pore Structure and Frost Susceptibility of Building Materials," Proceedings, RILEM/IUPAC Conference on Pore Structure and Properties of Materials, Prague, Vol. 2, 1973, p. F-17.
  13. Swenson, H.S., "Research on Concrete Durability as Affected by Coarse Aggregates," Proceedings, American Society for Testing and Materials, Vol. 48, 1948, p. 988.
  14. Blanks, R.F., "Modern Concepts Applied to Concrete Aggregates," Proceedings, American Society of Civil Engineers, Vol. 75, 1949, p. 441.
  15. Walker, A.D. and Hsien, T., "Relationship Between Aggregate Pore characteristics and Durability of Concrete Exposed to Freezing and Thawing," Highway Research Record 226, 1968, p. 41.
  16. Polach, J., "A Study on the Relationship Between Frost Resistance and Porosity of Heavy Clay Materials," Proceedings, RILEM/IUPAC Conference on Pore Structure and Properties of Materials, Prague, Vol. 2, 1973, p. F-63.
  17. Gorge, H. and Modry, S., "Determination of the Frost Resistance of Limestone Aggregates in the Light of Porosity Investigations," RILEM, International Symposium on Durability of Concrete, Prague, 1970, p. B-129.
  18. Koh, Y. and Kamada, H., "The Influence of Pore Structure of Concrete Made with Absorptive Aggregates on the Frost Durability of Concrete," Proceedings, RILEM/IUPAC Conference on Pore Structure and Properties of Material, Prague, Vol. 2, 1973, p. F-45.
  19. Verbeck, G. and Landgren, R., "Influence of Physical Characteristics of Aggregates on Frost-Resistance of Concrete," Proceedings, American Society for Testing and Materials, Vol. 60, 1960, p. 1063.
  20. Scholer, C.F., "Durability of Concrete," Proceedings, Highway Research Board, Vol. 10, 1930, p. 132.

21. Brown, R.H., "Pore Studies of Carbonate Aggregates by an Evaporation Technique," Ph.D. Thesis, Purdue University, 1968.
22. Lindgren, M.N., "The Prediction of Freeze-Thaw Durability of Coarse Aggregate in Concrete by Mercury Intrusion Porosimeter," M.S. Thesis, Purdue University, 1980.
23. Maage, M., Discussion, Proceedings, American Concrete Institute Journal, Vol. 81, No. 2, 1983. p. 305.
24. Shakoor, A., "Evaluation of Methods for Predicting Durability Characteristics of Argillaceous Carbonate Rock," Ph.D. Thesis, Purdue University, 1982.
25. Kaneuji, M., "Correlation Between the Pore Size Distribution and Freeze-Thaw Durability of Coarse Aggregate in Concrete," Ph.D. Thesis, Purdue University, 1978.
26. Campbell, N., "What is Science," Dover Publications, 1953.
27. Stevens, S. S., "On the Theory of Scales of Measurement," Chapter 1, in "Contemporary Problems in Statistics," B. Lieberman, editor, 1971.
28. Nunnally, J. C., "Psychometric Theory," McGraw Hill, 1978.
29. Klieger, P., Monfore, G., Stark, and Teske, W., "D-Cracking of Concrete Pavements in Ohio, Portland Cement Association, Report No. OHIO-DOT-11-74, 1974.
30. Hartgen, D.T., Shufon, J.J., Parrella, F.T., and Koepel, K., "Visual Scales of Pavement Condition: Development, Validation and Use," Transportation Research Record 893, 1981, p. 1.
31. Cooley, W. W. and Lohnes, P. R., "Multivariate Data Analysis," New York, Wiley, 1971.
32. Nie, N. H., Hull, C. H., Jenkins, J. G., Steinbrenner, K., Bent, D. H., "Statistical Package for the Social Sciences," McGraw Hill, 1975.
33. Walker, R.D., Pence, H.J., Hazlett, W.H., and Ong, W.J., "One-Cycle Slow-Freeze Test for Evaluating Aggregate Performance in Frozen Concrete," NCHRP Report 65, Highway Research Board, 1969.
34. Cordon, W.A., "Freezing and Thawing of Concrete - Mechanisms and Control," American Concrete Institute

Monograph No. 3, 1966, p. 99.

35. Verbeck, G.J. and Klieger, P., "Studies of 'Salt' Scaling of Concrete," Highway Research Board, Bulletin 150, 1956.
36. Klieger, P., "Durability Studies at the Portland Cement Association," Durability of Building Materials and Components, ASTM STP 691, American Society for Testing and Materials, 1980, p. 283.
37. Litvan, G.G., "Frost Action in Cement in the Presence of De-Icers," Cement and Concrete Research, Vol. 6, 1976, pp. 351-356.
38. Rosli, A. and Harnik, A.B., "Improving the Durability of Concrete to Freezing and Deicing Salts," Durability of Building Materials and Components, ASTM STP 691, American Society for Testing and Materials, 1980, p. 464.
39. Browne, F. and Cady, P., "Deicer Scaling Mechanisms in Concrete," SP 47-6, American Concrete Institute.
40. Harnik, A.B., Meier, U., and Rosli, A., "Combined Influence of Freezing and Deicing Salts on Concrete-Physical Aspects," Durability of Building Materials and Components, ASTM STP 691, American Society for Testing and Materials, 1980, p. 474.
41. Hartmann, E., "Effect of Frost and De-Icing Salts on Concrete with and without Air Entraining Agents," Zement-Kalk-Gips, Vol. 10, 1957, pp. 265-281, 314-323.
42. Snyder, M.J., "Protective Coatings to Prevent Deterioration of Concrete by, Deicing Chemicals," NCHRP Report 16, Highway Research Board, 1965.
43. Kesting, R. E., "Synthetic Polymeric Membranes," McGraw Hill, 1971.
44. Verbeck, G.J. and Gramlich, C., "Osmotic Studies and Hypothesis Concerning Alkali-Aggregate Reaction," Proceedings, American Society for Testing and Materials, Vol. 55, 1955, p. 1110.
45. Indiana Department of Highways, Materials and Test Division, "Proposed Modification of Freeze-Thaw Soundness Tests of Coarse Aggregates," Personal Communication, 1980.
46. National Research Council, "Minimizing Deicing Chemical Use," NCHRP, Synthesis of Highway Practice 24, 1974.



47. Powers, T. C., "The Mechanism of Frost Action in Concrete," Stanton Walker Lecture No. 3, National Sand and Gravel Association, Silver Spring, Maryland, 1965.
48. Dorsey, N.E., "Properties of Ordinary Water Substance," Reinhold Publishing Corp., 1940.
49. Chalmer, B., "
50. Turnbull, D., "The Undercooling of Liquids," Scientific American, January 1965, p. 38.
51. Wylie, R.G., "The Freezing of Supercooled Water in Glass," Proc. Phys. Soc. (London) B65, 1952, p. 241.
52. Kubelka, P., Z. Electrochem, Vol. 38, 1932, p. 611.
53. Sill, R.C. and Skapski, A.S., "Method for the Determination of the Surface Tension of Solids from their Melting Points in thin Wedges," Journal of Chem. Phys., Vol. 24, 1956, p. 645.
54. Blachere, J.R. and Young, J.E., "The Freezing Point of Water in Porous Glasses," Journal, American Ceramic Society, Vol. 55, 1972, p. 306.
55. Williams, P.J., "Properties and Behavior of Freezing Soils," Norwegian Geotechnical Institute, Publ. No. 72, Oslo, 1967.
56. Fagerlund, G., "Determination of Pore-Size Distribution from Freezing-Point Depression," Materials and Structures, Vol. 6, No. 33, 1973, p. 215.
57. Dolch, W.L., Personal Communication, 1983.
58. Drost-Hansen, W., "Structure of Water Near Solid Interfaces," Proceedings, Industrial and Engineering Chemistry, Vol. 61, No. 11, 1969, p. 10.
59. Hillig, W.B. and Turnbull, D., "Theory of Crystal Growth in Undercooled Pure Liquids," Journal of Chem. Phys., Vol. 24, 1956, p. 914.
60. Lindenmeyer, C.S., Orrok, G.T., Jackson, K.A., and Chalmers, B., "Rate of Growth of Ice Crystals in Supercooled Water," Journal of Chemical Physics, Vol. 27, No. 3, 1957, p. 822.
61. Helmuth, R.A., "Capillary Size-Restrictions on Ice-Formation in Hardened Portland Cement-Pastes," Proceedings, Vol. II, 4th International Symposium on Chemistry of Cement, Washington, D.C., 1960, p. 855.

62. Weast, R. C., editor, "Handbook of Chemistry and Physics," CRC Press, 58th edition, p. F-49, 1977-1978.
63. Winslow, D.N. and Diamond, S., "A Mercury Porosimetry Study of the Evolution of Porosity in Portland Cement," Journal of Materials, Vol. 5, No. 3, 1970, p. 564.
64. The Asphalt Institute, "Mix Design Methods for Asphalt Concrete and Other Hot Mix Types," Manual Series No. 2, March 1979.
65. Indiana State Highway Commission, "Standard Specifications," Indianapolis, Indiana, 1971.

## APPENDICES

## APPENDIX A

Physical Properties of Selected Samples

In this appendix some of the physical properties of samples P and G are given. The vacuum absorption, specific gravity, and specific surface of sample P are: 4.43%, 1.73, and 15.53  $\text{m}^2/\text{g}$  respectively. The same physical properties of sample G are: 9.0%, 2.72, and 1.53  $\text{m}^2/\text{g}$  respectively. The physical properties of sample CC-1 are given in reference (25).

Finally, the pore size distribution of each sample, obtained by mercury porosimetry, are shown in Figure A.1.

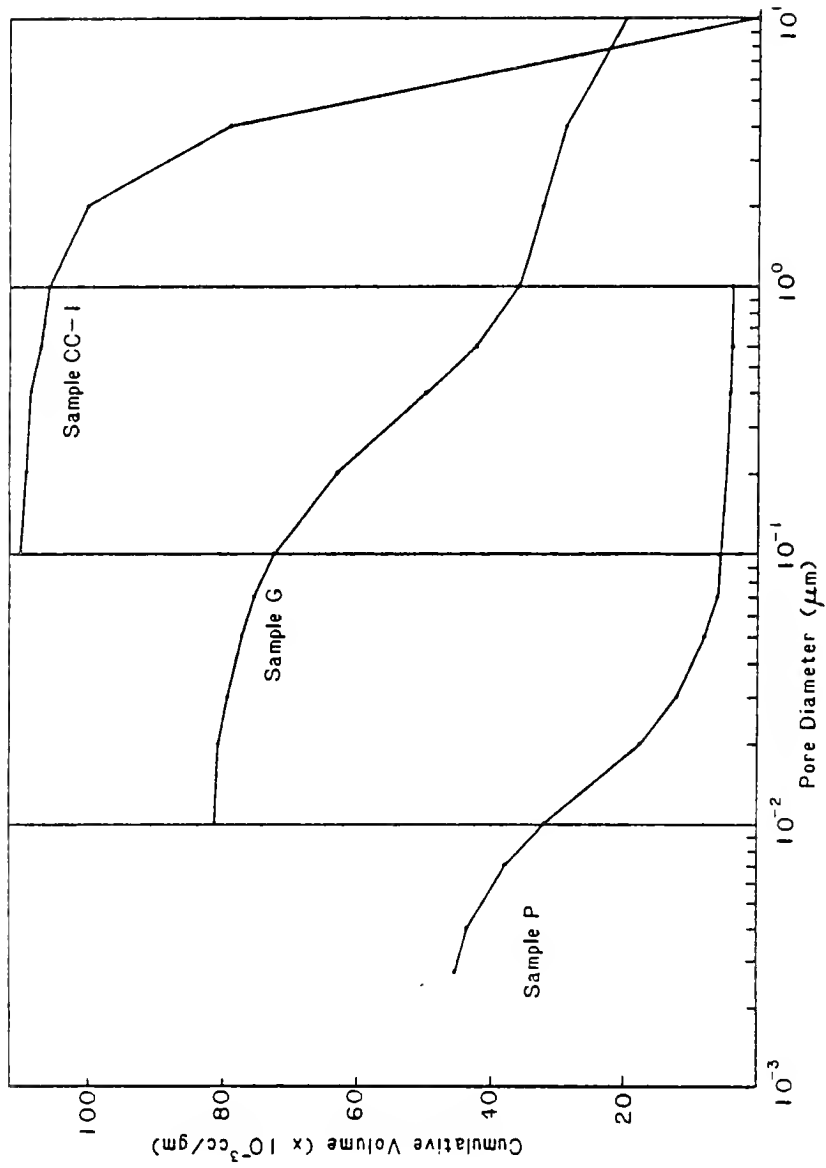


Figure A.1 Pore Size Distribution of Samples P, G, and CC-1

## APPENDIX B

Strain Gage Instrumentation

The freezing action in water saturated rock specimens was monitored by using electrical strain gages. Oven dry cylindrical specimens 2" in height and 1-3/8" in diameter were instrumented with four strain gages. Two measurements of longitudinal strains and two measurements of diametral strains were recorded from diametrically opposite points on the middle height of the test specimen.

The strain gages used were obtained from:

Micro-Measurements Division  
Measurements Group  
P. O. Box 27777  
Raleigh, North Carolina 2611

The type corresponds to the gage designation CEA-00-125UT-120 listed in the Catalog 200 of Micro-Measurements (M-M).

Before the application of the strain gages, the surface of the test specimen was prepared according to the Instruction Bulletin B-129 of M-M. M-Bond AE-10 bonding cement was used, and two protective coatings were applied on the strain gage: first, M-Coat D, and second, M-Coat G. The first is

a moisture barrier of negligible electrical leakage, and the second coat was used for further protection because the specimen was vacuum saturated with water. After several tests were performed, it was found that two or three layers of M-Coat D were enough to protect the strain gages from undesirable moisture penetration. The characteristics of the adhesive that was used and the properties of the protective coatings are listed in the Catalog A-100 of M-M. The strain gage application with M-Bond AE-10 was done according to the Instruction Bulletin B-137-7.

Each strain gage was hooked in a quarter bridge configuration, and two recording units were used for monitoring the strain readings. The recording of strains was performed manually.







COVER DESIGN BY ALDO GIORGINI